SERI/SP--231-3579

SERI/SP-231-3579
UC Category: 244
DE89009472

DE89 009472

Aquatic Species Program

Annual Report

W. S. Bollmeier
S. Sprague

September 1989

Prepared under Task No. BF911010
FTP No. 656

Solar Energy Research Institute
A Division of Midwest Research Institute

1617 Cole Boulevard
Golden, Colorado 80401-3393

Prepared for the
U.S. Department of Energy
Contract No. DE-AC02-83CH10093

NOTICE

Printed in the United States of America
Available from:
National Technical Information Service
U.S. Department of Commerce
5285 Port Royal Road
Springfield, VA 22161

Price: Microfiche A01
Printed Copy A08

Codes are used for pricing all publications. The code is determined by the number of pages in the publication. Information pertaining to the pricing codes can be found in the current issue of the following publications which are generally available in most libraries: *Energy Research Abstracts (ERA)*; *Government Reports Announcements* and Index (*GRA* and I); *Scientific and Technical Abstract Reports (STAR)*; and publication NTIS-PR-360 available from NTIS at the above address.

PREFACE

This report summarizes the progress and research accomplishments of the Aquatic Species Program, field managed by the Solar Energy Research Institute (SERI), through May 1989. This report includes an overview of the entire program and a summary of individual research projects. The program receives its funding through the Biofuels and Municipal Waste Technology Division of the Department of Energy.

For further details, contact the SERI Biofuels Program Office Aquatic Species Program Coordinator, Warren Bollmeier, at (303) 231-7669.

SUMMARY

When stimulated by environmental stress, many species of aquatic microalgae produce lipids, or oils, that can be processed into diesel oil or gasoline. These algae have growth rates as high as five times those of most terrestrial plants, and some species flourish in saline or brackish water unsuitable for human or traditional agricultural use. In addition, microalgae require large quantities of carbon dioxide for growth and lipid production, offering a way to mitigate increases in the concentration of atmospheric carbon dioxide, a major greenhouse gas. The Aquatic Species Program, funded by the Department of Energy and managed by the Solar Energy Research Institute, was designed to take advantage of these attributes.

The overall goal of the program is to provide the technology base for the cost effective production of diesel fuel from microalgae by the year 2010. The specific objectives are to identify or develop strains and culture (growth) requirements for high biomass and lipid production under fluctuating outdoor conditions, to develop design criteria for large scale culture systems, and to develop efficient harvesting, handling and conversion methods. Moreover, since the first applications of this technology are most likely to occur in the U. S. southwest where there are high levels of solar radiation, a large land base, and an inexpensive water source (saline), the research is driven by the conditions found in this area.

Significant progress has been made since the program focused exclusively on the production of fuels from microalgae in 1982. More than 3000 strains collected from desert and saline environments have been studied, resulting in the selection of numerous strains for improvement or development research. The strains selected grow over a wide range of salinities, produce significant quantities of lipid oils and achieve growth rates of nearly three doublings per day. Some of these strains can tolerate freezing temperatures and some as high as 100 degrees (F) or higher.

The most promising of these algal strains are maintained in a culture collection at SERI. This is the only collection of algae in the country that is focused on oil products for processing to fuels and serves as a resource for the program. However, many of these strains are distributed to industrial users, including shellfish growers and others interested in exploring microalgae for high-value products.

Analyses indicate that economic fuel production will require the microalgae to be grown in intensive culture in large outdoor ponds. The program has established an Outdoor Test Facility (OTF) to evaluate pond designs and to translate laboratory successes in strain development to outdoor conditions. The preliminary design consists of a 6-m-deep, raceway-shaped pond (0.25 acre) with a paddle wheel to circulate the water and systems for injecting carbon dioxide and other nutrients into the culture. The OTF became fully operational in 1988 and has two of the 0.25-acre ponds.

Recognizing the increased concern with global warming and the fact that large additions of carbon dioxide are required to obtain the production levels required for the technology, SERI has conducted a preliminary analysis coupling microalgae production facilities with power plants in the southwest. The preliminary results are promising and indicate that the carbon dioxide emissions from all the power plants in New Mexico and Arizona could be trapped by microalgae farms covering about ¼% of the combined land area of both states. Ongoing analysis will be used to guide and focus the research and to identify opportunities and other potential benefits of the technology.

Research is now focused on applying genetic techniques to enhance the lipid production of microalgae. This effort builds on extensive strain characterization research, as well as biochemical studies of the metabolic pathways for lipid synthesis. Using nongenetic methods, scientists have already improved the lipid content of the cell from the 5%-20% found in nature to more than 60% in the laboratory and 40% in outdoor culture. Recent results suggest that microalgae production goals of 70 dry tons per acre per year and lipid content of 60% can be achieved in outdoor culture. Research results suggest that if these goals are reached, oil produced from microalgae could be competitive with petroleum after the year 2010.

TABLE OF CONTENTS

TABLE OF CONTENTS (concluded)

1.0 PROGRAM OVERVIEW

Researchers in the Aquatics Species Program focus on the use of microalgae as a feedstock for producing renewable, high-energy liquid fuels such as diesel. It is important for the United States to develop alternative renewable oil sources because 42% of the current energy market in the United States is for liquid fuels, and 38% of these fuels are imported. The latter figure is expected to rise to more than 50% soon, increasing the U. S. trade deficit and our vulnerability to disruptions in petroleum supplies.[1] In 1979, the U. S. Department of Energy (DOE) and the Solar Energy Research Institute (SERI) initiated the Aquatic Species Program as part of the overall effort in biofuels. The program began to focus exclusively on fuels from microalgae in 1982. Estimates show that the technology being developed by the program can provide as much as 7% of the total current energy demand.

The program's basic premise is that microalgae, which have been called the most productive biochemical factories in the world, can produce up to 30 times more oil than per unit of growth area than land plants. It is estimated that 150-400 barrels oil per acre per year could be produced with microalgal oil technology. Initial commercialization of this technology is envisioned for the desert Southwest because this area provides high solar radiation and offers flat land that has few competing uses (hence low land costs). Similarly, there are large saline aquifers with few competing uses in the region. These could provide a suitable, low-cost medium for the growth of many microalgae.

Recently, the program has begun to assume additional importance for its potential contribution to the environment. Global warming, the primary "greenhouse effect," is caused by the release of carbon dioxide from fossil fuel combustion. This global warming has the potential of producing economic and geopolitical changes with profound impact on our economy and the energy industry. The production of diesel fuel by microalgae requires very large quantities of carbon dioxide as a nutrient. In areas where microalgae fuel plants operate, and in regions where these plants operate in tandem with fossil fuel plants to scrub carbon dioxide from flue gases, contributions to the greenhouse effect could be significantly reduced.

The program has supported research at SERI in Golden, Colo., as well as in industry, other government laboratories, and universities.

1.1 Program Goal

The goal of the Aquatic Species Program is to develop the technology base for large-scale production of oil-rich microalgae and conversion methods to convert the microalgae lipids into liquid fuels needed for industry and transportation by the year 2010.

---

[1] *Annual Energy Outlook 1989*, DOE/EIA-0383 (89), DOE/Energy Information Administration, Washington, DC, 1989.

1.2 Program Objectives

Specific long-term objectives of the program are to

- Genetically engineer microalgae for high lipid production at high growth rates
- Identify "trigger" points in biochemical pathways of algae that turn lipid production on and off
- Develop inexpensive, large-scale, outdoor mass culture technologies to grow microalgae
- Evaluate resource requirements for the growth and environmental impact of microalgae in the desert Southwest of the United States
- Develop technologies for converting microalgal lipids into high-value liquid transportation fuels, particularly diesel
- Transfer the technologies to the private sector for continued development and rapid commercialization by involving industry in the research process as early as possible.

1.3 Description of the Aquatic Species Program Elements

1.3.1 Production

Improvements are needed in algal growth and lipid production in order to produce economic liquid fuels from microalgae. The production element's goal is to reach target growth rates of 50 g/m^2-d in outdoor cultures and produce algae cells that are 50%-60% lipid. To do this, microalgae strains have been collected from many areas in the United States. These algae have been screened to select species that are temperature and salinity tolerant, have high productivities, and are good lipid producers. A collection of organisms is being maintained to provide a gene pool for direct exploitation as energy crop organisms in the laboratory and test facility and also as starting material for genetic engineering. It is also important to understand lipid biochemical pathways in algal cells in order to maximize lipid production and to develop genetic engineering techniques for improving microalgal production and lipid content.

1.3.2 Extraction and Conversion

Methods need to be developed for economical extraction of lipids from microalgae and conversion of lipids to gasoline and diesel substitutes. Untreated lipids have too high an oxygen content and viscosity to be used in standard engines. The primary goal of the conversion element is to economically convert a high proportion of the algal lipids to diesel fuels and to improve the overall economics by converting the balance of the biomass to biogas or other high energy products.

1.3.3 Engineering Design

The technology to produce economic liquid fuels from microalgae will require the growth of microalgae on a large scale. Systems to maintain optimal levels of nutrients, carbon dioxide, salinity, and temperature must be developed and tested. The engineering design element's goal is to develop large-scale outdoor facilities that allow the production goals to be met and to reduce the economic costs of such a system to those targeted by the program's economic analysis. The Outdoor Test Facility (OTF) located at Roswell, N. Mex. is being operated by a subcontractor, Microbial Products, Inc., so that various mass-culture and harvesting systems and technologies can be tested in an effort to increase outdoor algal productivities and decrease the cost of operating such a facility.

1.3.4 Analysis

Economic and resource analyses provide input to program management so research directions and priorities can be set. The analysis element's goal is to support the technology development by determining cost goals, economic sensitivities, resource assessments, and environmental impacts as new data are developed. To do this, researchers will conduct ongoing economic analyses. Resource and environmental assessments will be conducted to identify potential constraints, identify and address data gaps, and provide program guidance.

1.4 Program Highlights

1.4.1 FY 1988 Accomplishments

The microalgal screening program was completed, resulting in the identification of many productive strains and the establishment of a sufficient gene pool for future research. The most promising strains have been identified for genetic engineering. Protoplasts were produced and several potential genetic markers were developed. The key lipid biosynthetic enzyme acetyl-CoA carboxylase was purified and studied.

A report summarizing the carbon dioxide sources was completed. Up to 1 Petagram (Pg) of CO_2 is produced each year, primarily from fossil-steam power plants. A study was performed on the alternative approaches for disposing of brine from algal fuel facilities. The primary conclusions are that there are several potential solutions using existing technologies, such as deep well injection. The most cost-effective solution will depend heavily on the specific sites.

Operation of two 0.25-acre ponds began at OTF in Roswell. Two microalgal strains have been grown successfully since August 1988. The pond hydraulics and CO_2 injection system have operated successfully.

1.4.2 FY 1989 Plans

Research is now focused on applying genetic techniques to enhance the lipid production and growth characteristics of microalgae, as the program shifts from its complete reliance on wild algal strains

to genetically engineered strains. Field trials of strains from the culture collection will continue in the large scale (0.25-acre) outdoor ponds at Roswell. Work also continues on evaluating economic and environmental issues associated with production of liquid petroleum fuels. Advances in technology are used to readjust economic forecasts and economic analyses are used in setting research priorities.

MICROALGAL MASS CULTURE AND THE GREENHOUSE EFFECT: RESOURCES UPDATE

Paulanne Chelf and Lewis M. Brown
Biotechnology Research Branch
Solar Fuels Research Division
Solar Energy Research Institute
Golden, CO 80401

ABSTRACT

The purpose of this article is to review the resource requirements for algal mass culture, to discuss the feasibility of this technology for fuel production, and to examine the use of microalgae as a biological "sink" for carbon dioxide released from the burning of fossil fuels. Resource assessments have demonstrated that sufficient land and water for microalgal farms exists in a number of locations in the desert southwest. Technology assessments have demonstrated the long-term potential of fuels from microalgae, and have identified specific goals to make this technology economically feasible. We have utilized the existing data regarding availability of saline groundwater in Arizona and New Mexico, land and climate suitability in these states, and location, size, and carbon dioxide emissions from power plants in the area to assess the impact that microalgal energy farms could have on carbon dioxide emissions in these two states.

Background

The potential for global warming and other climate changes attributed to the greenhouse effect are attributed in large part to the accumulation of carbon dioxide in the atmosphere as a result of burning of fossil fuels (Schneider 1989). The carbon present in the petroleum burned today was fixed by marine plants, primarily phytoplankton, in the Tertiary and Mesozoic eras (Hunt 1979, Waples 1985). This carbon was trapped in sediments and slowly converted to the petroleum resources we rely on today. The massive quantities of fossil fuels combusted by modern society add large quantities of carbon dioxide to the atmosphere more rapidly than the biosphere can compensate.

Public attention has recently been focused on the greenhouse problem by a number of

articles, many of which predict grim consequences for life in a warming world (cf. Mintzer 1988, Pain 1988, Revkin 1988, Schneider 1989, Shabecoff 1988, Wald 1988). A rise in sea level is one of the most certain impacts of climate change, according to a recent draft report by the Environmental Protection Agency on the likely consequences of the greenhouse effect (USEPA 1988b). This rise in sea level threatens coastal areas, both urban and marshland. Vast areas of the grain belts of the United States and Western Europe may suffer decreases in agricultural production as a result of decreasing rainfall and increasing temperature (USEPA 1988a, Schneider 1989). In 1985 in the U.S., 35% of carbon dioxide emissions were attributed to electric utilities, mostly from coal burning. Carbon dioxide emissions from electric utilities are predicted to rise from 0.43 petagrams of carbon per year (PgC/yr; $1PgC = 10^{15}gC$) in 1985 to 0.77 PgC/yr in 2010, which is 44% of predicted total U.S. emissions (Edmonds et al. 1988).

A major problem which will need to be faced in reducing carbon dioxide emissions is how to trap and store carbon dioxide. The cost of trapping and concentrating carbon dioxide by conventional methods not involving biomass technologies is projected to increase the cost of electricity by 75 to 150% (Edmonds et al. 1988). There are also considerable problems and costs associated with transporting and storing large amounts of gaseous carbon. Methods must be found to trap and store this carbon dioxide. One proposed solution has been to grow trees and store them at the bottom of the ocean (Kellogg and Schware 1981). This process would delay the release of carbon back to the atmosphere, but is most likely impractical at a large scale. Reforestation has also been proposed, since trees can absorb 17 to 25 tons of carbon per acre per year. To absorb about 3 billion tons of carbon annually (the amount of carbon that is accumulating in the atmosphere) would require 740 million acres of trees, a land area roughly equal to that of Zaire (Booth 1988). Reforestation would need to continue at a rate sufficient to offset the predicted continued increase in fossil fuel consumption. In addition, reforestation requires arable land. Few areas of the world are amenable to reforestation at this scale. Another solution with perhaps greater practical potential is the use of biomass specifically grown in areas of current low productivity to displace fossil fuels. The combustion of biomass in this way releases recently fixed carbon back to the atmosphere where it can be refixed by biomass. Thus, no net increase in atmospheric carbon dioxide concentrations occurs.

An equally appropriate issue is how we can increase the amount of energy we obtain per petagram of carbon released from fossil fuel combustion today. Conservation and increased energy efficiency are alternatives available in the short term. Another way to obtain more energy per gram of carbon released is to reuse the released carbon for further energy generation before its eventual release to the atmosphere. Use of waste CO_2 from power plant flue gas as a feedstock for microalgal energy farms is one means to this end.

Certain microalgae are capable of accumulating intracellular lipids, thereby increasing their heat of combustion and their fuel value. Some organisms can accumulate up to 60% of their cellular organic mass as lipids, which can be readily converted to gasoline and diesel fuel. These organisms have been the subject of study of a program funded by the U.S. Department of Energy at the Solar Energy Research Institute. SERI researchers have been working since 1979 to develop microalgae as a biomass resource for the production of liquid fuels (Johnson and Sprague 1987). The present report extends this work to the issue of the potential impact of microalgal energy farms on global warming.

Land Climate and Water Resources

Microalgal lipid production requires land, water, sunlight, carbon dioxide, and inorganic nutrients. In order to minimize the cost of liquid fuels from microalgae, our work at SERI has focused on the desert Southwest, where abundant land, sunlight, and warm temperatures facilitate algal production. Fresh water is a precious commodity in this area, but highly saline water is present in abundance, primarily in underground aquifers. For this reason, SERI researchers have selected microalgae which can grow rapidly and produce lipids in very saline water, water which has no competing uses such as agriculture or municipal uses. Examination of the availability of land, water, and carbon dioxide resources required for microalgal production has revealed that sufficient resources are available in Arizona and New Mexico (Figs 1 and 2). Microalgal farms on a large scale could have a major impact on carbon dioxide emissions from power plants in these two states. Figures 1 and 2 demonstrate that most of the saline water resources in these two states coincides or is within a moderate distance (50-100 mi.) of existing fossil-fuel power plants. The total emissions from these two states (50 billion kg of carbon dioxide per year) could be absorbed by farms covering 1/4 % of their area.

We lack detailed land and saline water resource assessments for states neighboring this study area, and for other states with potential for microalgal culture. A study of carbon dioxide sources has demonstrated that sufficient carbon dioxide resources exist to support as much as 14.5 quadrillion Btu/yr of energy production, far exceeding the Department of energy goal of 2 quadrillion Btu/yr (Feinberg and Karpuk 1988). The modest 2 quadrillion Btu/yr goal for microalgal farming would nevertheless use a substantial amount (3.5 %) of U. S. carbon dioxide emissions. Microalgal farming for carbon dioxide capture has potential exceeding that analyzed in this study.

References

Booth, W. 1988. Johnny Appleseed and the greenhouse. Science 242:19-20.

Edmonds, J.A., Ashton, W.B., Cheng, H.C., & M. Steinberg. 1988. An Analysis of U.S. CO_2 Emissions Reduction Potential in the Period to 2010. U.S. Dept. of Energy Draft Report. 77pp. plus app.

Energy Information Administration. 1987a. Inventory of Power Plants in the United States 1987. DOE/EIA-0095(87).

Feinberg, D.A., & M.E. Karpuk. 1988. CO_2 Sources for Microalgae-based Liquid Fuel Production. Report on subcontract HK-8-18045-1 to the Solar Energy Research Institute. 42 pp.

Hunt, J.M. 1979. Petroleum Geochemistry and Geology. W.H. Freeman and Company, San Francisco. 617 pp.

Johnson, D.A., and S. Sprague. 1987. FY1987 Aquatic Species Program Overview. SERI/PR-231-3258, Solar Energy Research Institute, Golden, CO. 22 pp.

Kellogg, W.W. & R. Schware. 1981. Climate Change and Society: Consequences of Increasing Atmospheric Carbon Dioxide. Westview Press, Boulder, CO. 178 pp.

Lansford, R.R., Hernandez, J.W., Enis, P., & C.L. Mapel. 1986. Evaluation of Available Saline Water Resources for the Construction of Large-Scale Microalgae Production Facilities in New Mexico. Report on subcontract ZK-505091-1 to the Solar Energy Research Institute. 112 pp.

Maxwell, E.L., Folger, A.G., & S.E. Hogg. 1985. Resource Evaluation and Site Selection for Microalgae Production Systems. SERI/TR-215-2484, Solar Energy Research Institute, Golden, CO. 83 pp.

Mintzer, I. 1988. Weathering the storms in a warming world. Public Power 46:15-21.

Pain, S. 1988. No escape from the global greenhouse. New Scientist 128:38-43.

Revkin, A.C. 1988. Endless summer: living with the greenhouse effect. Discover, Oct., pp. 50-61.

Schneider, S.H. 1989. The greenhouse effect: science and policy. Science 243:771-781.

Shabecoff, P. "Energy dept. joins fight over global warming," New York Times, November 26, 1988.

United States Environmental Protection Agency. 1988a. Great Plains. In: The Potential Effects of Global Climate Change on the United States: Draft Report to Congress. J.B. Smith and D.A. Tirpak, eds. Vol. 1: Regional Studies, pp. 7-1 to 7-30.

United States Environmental Protection Agency. 1988b. Sea-level rise. In: The Potential Effects of Global Climate Change on the United States: Draft Report to Congress. J.B. Smith and D.A. Tirpak, eds. Vol. 2: National Studies, pp. 9-1 to 9-47.

Wald, M. "Fighting the greenhouse effect," New York Times, August 28, 1988.

Waples, D.W. 1985. Geochemistry in Petroleum Exploration. International Human Resources Development Corp., Boston. 217 pp.

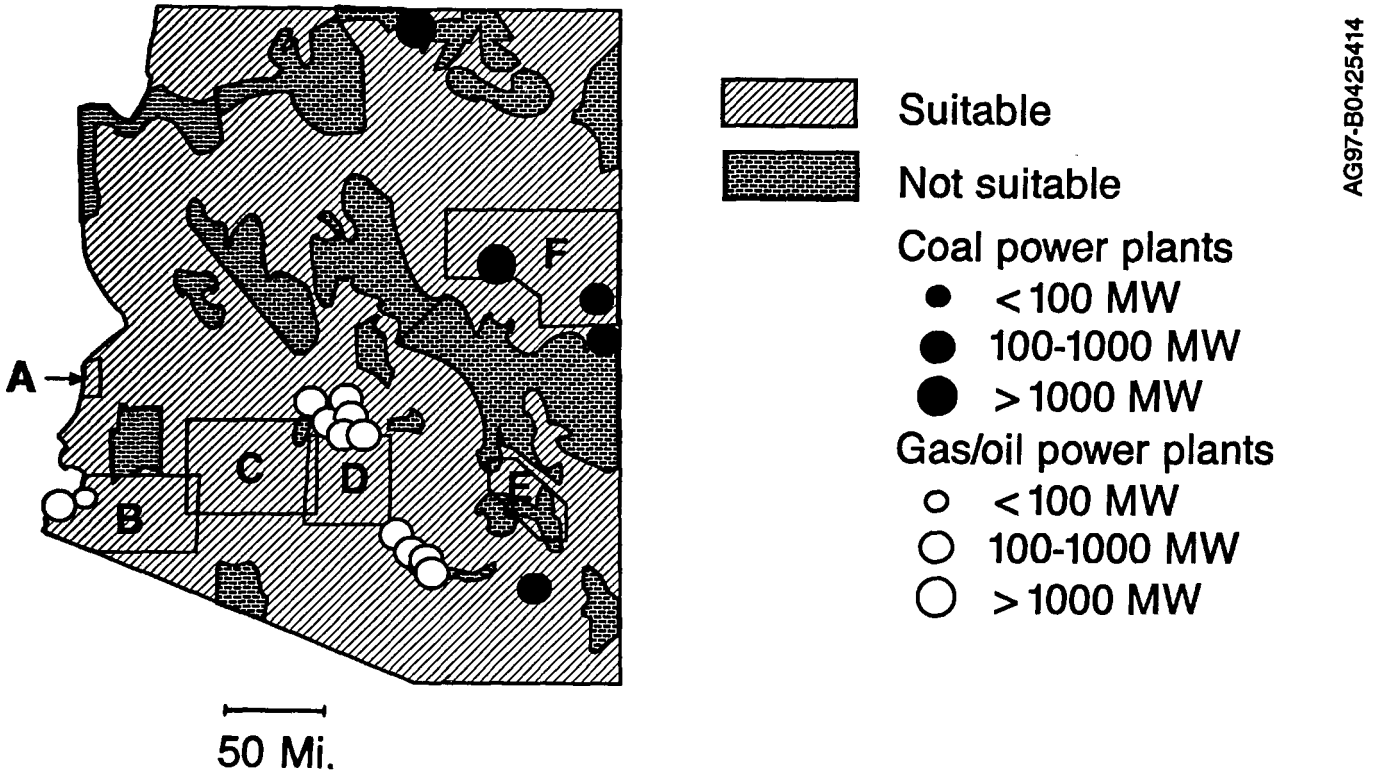

Fig. 1. Composite map showing size, type, and location of fossil-fuel burning power plants (EIA 1987) in Arizona in relation to saline groundwater resources (boxes A-F) and land/climate suitability (Maxwell et al. 1985) for microalgal mass culture. Clearly, there are large areas where all of the resources coincide, or are within a 100 mi. pipeline distance.

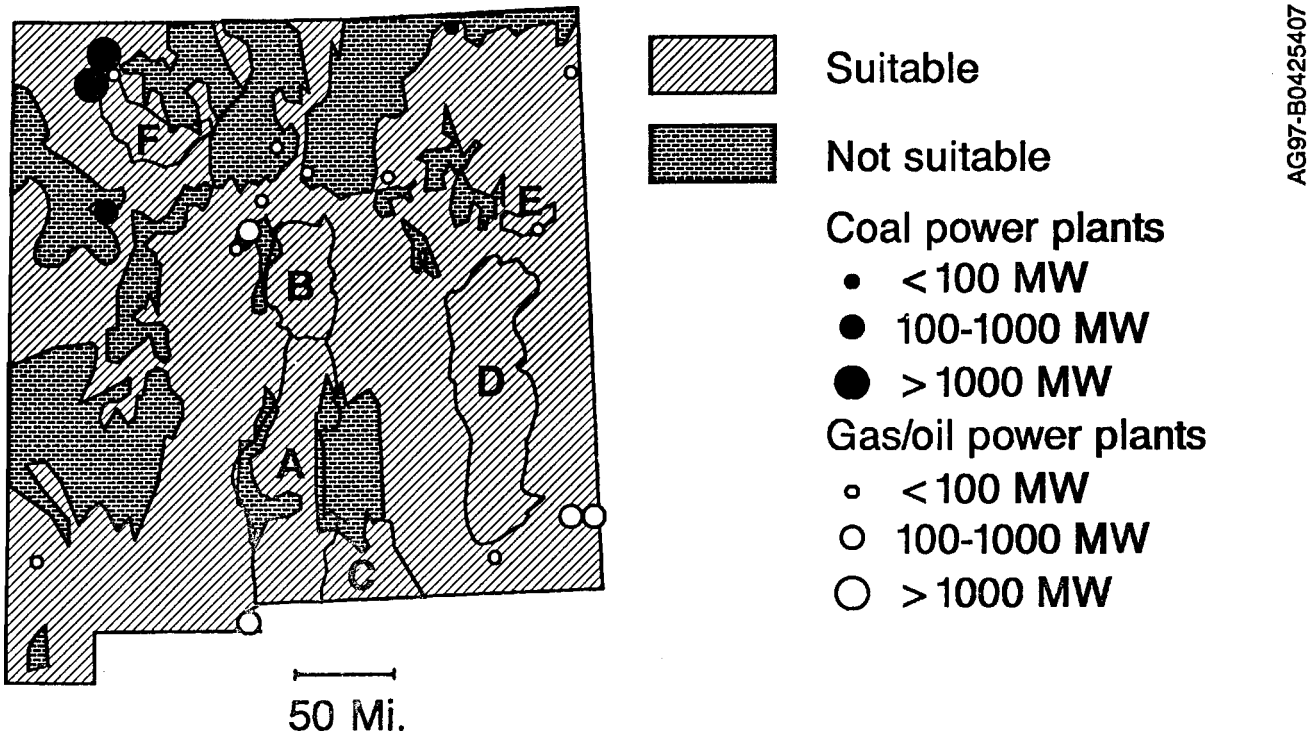

Fig. 2. Composite map showing size, type, and location of fossil-fuel burning power plants (EIA 1987) in New Mexico in relation to saline groundwater resources (Landsford et al. 1986) (boxes A-F) and land/climate suitability (Maxwell et al. 1985) for microalgal mass culture. Clearly, there are large areas where all of the resources coincide, or are within a 100 mi. pipeline distance.

CO_2 SOURCES FOR MICROALGAE-BASED LIQUID FUEL PRODUCTION

Prepared by:

Daniel A. Feinberg
Michael E. Karpuk

Technology Development Associates, Inc.
1667 Cole Blvd., Suite 400
Golden, CO 80401

for the

Solar Energy Research Institute
Contract No. HK-8-18045-1

June 1988

EXECUTIVE SUMMARY

The Solar Energy Research Institute's (SERI) Aquatic Species Program is developing microalgal species and culture technologies that result in microalgal cells with a high percentage of lipids. The lipids can be extracted and converted to a diesel fuel substitute. Optimal microalgae growth occurs in CO_2 saturated solutions. If these research efforts are successful, large quantities of low-cost CO_2 will be needed. The purpose of this study is to identify possible CO_2 sources for microalgae-based fuel production and to quantify the amounts available and possible costs. Because of the early stage of development of the fuel synthesis technology, and the current plentiful supplies of gaseous and liquid fossil fuels, the year 2010 was chosen as the earliest date that CO_2 for fuel synthesis would be needed.

The sources of CO_2 we have analyzed are:

Natural Reservoirs. Large natural reservoirs of CO_2 in the southwestern United States are currently being utilized for enhanced oil recovery (EOR). These reservoirs are expected to be depleted by the year 2010 and consequently unavailable for microalgae production. However, the CO_2 used for EOR will remain in the depleted oil fields, and could be recovered for microalgae production. Significant quantities of CO_2 are also present in some natural gas fields which are not currently being produced due to high separation costs. If the economics of these fields improve, then this CO_2 could become available.

Fossil Fuel Combustion. The U.S. has very large coal reserves, and coal is expected to remain a primary energy source in 2010 and beyond. Coal combustion in power, synthetic fuels, and chemical process plants will produce large quantities of CO_2. Clean coal technologies under investigation by the Electric Power Research Institute (EPRI) and the U.S. Department of Energy (U.S.D.O.E.) have the potential to produce large quantities of concentrated CO_2 at low cost. Concern and possible regulation of global warming caused by the release of CO_2 into the atmosphere may make CO_2 available from these sources at low or even negative costs.

Air Separation. It is conceivable that CO_2 could be recovered directly from the atmosphere, where it is the fourth-largest constituent. However, since the atmospheric CO_2 concentration is very low (330 ppm), significant technical breakthroughs are required to make the process viable.

Anaerobic Digestion. Anaerobic digestion of biomass and wastes is currently being investigated as a source of methane. Methane and CO_2 are coproduced in approximately equal molar volumes and are easily separated. Large quantities of CO_2 could be available from fuel-scale anaerobic digestion plants.

The results of this study indicate that there are several large sources of CO_2 that could support microalgae-based fuel production. The possible quantities and costs of CO_2 are listed in Table S-1.

Table S-1 Potential Sources of CO_2 for Fuel Synthesis in 2010

CO_2 Source	Potential CO_2 (10^9 kg/yr)	Estimated Cost (1986 $/kg)	(1986 $/MSCF)
Concentrated, high pressure sources:			
Liquid synthetic fuels plants	40	0.012-0.016	0.64-0.85
Gaseous synthetic fuels plants	220		
Gasification based combined cycle power plants	0-790		
Subtotal	260-1050		
Concentrated, low pressure sources:			
Enhanced oil recovery[ab]	8-32	0.009-0.016	0.47-0.85
Ammonia plants	9		
Ethanol plants	< 0.1		
Subtotal	17-41		
Dilute, high pressure sources:			
Noncommercial natural gas[a]	52-100	0.011-0.053	0.57-2.77
Refineries[c]	13	0.054-0.095	2.80-5.00
Dilute, low pressure sources:			
Anaerobic digestion (biomass)	130	0.011-0.084	0.57-4.40
Anaerobic digestion (wastes)	100		
Cement plants	26	0.051-0.084	2.78-4.40
Fossil-steam power plants[de]	0-790	0.029-0.048	1.50-2.50
Subtotal	321-1159		

a Assumes 25-yr depletion

b Based on 20% recycle of CO_2 used for EOR

c Includes fluid catalytic-cracking units (FCCU) and hydrogen plants

d Totals for 10-state region (AL, AZ, CA, FL, GA, LA, MS, NM, OK, TX)

e Based on U.S.D.O.E. projections for 2010

Sources: Zimmerman et al. (1979), Anada et al. (1982), U.S.D.O.E. (1983, 1987), Nelson (1983)

The lowest cost sources of CO_2 are from systems that produce CO_2 at high pressure and in high concentration. These systems include liquid and gaseous synthetic fuel plants, and gasification combined cycle power plants. From these sources, a total of 260-1050 x 10^9 kg (5.0-20.1 TSCF) per year of CO_2 could be available at a price of $0.012-$0.016/kg ($0.64-$0.85/MSCF). CO_2 costs will be higher or lower due to variations in flowrate, allocation of costs between main product and CO_2, process operating pressures, and other factors. Based on a requirement of 80 x 10^9 kg CO_2/quad (10^{15} Btu) of microalgae-derived lipid fuel, we estimate that sufficient CO_2 from these sources is available to support 3.3-13.1 quads annually of microalgae-based liquid fuel production. Gasification-based combined

cycle power plants have been included in this total, even though only one commercial plant of this design exists. If this type of plant design gains favor with electric utilities, a significant portion of the estimated 790 x 10^9 kg/yr of CO_2 could actually be produced.

If these sources were not adequate or available in a particular location, low pressure, high purity sources could be exploited. These sources include recovery from ammonia plants, ethanol fermentation plants, and depleted oilfields that have been flooded with CO_2 in enhanced oil recovery operations. A total of 17-41 x 10^9 kg (0.3-0.8 TSCF) per year are potentially available from these sources. The costs of recovering CO_2 from these sources range from \$0.009-\$0.016/kg (\$0.47-\$0.85/MSCF). This CO_2 would support an additional 0.2-0.5 annual quads of microalgae-based fuel production, bringing the total from high purity sources to 3.5-13.6 annual quads.

An additional 321-1159 x 10^9 kg (6.1-22.2 TSCF) per year of CO_2 could be available from high and low pressure dilute streams, primarily flue gas from coal-fired power plants and biomass anaerobic digestion plants. This quantity, which could be available in a ten-state region in the sunny part of the U.S., is enough to support 4.0-14.5 annual quads of microalgae-based fuel production. However, except for special cases, e.g., high demand for biogas leading to natural gas pipeline companies bearing the cost of CO_2 separation from biogas, recovery of CO_2 from such dilute streams is expensive, ranging from \$0.029-\$0.095/kg (\$1.50-\$5.00/MSCF). For flue gas, the situation is further complicated by the presence of sulfur compounds. Unless improved separation processes are developed, these sources may not be economical for microalgae-based liquid fuel production.

We have also evaluated the costs of transporting CO_2. Supercritical pipelines are the most economical method of transporting CO_2 for the flowrates required for fuel synthesis. Transportation costs are typically \$0.008/kg (\$0.40/MSCF) per 100 miles for a pipeline capacity of approximately 2.6 x 10^6 kg/d (50 MMSCFD). Therefore, transportation of CO_2 is feasible only from large concentrated sources, over relatively short distances. This implies that microalgae production facilities should be sited near CO_2 sources.

THE ECONOMIC IMPACT OF BRINE DISPOSAL ON ALGAL FUEL FACILITIES

Paul Bergeron
Engineering Research Section
Biotechnology Research Branch
Solar Fuels Division
Solar Energy Research Institute

May, 1989

THE ECONOMIC IMPACT OF BRINE DISPOSAL ON ALGAL FUEL FACILITIES

SUMMARY

Three brine disposal options were found that may be environmentally and economically acceptable: deep-well injection; transport by pipeline to the ocean or other large body of saline water (e.g., the Great Salt Lake); and containment in evaporation ponds as described in studies by the Bureau of Reclamation. The selection of an alternative for a particular algal fuel facility site depends on the topography, geology, and remoteness of that site. Transport by rail or truck does not appear to be an economically viable option. The possibility of generating revenue by producing salable salts, potable water, and electricity (via solar pond power plants) was investigated, but found to be economically unattractive unless the prices of the competition increase considerably. In general, the greater the distance to an environmentally acceptable disposal site and the higher the salinity of the feed water to the algae production ponds, the greater the cost of brine disposal to the algal fuels facility. Overall, brine disposal is not an intractable problem for microalgae farming for fuel, and can be handled by existing technologies.

INTRODUCTION

A report by Neenan et al entitled "Fuels from Microalgae: Technical Status, Potential, and Research Requirements" (1) has documented the results of a study to determine the potential of microalgae for fuel production. In this study, a typical algae "farm" was designed based on estimates of current technical performance, and processing plants were also designed to convert the algae and its oil from this reference pond system into various fuel products. The costs of the algae production facility and the conversion options were estimated from the designs, and the results were reviewed with several experts in the field. The study did not include the issue of disposal of the brine that is generated by the algae growth facility. It is this issue that will be addressed by this report. Alternatives for brine disposal will be presented along with estimates of their impact on the economics of the microalgal fuel facility.

BACKGROUND

The reference pond for the study is composed of forty three 20 hectare (ha) modular ponds with a total surface area of 860 ha, for a nominal facility size of 1000 ha. Ninety per cent of the pond area is assumed to be active at all times for a total active growth area of 770 ha. The study by Neenan et al. predicted that economic viability for the production of gasoline and ester fuel would be achieved for the following 1000 ha algal production

characteristics: an algal productivity of 50 g/m^2-day, a photosynthetic efficiency of 16% of photosynthetically active radiation (PAR), a specific growth rate of 0.37, a lipid oil content of 50% by weight, a salinity tolerance of 80 g TDS/L, and an algal yield of 130,000 tons/year. These characteristics may be attained through further research.

Based on the design assumptions and associated costs from the study cited above, Wyman (2) calculated the capital and operating costs for a 10,000 ha facility that would produce one million tons of algae per year from which 76.7 MM gallons of gasoline would be manufactured. The total capital cost was estimated at $446.1 MM which, when annualized, came to $61.3 MM per year. With operating costs estimated at $159.2 MM, the total annual charge was $220.5 MM. This resulted in a gasoline price of $1.59 per gallon after co-product credits.

DEFINITION OF THE ISSUE

The desert southwest with its high insolation levels and large underground reserves of saline water unsuitable for most other purposes has been considered best suited to support large-scale microalgae production facilities in the future. This area also has a high evaporation rate of approximately 0.0035 m/day on average. This results in large evaporative losses from the algae ponds which in turn causes an increase in the salinity of the water remaining in the ponds. This salinity is controlled by purging brine from the system in a bleed stream.

The water stream from the harvesting ponds is split into a recycle stream and a purge stream in order to reduce the feed water requirements. The amount of recycle is a function of the detention time in and the depth of the growth ponds, while the size of the purge brine stream is set by the salinity tolerance of the algae and the amount of salt entering with the saline water feed stream (all of which is assumed to leave with the purge brine stream). The size of the water evaporation stream is simply a function of the assumed average evaporation rate of 0.0035 m/day and the active algae growth area. The amount of water consumed by the algae is less than 1% of the feed water stream.

Table 1 lists the flow rates of the major streams for feed water salinities of 1.0 and 2.5% combined with a purge brine stream salinity of 8%. These feed stream salinities were chosen because there is a large supply of such underground saline water in the southwest and there is little competition for its use. The purge brine stream salinity was set at the assumed salinity tolerance of the algae. An algae growth pond depth of 0.15 m and detention time of 7 days were used to calculate the size of the recycle stream. The flow rates of the feed and brine streams are relatively insensitive to the values of the pond depth and detention time because any changes in them first affect only the recycle stream which is much larger than either the feed or brine streams. For

example, the detention time must be increased to 30 days in case 1 and 38 days in case 2 before the recycle rate shrinks to zero and the feed and purge rates start to be affected.

BRINE DISPOSAL ALTERNATIVES

Having determined the size of the purge brine stream, one must next decide what to do with it. The brine disposal methods investigated in this study are: 1) transportion to either a market or remote disposal site of the salt (dried in evaporation ponds) by truck, rail, or brine by pipeline; 2) containment in the evaporation ponds used to dry the salt; 3) deep-well injection at or near the facility. Three ways to generate revenues from the brine were also investigated: 1) creation of solar ponds to generate electricity; 2) desalinization to produce potable water; 3) fractional crystallization of salts for sale. The relative attractiveness of these disposal and revenue generation alternatives will depend on the economic climate within which the decision must be made and the physical attributes of the exact location (e.g., remoteness, geology, topography, hydrology,...) of the facility.

The assumptions used to calculate the annual cost of the various options include: financing at seventy percent equity at a 15% rate of return and thirty percent debt at an interest rate of 11%; twenty year plant life; a labor rate of $15.40/hr with man-hours of labor per year at 0.1% of the total investment; maintainance cost at 4% of total investment; and overhead at 60% of the labor plus maintenance cost total.

Salt Transport by Truck or Rail and Brine Transport by Pipeline

Dried salt could be transported from the site by truck or rail in order to deliver it to a market or to dispose of it at a remote location. As shown in Table 1, approximately 4 MM tons (case 1) or 1.25 MM tons (case 2) of salt would be generated per year from the brine. The capital and operating cost of using a bulldozer, front-end loader, and scale to load the salt onto the trucks or rail car is estimated to be approximately $0.54/ton which includes a two-man crew working at the loading end. The cost of transporting the salt by truck or rail is very dependent on the location of the algal fuel facility (AFF) and the distance to the delivery point.

Rail freight numbers can be obtained from Carload Waybill Statistics reports (3) of the Interstate Commerce Commission. The rate structure is a function of location in the country and weight. For carload shipments within the southwest territory, the rate in 1986 for rock salt was 4.5 cents/ton-mile. Including the $0.54/ton loading cost, the cost of salt transport by rail for 200 miles would be $9.50 per ton or $38 MM per year for case 1 and $12 MM per year for case 2; for 500 miles the costs increase to $23 per ton or $92 MM for case 1 and $29 MM for case 2. This does not include the cost of putting in a spur to the AFF or any unloading and final

delivery costs at the other end.

The cost of loading and moving 25-ton trucks was derived from from a study by Morbark Industries of Winn, Michigan based on their woodchip operations. The cost came to $.08 per ton per mile plus the loading charge of $0.54 per ton mentioned above. For a 200-mile trip (400 miles round trip), the cost comes to $16.54 per ton. For the 4 MM tons of salt per year of case 1, the annual charge is $66 MM ; for the 1.25 MM tons salt/year of case 2, the annual charge is $21 MM. This does not include the cost of putting in a road to the AFF or unloading and any disposal costs at the other end. The minimum number of truckloads necessary to do the job can be calculated using a load capacity of 40 tons per truck. This roughly corresponds to the maximum allowable limits for interstate and state highways. For case 1, 100,000 truckloads are required per year, or 274 truckloads per day for 365 days per year. The corresponding numbers for case 2 are 31,250 per year and 86 per day.

Since both truck and rail transport options are assumed to handle dry salt, the cost of removing the salt from the brine must be added. An evaporation/crystallization pond system would be used for this, and the costs associated with it are factored into the rail and truck options in the "Evaporation Ponds" section below. An alternative to transporting dry salt is to pump the 8% brine to the disposal destination via a reinforced concrete underground pipeline. Estimates for this option are based on a study done by the Bureau of Reclamation (BUREC)(4) to determine the economics of alternative salinity control projects for the Big Sandy River in the state of Wyoming. The pipeline system includes a 2 MM gallon regulating reservoir and a pumping station every ten miles. Installed pipeline costs are listed in the BUREC report in terms of pipe diameter which is determined by assuming a velocity of 5 ft/sec at the required capacity. The size and cost (capital and operating) of the pumps are determined by standard engineering techniques.

Tables 2 and 3 list the capital and power costs as a function of pipeline distance for cases 1 and 2, respectively. Any costs related to the disposal of the brine at the point of discharge are not included. This scenario is valid if the environmental impact at the point of discharge is negligible; for example, if the brine is discharged into the ocean, the Great Salt Lake, or existing salt flat where seepage of the brine into the water table is not a concern. An appropriate salt flat location that would meet with EPA approval would be difficult to find. The brine salinity was not concentrated above 8% in the above pipeline economics to minimize the local environmental impact at the point of discharge in the ocean which a salinity of approximately 3.5%. This restriction would not apply if the destination were the Great Salt Lake because its salinity is at or near saturation depending on the recent rainfall and snow melt history of the area.

Evaporation Ponds

The use of evaporation ponds to remove water from waste slurries is common practice wherever there is cheap land in sufficient quantity to handle the amount of such effluent. The BUREC has done considerable work in the last ten years to design and cost systems to control salinity levels in the Colorado River basin. Their approach has been to intercept highly saline ground water from agricultural irrigation runoff or other natural sources before this water enters the Colorado River basin. Once intercepted, the water can be sent to an industrial user for process water, to a utility for cooling water, to a desalinization plant, or straight to an evaporation pond. All of the potential uses require an evaporation pond as the final destination of the saline water not consumed in the intermediate use. The salinity of the water under study in the BUREC report (4) is approximately 0.4%. At this low salinity level compared to the 8% of the AFF brine, the saline water has much greater potential for a variety of uses than would the 8% brine. However, the design and costing of the components (pipelines, evaporation ponds,..) of the BUREC disposal alternative systems are directly applicable to the AFF brine disposal study.

The BUREC evaporation pond strategy involved locating the pond in an area that minimized pond construction costs and pumping the saline water via a pipeline to that location. Topographical attributes are sought such as availability of level terrain, suitability of relatively inexpensive remolded native clay liner (which still represented greater than 85% of the pond cost), natural enclosures, and high evaporation rates. Depending on these attributes, the evaporation pond cost varied from $11,000 to $22,000 per acre among the locations selected in the BUREC study. These costs included the clay liner and monitoring wells to detect seepage from the pond. The cost of the pumps and a 13 mile pipeline necessary to deliver the saline water to the pond are not included in the above figure. No cost was included to remove the salt since it was assumed to remain in the ponds which were in remote locations.

Three strategies are possible for the disposal of the salt for the AFF brine evaporation ponds: 1) evaporate all of the water and leave the salt in place as in the BUREC study; 2) concentrate the brine to saturation (approximately 25%) and inject the saturated solution into a geologically suitable underground area; 3) evaporate all of the water and transport the dry salt by rail or truck to an appropriate disposal site.

An enhanced evaporation system (EES) has been developed in the last 5 years that greatly reduces the amount of land area necessary to evaporate a given amount of water. The system was developed in Israel (5) (Hygroscopic Dew Point Conversion by Gad Assaf) and installed in the solar pond at Biet Ha' Arava, Israel which is used to generate electricity. The system comprises an elevated spray system which provides a larger evaporation surface area by creating

droplets which enhance the ground area efficiency by a factor of six to ten. EES costs were determined from a proposal submitted by the Imperial Irrigation District in 1988 (6) to construct a electricity-generating solar pond as a mitigation measure to manage the increasing salinity in the Salton Sea in southern California. Saline water would be withdrawn from the Salton Sea and sent to the EES where it would be concentrated to saturation. The saturated solution would then be pumped to the solar pond to be used as the bottom, heat absorbing layer of the pond. The estimated cost of the EES came to $19,000/acre for the 86 acre EES pond, and a ten-fold reduction in land area needed for the evaporation was assumed.

In Table 4 is listed the evaporation pond land areas needed to remove the water in the brine at the same rate that it is introduced using an EES with a tenfold increase in evaporation efficiency over a standard evaporation pond. The cost of the EES is assumed to scale with size to the 0.6 power. This cost has been added to the high end of the evaporation pond cost of $22,000 per acre from the BUREC study and used to calculate the cost per acre in Table 4. The evaporation pond is assumed to be located within a 10 mile radius of the AFF, and the pipeline cost in Table 4 was extracted from Table 2. These costs represent the cost to dry the salt prior to transporting it via rail or truck and must be added to those transport costs given in the previous section. This increases the annual 200-mile rail transport cost from $38 MM to $45.4 MM ($11.35 per ton) for case 1 and from $12 MM to $14.6 MM ($11.68 per ton) for case 2. The 500-mile rail transport costs rise to $99.4 MM and $31.6 MM for case 1 and 2, respectively. The annual 200-mile truck transport costs increase from $66 MM to $73.4 MM in case 1 and from $21 MM to $23.6 MM in case 2.

If the salt is to be left in the pond as was assumed in the BUREC study, then there must be enough land area to contain the salt produced over the life of the facility. The brine in case 1 produces 1354 acre-ft of salt per year and that in case 2 produces 423 acre-ft per year. If the pond is assumed to be 10 feet deep (solar ponds for generation of electricity are roughly 13 feet deep), then the storage area needed each year is 135.4 acres for case 1 and 42.3 for case 2. Assuming a life of the AFF of 20 years, the land areas needed are 2708 acres in case 1 and 846 acres in case 2. Adjusting the annual costs in Table 4 to reflect this increase in pond area brings them to $18.7 MM for case 1 and $6.8 MM for case 2.

The final evaporation scenario involves the concentration of the brine to saturation prior to injection of the saturated brine into a geologically suitable underground area. Concentrating from 8% to 25%, approximately 75% of the water in the 8% brine is removed, thereby substantially reducing the volume of brine to be injected. The evaporation pond land area necessary to do this is simply 75% of the area listed in Table 4--620 acres for case 1 and 207 acres for case 2. Assuming that the pond is once again located within a ten mile radius of the AFF, the cost data in Table 4 are

easily adjusted to arrive at an annual cost, exclusive of injection costs, of $5.8 MM for case 1 and $2.1 MM for case 2.

Deep Well Injection

Deep well injection of brine is a common practice in the oil and gas industry and has also been done by the BUREC for salinity control projects in the Colorado River basin area. All such injection sites must be approved by the Environmental Protection Agency (EPA). The main constraint imposed by the EPA is proof that the injected brine will not contaminate fresh water aquifers. This is accomplished by mapping the geology of the proposed area to determine if the geologic conditions exist to confine the brine. The survey also defines the depth to the proposed formation and the porosity and permeability of the proposed formation in order to calculate the storage capacity and the injection rate/pressure drop relationship. The cost of constructing and operating an injection well is dependent upon these characteristics of the proposed underground formation.

Through communication with the Oil and Gas Commissions of New Mexico and Colorado and a survey of brine disposal literature, the highest injection rates currently used in the southwest appear to be 250 to 300 gpm, and 200 gpm is is still considered high. This can be compared to a flow rate after concentration to saturation of 6000 gpm of saturated brine for case 1 and 2000 gpm for case 2. If a maximum injection rate of 200 gpm is assumed possible, then 30 wells will be needed for case 1 and 10 for case 2. As the number of wells in an injection system increase, care must be taken in situating the wells to avoid pressure feedback among them which increases pressure requirements.

A worst case cost scenario is provided by an injection well installed in Paradox, Colorado by the BUREC as part of their Colorado River Basin salinity control effort. Because the formation used was 16,000 feet deep and had a fairly low permeability and porosity, the system was designed for 5000 psi. The brine was saturated and contained enough hydrogen sulfide and carbonates to be very corrosive. Because of this and the stipulation of a 100 year well life, the pipe was constructed of Hastalloy. The cost of the well came to $13 MM to inject 200 gpm of brine (7). The annualized fixed cost for 20 years of $2.8 MM combines with the yearly power cost of $0.17 MM (at 3 cents/kw-hr) to obtain a yearly cost of approximately $3 MM for each of 30 wells for case 1 ($90 MM total system) and 10 wells for case 2 ($30 MM total system).

An example of a much lower cost system is provided by a study done by the EPA (8) to rehabilitate a brine-polluted aquifer by withdrawing brine from the region of the aquifer that was polluted and injecting the brine into a nearby, isolated underground formation. The well (500 feet deep, 200 gpm rate, 217 psi head), pump, piping, and associated hardware and construction costs came to $615,000 (1984 $)--two-thirds of which is for the well itself. The yearly operating and maintainance costs were estimated to be

$102,000, and the annual power costs to be approximately $5000. Therefore, the 20-year annualized cost comes to $242,500 per well of this type. The annual cost for the 30 wells of case 1 is $7.4 MM and for the 10 wells of case 2 is $2.5 MM.

Engineers at the Layne-Western Company, a major well-drilling company in the western U.S., estimated that injection well costs can be expected to be approximately $300 per foot for the type of well envisioned in this study. This covers the cost of a special casing sealing technique and two monitoring wells. If this figure is divided by 2/3 to account for non-well site costs (as estimated in the above EPA well example) and the resulting figure of $450/foot is multuplied by 500 feet (also from the above EPA well example), the well system cost is $225,000. The $615,000 estimated in the above-cited EPA study, therefore, appears to be a reasonable estimate and will be used for this study.

To the injection well system cost must be added the cost of the evaporation pond system which greatly reduces the volume of brine by concentrating it from 8% to 25% salt. These figures are $5.8 MM for case 1 and $2.1 MM for case 2. Assuming the injection well system is connected to the evaporation pond by a 10-mile pipeline, the annual pipeline cost comes to $0.6 MM and $0.3 MM for cases 1 and 2, respectively. The evaporation pond-injection well system total annual cost now totals $13.8 MM for case 1 and $4.9 MM for case 2 assuming that the EPA study injection well cost is applicable.

Another possibility for injection well siting is to use the saline water aquifer from which the AFF feed water is being drawn as the receptacle for the saturated brine. This is a common practice in oil and gas wells, serving to dispose of the brine and improve pressure in the reservoir. The costs associated with this scenario would be approximately the same as the $10.4 MM for case 1 and the $3.7 MM for case 2 as cited above. This scenario eliminates the possibility of having to locate the injection wells a great (uneconomical) distance from the AFF due to the lack of an appropriate nearby site.

Injecting the brine into the aquifer would raise the average salinity in the aquifer; however, an injection strategy could be devised to minimize the mixing of the injected brine with the less saline feed water already in the aquifer. For example, the difference in specific gravity between the approximately 2.5% saline water (SG=1.02) and the 25% brine (SG=1.2) would tend to inhibit mixing if the brine were injected near the bottom of the aquifer while the feed water withdrawn nearer the top. The main mechanism for increasing the feed water salinity would be diffusion of the salt from the more to the less concentrated water. This is normally a slow process and is slower still through a porous media such as the saline water rich formations under discussion. The actual rates depend heavily on the physical characteristics of the formation (e.g., porosity and permeability) and the degree of mixing at the boundary between the brine and the feed water. Of

course, this becomes irrelevant if the volume of water in the aquifer is large enough that the addition of the brine increases the average salinity only slightly during the lifetime of the AFF.

REVENUE GENERATION FROM BRINE

The three revenue-generating products from the 8% brine that were reviewed are: 1) sodium chloride and salts of magnesium and potassium obtained via fractional crystallization; 2) potable water via desalinization technology; 3) electric power via salt gradient solar ponds.

Salt Recovery

The possibility of selling the salt as is for road salt was briefly investigated; but it was found through conversations with the New Mexico State Highway Department and the EPA that such salt is required to be at least 95% sodium chloride (9). Therefore, a process like fractional crystallization is required to attain the necessary purity. Salts of potassium and magnesium could be generated as coproducts from this process. BUREC looked at this in their Colorado River Basin salinity control project and concluded that, even with their very large streams of 3 to 5 percent brine, the quantities of salt, the large water evaporation cost, and the remote location of the operations would make salt recovery not competitive with existing large-scale commercial operations. There are two companies on the shore of the Great Salt Lake that produce sodium chloride using evaporation ponds. Since the salinity of the Great Salt Lake is near or at saturation, the amount of water to be removed is one third to one quarter that for the 8% brine effluent from the AFF. This advantage along with the proximity of the Great Salt Lake operations to major rail and trucking lines makes that area a tough competitor for this market.

Desalinization

High efficiency distillation processes such as vapor compression evaporation (VCE) are the most widely used desalinization process today. Reverse osmosis membrane systems are also used for this purpose, but can tolerate salinities up to only 4.5%. The latest eficiency and cost information on VCE systems was obtained from a company that analyzes and designs wastewater treatment systems and has a great deal of experience with evaporators (10). A recently completed design of a VCE system that produced 2.2 MM gpd of product water from 2.5 MM gpd of 5% brine had an installed cost of $20 MM. As a rule of thumb, 150 kw-hr are required per 1000 gallons of product. A similar but larger system can generate 25 MM gpd of product from 30 MM gpd of 8% brine (case 1), or 8.3 MM gpd from 10 MM gpd of 8% brine (case 2). The costs presented in Table 5 were obtained by scaling the fixed costs by the 0.6 power and assuming an electricity requirement of 150 kw-hr per 1000 gallons of product. As seen in Table 5, the product cost is dominated by the cost of power, and is, therefore, very sensitive to the assumed cost of electricity. The assumed rate of 3 cents/kw-hr is probably at the low end of what can be expected. Also, the approximately 6 MM gpd (4325 gpm) of supersaturated brine

produced by this process for case 1 and 2 MM gpd (1442 gpm) for case 2 must still be disposed of in some manner.

Electricity Production via Solar Ponds

Solar pond power plant (SPPP) technology exploits the phenomenon that, in a standing pond of salt water, the more saline water is heavier and stays at the bottom. Heat from solar energy penetrates to the saturated brine solution trapped at the bottom where temperatures can exceed 80C. This is hot enough to drive special organic fluid Rankine cycle turbine generators. The largest such plant in the world is a 62 acre pond in Israel at Bet Ha' Arava which is designed for 5 MW, 1000 hr/year.

Engineering studies based on the operation of this SPPP and other demonstration ponds in the U.S. and Australia have defined the potential economics of large-scale SPPP's of the future (11,12). As a rough approximation, an SPPP is capable of producing 2 watts (net) per square meter of pond at a cost of approximately 10 cents/kw-hr. It is estimated that with continued research the conversion efficiency can be raised from 7% to 9% (out of 16% potential), and the parasitic power losses can be reduced from 25% to 15% of power output (12). These improvements can reduce the cost to approximately 7.7 cents/kw-hr. This cost does not include the cost due to salt which would raise the price by 2.3 cents to 10 cents/kw-hr. Some of this additional salt cost would not be incurred if the salt were obtained from a nearby AFF. The fraction of the 2.3 cents that remains depends upon whatever must be done to the salt for it to be usable in the SPPP.

The AFF design in the report by Neenan et al was based on a 1000 ha algae production unit and consumed 15 MM kw-hr/yr of electricity under the case 1 assumption that the fee water salinity is 2.5%. The ten-fold scale-up considered by Wyman and this current report will require 150 MM kw-hr/yr. If power is assumed to be needed 24 hours/day for 365 days/yr, an SPPP with a 17MW output will be required to satisfy the electrical requirements of the AFF. At a capacity of 2 watts per square meter, the SPPP must be 2100 acres--21% of the area of the algae production unit.

The advisability of installing an SPPP depends on the going rate for electricity, the availability of sufficiently level land, and the presence of any chemicals or matter in the salt solution from any of the processing in the AFF that might adversely affect the performance of the SPPP. The SPPP option only addresses the question of salt disposal if the solar pond is to be the final resting place of the salt, or if the lifetime of the SPPP goes beyond that of the AFF. The latter possibility assumes that the SPPP could be hooked up to the national grid. This should not present a problem since the AFF would require power from the grid for the first two to three years of its existance--the time necessary to produce enough salt from the AFF and commission the SPPP.

DISCUSSION AND CONCLUSIONS

This study has reviewed several brine disposal options that might be available to an algal fuel facility (AFF). The selection of the most appropriate option and the impact on algal fuel price will depend on the relative costs of each option and on the characteristics--geological, topographical, hydrological-- of the particular location. Also of great importance is the distance of the particular location from the destination (market or final disposal site) of the salt or brine. The decision on by-product generation from the brine is dependent upon the costs of the competition at the time. All of these variables make it impossible to predict an optimum disposal method or assess the final fuel cost; but the number of potentially viable options can, perhaps, be reduced, and an estimate of their impact on the economics of the AFF presented.

The impact of the various options is presented in Table 6 in terms of the annual charge of each and as a per cent of the $220.5 MM AFF annual charge calculated by Wyman for the 10,000 ha AFF without brine disposal costs. The level of acceptability for brine disposal cost has been arbitrarily set at roughly 10% or less of the annual AFF charge.

In general, the greater the distance to an environmentally acceptable disposal site and the higher the salinity of the feed water to the algae growth ponds, the greater the disposal cost to the AFF. Transport of dry salt by rail is acceptible only for case 2 when the distance is less than 200 to 300 miles. This assumes a negligible disposal cost at the destination. Trucking the salt for 200 miles is prohibitively expensive for case 1, and moderately expensive for case 2. This option may be feasible if the AFF feed water salinity is 1% or less, and if the additional disposal costs at the destination are modest.

The use of a pipeline to ship the 8% brine may be attractive for either case 1 or case 2 if the distance is not too long and the destination is an environmentally acceptible dumping area with little or no modification. The ocean may be such a destination, and, therefore, the AFF may roughly be located within 100 miles of the coast if the feed water salinity is 2.5% and 300 miles if it is 1%. As a point of reference, southwest New Mexico is approximately 300 miles from the Gulf of California. If the salinity of the brine sink were at or near saturation as is the Great Salt Lake, the pipeline costs would be reduced since pumping the reduced volume of saturated brine would reduce the pipeline size. However, if there is insufficient level land area available near the AFF site, the saturated brine pipeline would not be an option.

The use of an evaporation pond as the final containment site is economically very attractive, but would require the approval of

the EPA and the availability of sufficiently level land. By combining the evaporation pond and pipeline costs in Table 6, it can be seen that this option would be acceptable if such a site were located within 50 miles of the AFF of case 1 or within 200 miles of the AFF of case 2.

Deep well injection of brine at saturation appears to be economically acceptable if the injection sites are within 200 miles of the AFF for case 1; but can be even greater distances if the feed water salinity is 1% or so as in case 2. This, of course assumes that an EPA-approved site is available within that range. Using the feed water aquifer as the injection site eliminates doubts associated with finding an EPA-approved site. Whether or not this is practical depends upon the characteristics of the aquifer--size,porosity,permeability-- that determine the rate at which the salinity of the feed water in the aquifer is raised.

Generation of income from the sale of salts, electricity, or potable water requires prices of the competition of these by-products that are considerably higher than currently exist. In the case of electrical generation by solar pond power plants, the disposition of the salt at the end of the SPPP life is still an issue if it cannot be left in the ponds. The production of potable water greatly reduces the volume of the brine to be disposed of, but the issue of the disposal of that brine remains. The option of fractional crystallization of the salt to produce salable salts needs to be looked at in more detail. However, transportation costs to market could be prohibitive if the AFF location is remote; also, there appears to be no economic advantage to using AFF brine at 8% salinity compared to Great Salt Lake brine at 15-25% salinity as is currently done.

REFERENCES

1. Neenan, B. et al. 1986. "Fuels from Microalgae: Technology Status, Potential, and Research Requirements," Solar Energy Research Institute, Golden, Colorado. Report No. SP-231-2550.

2. Wyman, C.E. 1988. Unpublished internal report for the Solar Energy Research Institute.

3. "Carload Waybill Statistics,1986," 1988. U.S. Federal Railroad Commission, Washington, D.C. Publication No. PB38-189345.

4. "Big Sandy River Unit-colorado River Water Quality Improvement Program," 1982. Prepared by Sage Murphy and Associates for the USDI/Bureau of Reclamation under contract No. 1-07-40-S1494.

5. Assaf, G. 1984. "Hygroscopic Dew Point Conversion,"

PhisicoChemical Hydrodynamics, 5:5/6, pp.363-368.

6. "Salton Sea Mitigation Plan Phase 1," 1988. Submitted by the Imperial Irrigation District of California to the State of California.

7. Personal communication with Paul Osborne of the Environmental Protection Agency in Denver, CO.

8. Fryberger, J.S. 1972. "Rehabilitation of a Brine-Polluted Aquifer," Environmental Protection Agency report No. EPA-R2-72-014.

9. Carstens, M. et al. 1988. "Modifications to the Design and Operations of an Outdoor Microalgae Facility," Unpublished report.

10. Personal communication with Thomas Wolfe of Personal Science, Inc.

11. Personal communication with Federica Zangrando of the Solar Energy Research Institute.

12. Doron, B. 1987. "Economic Analysis of Solar Ponds and Solar Pond Power Plants," Published in the proceedings of the Solar Pond Science and Technology Workship sponsored be IIE, Cuernivaca, Mexico.

Table 1. Flow rates of major streams for assumed feed water salinities of 2.5% and 1.0% in a 10,000 ha algae production facility operating 365 days/yr and producing 1.0 MM tons of dry algae per year.

	Case 1	Case 2
Feed Water Salinity (%)	2.5	1.0
Evaporation Rate (MM tons/yr)	108	108
Saline Feed Water Rate (MM tons/yr; gpm)	159;72,000	125;57,000
Brine Rate (MM tons/yr; MM gal/day)	50;30	16;10
Salt in Brine (MM tons/yr)	4.0	1.25
Recycle Rate (MM tons/yr)	538	568

Table 2. Pipeline costs for case 1 disposal of 8% brine which includes a 42 inch reinforced concrete pipe and a 2500 hp pump every 10 miles.

Distance (miles)	Capital Cost ($MM)	Annual Power Cost ($MM at 3cents/kw-hr)	Total Annual Cost ($MM)
10	7.5	0.4	2.0
20	14.5	0.8	4.0
50	35.5	2.0	10.0
100	70.5	4.0	20.0
500	350.5	20.0	96.3

Table 3. Pipeline costs for case 2 disposal of 8% brine which includes a 24 inch reinforced concrete pipeline and at 750 hp pump every 10 miles.

Distance (miles)	Capital Cost ($MM)	Annual Power Cost ($MM at 3cents/kw-hr)	Total Annual Cost ($MM)
10	3.5	0.1	0.9
20	6.6	0.3	1.7
50	15.7	0.7	4.1
100	30.9	1.3	8.0
500	152.5	6.7	39.9

Table 4. Cost of an evaporation pond with EES capable of evaporating 100% of the water in the brine annually from a 10,000 ha AFF.

	Case 1	Case 2
Area for 100% evaporation (acres)	825	275
Cost ($/acre);($/ha)	29,690;73,330	33,930;83,800
Total Pond Cost ($MM)	24.5	9.3
Cost for 10 mile pipeline ($MM)	7.5	2.0
Annualized Fixed Cost ($MM)	7.0	2.5
Annual Operating Cost ($MM)	0.4	0.1
Total Annual Cost ($MM)	7.4	2.6

Table 5. Costs associated with desalinization of 8% bring via vapor compression evaporation. Electricity cost assume to be 3 cents/kw-hr.

	Case 1	Case 2
Installed Cost ($MM)	89	43
Electricity Required (MW)	160	53
Annualized Fixed Cost ($MM)	19.4	10.0
Annual Electricity Cost ($MM)	41.0	13.7
Product Flow Rate (MM gal/yr)	9205	3068
Product Cost ($/1000 gal)	6.50	7.72

Table 6. Comparison of costs of the brine disposal alternatives--$MM annually and percent of AFF annual charge.

		Case 1 ($MM), (%AFF)	Case 2 ($MM), (%AFF)
Dried Salt by Rail[1]			
	200 miles	45.4 (21)	14.6 (7)
	500 miles	99.4 (45)	31.6 (14)
Dried Salt by Truck[1]			
	200 miles	73.4 (33)	23.6 (11)
8% Brine Pipeline[2]			
	50 miles	10.0 (5)	4.1 (2)
	100 miles	20.0 (9)	8.0 (4)
	300 miles	57.8 (26)	23.9 (11)
Evaporation Pond as Containment Site[3]		18.7 (9)	6.8 (3)
Deep Well Injection of Saturated Brine[4]			
	10 miles from AFF	13.8 (6)	4.9 (2)
	100 miles from AFF	19.5 (9)	8.8 (4)
	200 miles from AFF	25.5 (12)	10.6 (5)

[1]Includes amortized cost of the evaporation pond to concentrate the 8% brine to dryness.
[2]Pipeline costs would be reduced if saturated brine could be sent to a sink already at saturation like the Great Salt Lake.
[3]Evaporation pond size increased above that for drying in order to contain all of the salt. Includes the cost of a 10-mile pipeline from the AFF.
[4]Includes the cost of a 10-mile pipeline to transport the saturated brine from the evaporation pond.

DESIGN AND OPERATION OF AN OUTDOOR MICROALGAE TEST FACILITY

Joseph C. Weissman and David M. Tillett
Microbial Products, Inc.
Vacaville, CA 94533

ABSTRACT

The Outdoor Test Facility of the Aquatic Species Program was completed during 1988. It features a small-scale system comprised of six 3-m^2 fiberglass ponds and a large-scale system with two 0.1 hectare raceway ponds. One of these is lined with a plastic membrane, the other with clay and rock. An engineering analysis of the hydraulic and carbonation systems of the 0.1 hectare ponds was performed. Velocity profiles, head losses, and power requirements were measured in each raceway. Manning's roughness coefficient was 0.010 for the plastic-lined pond and 0.0173 for the pond lined with earthen materials. Thus considerably less power was consumed in mixing the former. The overall efficiency of converting inorganic carbon into algal biomass was estimated to be 60% in the large raceways. Outgassing through the pond surface accounted for half of the loss of CO_2 at pH 7.5. The small-scale system was used to screen over fifteen strains of algae for yield in outdoor culture, to estimate annual yield at the site, and to evaluate capacity for production of lipids under nitrogen or silicon deprivation.

DESIGN AND OPERATION OF AN OUTDOOR MICROALGAE TEST FACILITY

INTRODUCTION

The overall objective of this project is to develop and operate a test facility in the American Southwest to evaluate microalgal productivities and to examine the problems and potential of scaling up and operating large microalgal production systems. This includes testing specific designs, modes of operation, and strains of microalgae; proposing and evaluating modifications to technological concepts; and assessing the progress in meeting cost objectives of the Aquatic Species Program (ASP).

The project is located at an established water research facility in the city of Roswell in the southeastern part of New Mexico. The site is representative of those that may be available for construction of an actual production plant. It is characterized by high insolation, low precipitation, flat land, and an abundant supply of highly saline groundwater. Much of the infrastructure required for this type of project was already in place: triple-lined evaporation ponds for disposal of pond effluents, land at very affordable rental rates, and laboratory and office space. There is, in addition, an existing chemical analysis laboratory, much of which is common space for the tenants of the facility.

The objective during the first year of the project (3/9/87 to 3/11/88) was to evaluate the outdoor production performance of prescreened species of microalgae in six small-scale reactors (3 m^2) and to begin the development of a larger-scale facility (Weissman, Goebel, and Tillett 1988). During the second year (3/12/88 to 3/11/89) the objectives were to continue evaluating biomass and lipid productivity in the 3-m^2 pond system, to finish construction of the two 0.1-hectare raceways, to evaluate the large system in terms of hydraulics and carbonation, and to begin year round operation of the large system. The basic results obtained are summarized here.

LARGE-SCALE SYSTEM ENGINEERING ANALYSIS

The large-scale system was designed to be a research vehicle intermediate in scale between the small fiberglass (3-m^2) raceways and a larger 0.5-ha demonstration raceway. Biological and engineering scale up problems are uncovered, and solutions elucidated, using these 0.1-ha raceways. As a first step in this process, an engineering analysis was performed on the system. The goals were to evaluate performance of construction techniques, hydraulic operation, and carbonation systems in terms of design expectations and future scale up.

Grading and Pond Depth

The grade was designed with a 0.0006 slope from east to west, resulting in a 4.5 cm depth differential from one end of each channel to the other. This was done for ease of construction (of this relatively small system) and as an aid in draining and cleaning the ponds. Generally, the design intent would have been accomplished, except that the soil structure at the site was poor. Earth compacting was extremely limited; the spongy clay soils did not fully compact. Instead, certain areas compacted and sank subsequent to the grading efforts. The result is that the depth profiles undulate. This has had two deleterious consequences. First, the ponds are not easy to drain and clean. Second, the contractions and expansions of flow, due to the depth changes, complicate the hydraulics in the ponds and lead to an increased problem of in-pond deposition of particulates. The ponds were operated at an average depth of 14 cm. The standard deviation of depths from the mean was about 2 cm. Greater depths will be used in 1989 to reduce the magnitude of depth changes along the lengths of the channels.

Velocity Profiles

A simple logarithmic relationship was used to fit data from velocity-depth profiles: $A + B \log(y/d)$, where A and B are constants, d is the depth, and y is the distance from the bottom to the measuring point. Obviously this fit breaks down at $y = 0$ (the velocity profile changes shape as it approaches zero at the pond bottom) and usually at $y = d$ (the surface velocity may even be lower than beneath the surface). The average velocity is equal to $B - A$ (or V at $y/d = 0.368$).

Velocity profiles were taken 1.4 m upstream from the sump in each pond (Figure 1). There were six measurement stations in each channel, 0.60, 1.83, 3.05, 4.27, 5.49, and 6.10 meters from the center wall. Thus the 6.85 m width of a given channel was divided into seven sections, each bounded by two measurement stations. Section averages were determined, assigned a weight, and used to calculate the average velocity in the channel at the measurement cross section. An overall average flow rate for each raceway at each of six paddle wheel rotation speeds was determined from the average velocities, average depth, and channel width. Given the average depth of any reach of channel and the average flow rate, the velocity of flow in that reach could now be calculated.

Examples of the velocity-depth profiles obtained are shown in Figure 2. The velocity profiles across the return flow channel in each raceway are shown in Figure 3. Overall average velocities for both ponds, based on flow rate and average pond depth are shown in Table 1. The mixing system was designed to allow variation in mixing velocity from 15 to 40 cm s^{-1}. The top speed could not be reached, due to mixer inefficiency at the high lifts engendered.

Table 1. Average Velocities in 0.1-hectare Raceways (cm s^{-1}).

	Paddle Wheel Rotation Speed, rpm					
	2.7	3.6*	4.4	5.3*	6.1	7.8
North Pond	16.7	24.4	27.6	30.8	33.0	39.5
South Pond	15.8	17.1	21.3	22.1	23.0	25.0

Velocities calculated from measured flowrate and average depth of 13.7 cm for North Pond and 13.5 for South Pond.
* Velocity determined from interpolated flowrate.

Head Losses

Depth of flow was measured across the channel at six locations in each pond at a series of paddle wheel rotation speeds. Using the still water level as a datum, the potential energy of the water was estimated at each measuring station from the difference between the measured depth of the moving water and that of the still water. If flow were steady and uniform, these measurements would be enough to determine total head losses, since flow velocities would be equal (that is kinetic energy associated with the flow would be constant). We know from the depth profile, however, that even under steady flow conditions attained, the flow was not uniform: in one channel of each pond the slope of the pond bottom was adverse (increasing in the direction of flow); there were depth contractions and expansions; and there were non-uniformities associated with bends, sumps, and the lift stations. Thus, some estimate had to be made of the velocity head at each location in order to get an approximate estimate of total head. Once this was done, differences in total head between locations could be estimated.

Measurements taken before and after the paddle wheel were used to indicate total losses in mixing the pond. When multiplied by water density and flowrate, these losses gave an estimate of hydraulic power requirments for mixing. Measurements taken before and after each bend were used to estimate bend losses. Measurements were also taken before and after the carbonation sumps, to determine their contribution to losses; and at the beginning and end of the channels in each pond to isolate the "open channel flow" losses. Estimates of the head loss for each pond section are given in Table 2.

There was a considerable level of approximation in each of these meaurements. There was an error of 0.05-0.1 cm associated with each depth measurement at the lower mixing speeds, and an error of twice this at the higher speeds. Since there were two subtractions needed to obtain a head difference, the minimum measurement error for potential head loss was 0.1

to 0.2 cm. The errors in estimating velocity head were composed of the individual velocity measurement errors (about 10% of the mean at low velocity and 3% at high velocity), the errors in determining average velocity over pond depth and channel width (about 10%), the propagation errors in the translation of velocity from the velocity-measuring station to the head-measuring station (using the equation of continuity for flowrate), the underestimate of the correction to kinetic head deriving from highly non-uniform velocity distributions (especially near bends, sumps, and around the paddle wheel), and the propagation errors in subtracting to get velocity head differences. At low mixing speeds, errors in measuring depths, and error propagation led to about a 0.2 cm limit to precision. At high mixing speeds, errors were 20% of the mean. There were also limitations to the accuracy of the measurements. Velocity was only measured in the direction along the channel. Although the flow was predominantly in this direction, large eddies, cross flows, and vertical flows all contributed to the kinetic energy of the flow, but were not included in the measurements. At the higher mixing speeds, the effects of wave action were averaged when head and velocity were estimated. Their contribution to the energy of flow may have been greater than the average used.

Roughness Coefficients

For design purposes, open channel flow is characterized by the Manning equation and the Manning's roughness coefficient. Although this is most useful for conditions of uniform flow, it is still a guide in the estimation of head loss of large channel reaches. We used the data from the first channel (outgoing flow from the paddle wheel) and second channel (return flow) to derive estimates of Manning's n. In the return channels, the average grade was at least in the direction of flow. However, due to the depth variations, flow was probably never uniform. The roughness coefficients calculated are given in Table 3. Both the 0.010 value for the lined pond and the 0.0173 for the unlined pond are within the range expected.

Mixing Power

From the measurements of total head loss around the ponds and the flow rates, the power dissipated by the fluid motion was calculated. This is called the hydraulic power. The power delivered to the paddle wheel shaft (the net shaft power) was estimated for the North (lined) pond. This was done, at each paddle wheel rotation speed, by taking the difference between the wattage input to the mixing drive system (motor, speed reducers, shaft) with (load power) and without (no-load power) water in the pond. The hydraulic power divided by the net shaft power is an estimate of the paddle wheel efficiency. The mixer efficiency decreased with increasing mixing speed, from 76% to 40%. At the two highest mixing speeds, the kinetic energy of the water entering the paddle wheel lowered the total hydraulic head loss 30 and 50 percent, respectively. However,

little of this velocity head could be conserved by the mixer, resulting in the lower efficiency. Table 4 summarizes the power measurements taken.

Table 2. Total Head Loss (cm) for Each Section of 0.1-hectare Raceways.

	Paddle Wheel Rotation Speed, rpm					
	2.7	3.6	4.4	5.3	6.1	7.8
NORTH POND						
First Channel	0.33	0.53	0.60	0.66	0.61	0.64
	(20)	(19)	(15)	(13)	(9)	(10)
Second Channel	0.19	0.43	0.68	0.97	1.20	1.53
	(11)	(15)	(17)	(19)	(19)	(24)
First Bend	0.40	0.57	0.82	0.92	1.17	1.17
	(24)	(20)	(21)	(18)	(18)	(19)
Second Bend	0.34	0.74	1.15	1.59	2.32	1.65
	(20)	(26)	(29)	(31)	(36)	(26)
Carbonation Sump	0.41	0.58	0.67	0.97	1.09	1.30
	(25)	(20)	(17)	(19)	(17)	(21)
Total	1.66	2.85	3.91	5.12	6.39	6.30
SOUTH POND						
First Channel	0.40	0.60	0.82	0.99	0.98	
	(14)	(13)	(13)	(12)	(10)	
Second Channel	0.78	1.24	1.97	2.30	2.74	
	(27)	(26)	(30)	(27)	(27)	
First Bend	0.80	1.42	1.69	2.12	2.23	
	(27)	(30)	(26)	(25)	(22)	
Second Bend	0.49	0.99	1.51	2.53	3.53	
	(17)	(21)	(23)	(30)	(35)	
Carbonation Sump	0.47	0.47	0.50	0.59	0.68	
	(16)	(10)	(8)	(7)	(7)	
Total	2.94	4.69	6.51	8.54	10.17	

Numbers in ( ) are percentage of total head loss.

Table 3. Manning's Roughness Coefficient for 0.1-Hectare Raceways.

	Paddle Wheel Rotation Speed, rpm				
	2.7	3.6	4.4	5.3	6.1
NORTH POND (lined)					
Flow Rate, m^3/s	0.157	0.209	0.260	0.289	0.310
1st channel					
Av. Depth, cm	13.8	14.1	14.2	14.5	14.7
Head Loss, cm	0.33	0.53	0.60	0.66	
Manning's n	0.0120	0.0118	0.0090	0.0110	
2nd channel					
Av. Depth, cm	13.0	12.8	12.5	12.3	12.2
Head Loss, cm	0.19	0.43	0.66	0.97	1.20
Manning's n	0.0083	0.0090	0.0088	0.0092	0.0093
SOUTH POND (unlined)					
Flow Rate, m^3/s	0.146	0.158	0.198	0.205	
1st channel					
Av. Depth, cm	13.9	14.2	14.7	15.1	
Head Loss, cm	0.40	0.60	0.82	0.99	
Manning's n	0.0143	0.0168	0.0165	0.0183	
2nd channel					
Av. Depth, cm	12.5	12.3	12.0	11.7	11.5
Head Loss, cm	0.78	1.24	1.97	2.31	2.74
Manning's n	0.0167	0.0189	0.0182	0.0184	0.0187

Table 4. Mixing Power Requirements (watts) for 0.1-Hectare Raceways.

	Paddle Wheel Rotation Speed, rpm					
	2.7	3.6	4.4	5.3	6.1	7.8
NORTH POND (lined)						
Flow Rate, m^3/s	0.157	0.209	0.260	0.289	0.310	0.371
Head Loss, cm	1.66	2.85	3.91	5.12	6.39	6.30
Net Shaft Power	14	77	154	226	334	580
Hydraulic Power	26	58	100	145	194	229
Paddle Wheel Eff, %	183	76	65	64	58	40
SOUTH POND (unlined)						
Flow Rate, m^3/s	0.146	0.158	0.198	0.205	0.213	
Head Loss, cm	2.79	4.69	6.51	8.54	10.17	
Hydraulic Power	40	73	126	172	212	

A paddle wheel efficiency greater than 100% was calculated for the lowest mixing speed. The errors associated with the measured power were large at low mixing speeds. Since the system was designed to produce velocities ranging from 15 to 40 cm s^{-1}, large motors and speed reduction units were used. These were not very efficient at low mixing speed. A large amount of power was dissipated even under no-load conditions. At all mixing speeds both the load and no-load power were large numbers (500-1500 watt), but at low mixing speeds, the difference was small (less than 20 watts). The propagated error of subtraction was 15 watts, so the errors in estimates of net shaft power were large. Another error, stemming from the influence of wind on the power measurements (especially no-load measurements), is difficult to estimate. The standard deviation of replicate watt-meter readings taken one right after the other was about 0.5%. However, the standard deviation of sets of replicates, taken at various temporal separations was greater, about 3%. In addition to these precision errors, there was an accuracy error in the method. The no-load wattage is an estimate of the power dissipation in the drive train under load conditions, as opposed to the power delivered to the paddle wheel shaft. This power is not independent of load, so that use of the no-load measurement probably resulted in an underestimate of the drive train power dissipation and thus an underestimate of the paddle wheel efficiency.

OPERATION OF THE SMALL-SCALE SYSTEM

The small-scale system consists of six 2.74-m^2 fiberglass tanks operated at 15-cm depth, mixed by paddle wheel, and pH controlled by injection of 100% CO_2 on demand. Two 1000 W heaters were available per pond to maintain a given minimum temperature for certain experiments performed during the fall and winter.

Cultures were diluted continuously 8-14 hr per day (depending on temperature and insolation) from May through October. Effluents were sampled every hour and composited. Daily productivity was calculated as grams ash-free dry mass harvested (mass per liter of the composited samples, times liters harvested) divided by 2.74 m^2 (pond area). During periods of potential freezing temperatures, cultures were operated as sequential batches.

Heat of combustion was estimated at 6.0 kcal/g AFDM. Photosynthetic efficiency was calculated based on photosynthetically active radiation (using 45% of the cumulated outdoor energy input) and the estimated heat of combustion to convert from mass units to thermal units.

Overall Results

Fifteen organisms were inoculated into outdoor cultures. Two species invaded: the Amphora sp. that was present during

the previous year and a Cyclotella sp. which was isolated from a bloom in the 0.1-hectare raceways. Six of these could be cultured: Chaetoceros muelleri CHAET9, Chaetoceros muelleri CHAET63, the indigenous Amphora, the indigenous Cyclotella, Tetraselmis suecica TETRA1 and Monoraphidium minutum MONOR2. The ten that could not be cultured were a Chlorella sp. 12P, Nitzschia sp. NIT2, Chaetoceros muelleri CHAET61, Green 7.1, Green 7.2, Nannochloropsis sp. NANNP2, Nannochloris sp. NANNO2, Cyclotella cryptica CYCLO1, Thallasiosira fluviatilis, and Thallasiosira sp. THAL1.

The overall productivity results for the year are shown in Table 5. Two strains were found to be stable during the cold season: M. minutum and T. suecica. Five species performed well during the warm season: T. suecica, Cyclotella sp. RTF (Roswell Test Facility), Amphora sp. RTF, Chaetoceros muelleri CHAET9, and Chaetoceros muelleri CHAET63. All of the results shown in this table are from unheated cultures. The weather was quite similar during 1987 and 1988. So was the species succession.

Productivities were very low during the coldest months (December, January, February). Due to severe conditions of ice or slush in the small ponds every day, there was very little opportunity to dilute the cultures. Of course, growth was very slow anyway. The productivities averaged 25 to 30 g AFDM m^{-2} d^{-1} during the warm months of May, June, July, and August. Due to the effort to screen many species, the most productive organisms were not cultivated during most of July and August. Yields of about 20 g AFDM m^{-2} d^{-1} were obtained from several strains during the transition months of September and October. These months have 10 to 20% less insolation than the months of April and March, but are much warmer. It is the months of March and April for which productivities may be improved. If 15-20 g AFDM m^{-2} d^{-1} were attained during these two months as well, the yearly average would be close to 20 g AFDM m^{-2} d^{-1} rather than the 16 g AFDM m^{-2} d^{-1} achieved this year. The greater thermal insulation of the large-scale raceways compared to the 3-m^2 raceways will help keep pond temperatures and hence productivities a little higher during the transition months.

The results from all the species are shown in Table 6. As we have seen in previous years, the diatoms were more productive than the green algae.

Effects of Reduced pCO_2.

Amphora sp. RTF, T. suecica TETRA1, and C. muelleri CHAET9 were grown at several pHs to test the effect of reducing the concentration of CO_2 in the bulk liquid. Although the pH had to be raised to accomplish this, the assumption was that at the values tested higher pH would not affect productivity. Three pH values were used. At pH 7.2, CO_2 concentration was about 285 uM; at pH 7.8, it was 75 uM; and at pH 8.3 it was about 20 uM. Thus outgassing losses of CO_2 could be lowered greatly by operating at the higher pH.

The results of cultivation at different pH values are shown in Table 7. Productivity was significantly lower in a statistical sense (t test for difference of correlated means, data not shown). However, in a practical sense the 10-15% lower productivity at higher pH is not important. It remains to be seen whether the difference remains small when such an experiment is performed at productivities above 30 g AFDM m^{-2} d^{-1}.

Table 5. Monthly Results from Roswell Algal Cultivation.

MONTH	INSOL. $cal/cm^2/d$	AMBIENT TEMP. max(C)	min(C)	PROD. g AFDM/m^2/d	EFFIC. %PAR	SPECIES
JAN	235 (104)	9.6 (7.2)	-8.1 (2.7)	1 (2)	0.4	MONOR2
FEB	353 (102)	15.4 (7.1)	-4.8 (4.6)	2 (4)	0.8	MONOR2
MAR	494 (77)	20.9 (5.9)	-2.0 (4.7)	8 (7)	2.2	MONOR2
APR	537 (138)	25.5 (4.7)	3.4 (3.2)	12 (10)	3.0	MONOR2
MAY	606 (104)	29.4 (5.1)	9.8 (3.6)	29 (6)	6.4	MONOR2 to AMPHO
JUN	616 (106)	35.9 (2.6)	15.2 (2.8)	33 (4)	6.7	AMPHO
JUL	582 (103)	35.4 (3.2)	17.5 (2.2)	21 (3)	4.8	TETRA1 or CHAET9
AUG*	484 (139)	34.5 (5.0)	18.0 (2.6)	26 (3)	7.7	AMPHO
SEP	473 (94)	30.2 (3.8)	9.8 (3.9)	22 (7)	6.2	AMPHO
OCT	388 (62)	25.7 (3.6)	5.0 (2.3)	20 (2)	7.0	CYCLO or AMPHO
NOV*	326 (46)	18.7 (6.8)	-3.6 (6.7)	14 (2)	5.4	AMPHO

(SD)
* Half month

The results of cultivation at different pH values are shown in Table 7. Productivity was significantly lower in a statistical sense (t test for difference of correlated means, data not shown). However, in a practical sense the 10-15% lower productivity at higher pH is not important. It remains to be seen whether the difference remains small when such an experiment is performed at productivities above 30 g AFDM m^{-2} d_1.

Table 5. Monthly Results from Roswell Algal Cultivation.

MONTH	INSOL. $cal/cm^2/d$	AMBIENT TEMP. max(C)	min(C)	PROD. g $AFDM/m^2/d$	EFFIC. %PAR	SPECIES
JAN	235 (104)	9.6 (7.2)	-8.1 (2.7)	1 (2)	0.4	MONOR2
FEB	353 (102)	15.4 (7.1)	-4.8 (4.6)	2 (4)	0.8	MONOR2
MAR	494 (77)	20.9 (5.9)	-2.0 (4.7)	8 (7)	2.2	MONOR2
APR	537 (138)	25.5 (4.7)	3.4 (3.2)	12 (10)	3.0	MONOR2
MAY	606 (104)	29.4 (5.1)	9.8 (3.6)	29 (6)	6.4	MONOR2 to AMPHO
JUN	616 (106)	35.9 (2.6)	15.2 (2.8)	33 (4)	6.7	AMPHO
JUL	582 (103)	35.4 (3.2)	17.5 (2.2)	21 (3)	4.8	TETRA1 or CHAET9
AUG*	484 (139)	34.5 (5.0)	18.0 (2.6)	26 (3)	7.7	AMPHO
SEP	473 (94)	30.2 (3.8)	9.8 (3.9)	22 (7)	6.2	AMPHO
OCT	388 (62)	25.7 (3.6)	5.0 (2.3)	20 (2)	7.0	CYCLO or AMPHO
NOV*	326 (46)	18.7 (6.8)	-3.6 (6.7)	14 (2)	5.4	AMPHO

(SD)
* Half month

Table 6. Algal Productivity in 3-m^2 Ponds--1988

SPECIES	DATE	INSOL. cal cm^{-2} d^{-1}	PRODUCTIVITY g AFDM m^{-2} d^{-1}	EFFIC %PAR
RTF CYCLO	9/27-11/8	389	20.3	7.0
RTF AMPHO	5/17-7/3	608	30.9	6.8
	8/16-11/16	420	20.7	6.6
CHAET9	6/26-8/13	552	20.6	5.0
CHAET63	9/15-10/6	476	18.5	5.2
TETRA1	5/14-11/16	506	18.4	4.8
MONOR2	1/1-5/14	427	7.9	2.5
	9/15-10/23	435	15.7	4.8

Table 7. Effect of pCO_2 on Productivity (g AFDM m^{-2} d^{-1}).

SPECIES	pCO_2	PRODUCTIVITY	n
RTF AMPHO	0.0090	24.0 (2.0)	5
	0.0024	22.6 (2.6)	
CHAET63	0.0090	19.0 (1.7)	14
	0.0006	16.8 (1.7)	
TETRA1	0.0090	21.3 (1.6)	15
	0.0024	18.1 (1.3)	
TETRA1	0.0090	19.5 (3.4)	18
	0.0006	16.5 (1.0)	

pCO_2 of 0.0090, 0.0024, and 0.0006 atm correspond to pH 7.2, 7.8 and 8.3 respectively. 0.01 atm = 320 uM.
(SD)

Growth under Nitrogen or Silicon Deficiency

A number of experiments were performed to monitor production of biomass and lipid under nutrient deficient conditions. Nutrient sufficient biomass was taken from continuously diluted cultures, diluted with N-free or Si-free growth medium, and allowed to grow in batch. Sampling was daily. The cell density (and thus time) at which the cultures reduced intracelluar nutrient below levels typical of nutrient sufficiency, was estimated from the initial concentration of nutrient. Nitrogen sufficiency was taken to end when biomass N content dropped below 8%; silicon sufficiency at 20%. The point at which the experiment was terminated was when calculated intracelluar nutrient concentration reached half its sufficiency value. Lipid samples were saved for subsequent analysis at SERI.

The effect of nutrient deficiency on biomass productivity is shown in Table 8. Without the nutrient analyses it is difficult to determine where the optimal stopping point of the induction shoud be, as well as to what extent the lipid productivity increased or decreased. In general, the biomass productivities of the induction batches were less than concurrently operated nutrient sufficient continuous cultures even before the nutrient became limiting. An experiment with T. suecica was the only exception. The reasons may be that the cultures were both too dilute for optimal production at the beginning of the batches, and then not adapted to the "shade" conditions as the batches got denser (Weissman and Goebel, 1988). Setting the initial conditions of an induction batch will prove to be an important controlling factor. For the most part, biomass productivity dropped after the time at which nutrient sufficient growth turned to nutrient limiting growth.

OPERATION OF THE LARGE-SCALE SYSTEM

Operation of the two 0.1 hectare raceways began in August 1988 with the inoculation of T. suecica TETRA1. The mixing speed was set at 30 cm s^{-1} to try to alleviate in-pond sedimentation of biomass. The T. suecica grew from the middle of August to the middle of September, averaging 10-11 g AFDM m^{-2} d^{-1}. Even with the high mixing speed, the poor mixing in the large ponds at this time may have been responsible for both the low productivity (relative to the smaller ponds) and the culture instability. M. minutum was subsequently inoculated, and has remained throughout the winter of 1988-89. Its productivity was 12 g AFDM m^{-2} d^{-1} (in the lined pond) during October versus 15 g AFDM m^{-2} d^{-1} in the 3-m^2 ponds. Photosynthetic efficiency was 3.8% of PAR. During operation of the large-scale system, the total input of CO_2 was monitored. Average efficiency of carbon utilization (in the lined pond) was 60-70% during September, October, and November. The major

losses of CO_2 were due to outgassing and during injection in the carbonation sumps. Outgassing was calculated to account for 22% of the total loss at pH 7.5 and 15% at pH 7.8 (the mass transfer coefficient was 1.7×10^{-5} m s^{-1}). Thus the injection efficiency was estimated to be almost 80% in both cases.

Table 8. Productivities of Nutrient Sufficient and Deficient Algal Cultures (in g AFDM m^{-2} d^{-1}).

SPECIES	N or Si SUFF. CONT. CULTURES	INDUCTION BATCH BEFORE DEPLETION	AFTER DEPLETION	OVERALL
CHAET63				
Nitrogen	18	9.8 (4)*	13.4 (5-7)**	11.4
Nitrogen	20	14.2 (3)	19.2 (4-6)	12.2
CHAET9				
Nitrogen	22	15.4 (2)	14.4 (3-4)	14.9
Nitrogen	22	17.6 (2)	12.0 (3-4)	14.8
MONOR2				
Nitrogen	16	6.9 (5)	8.6 (6)	7.2
Nitrogen	13	7.9 (5)	2.1 (6)	6.3
RTF CYCLO				
Nitrogen	22	16.4 (2)	16.1 (3-5)	16.2
Nitrogen	20	12.2 (3)	12.1 (3-5)	12.1
Silicon	20	16.4 (3)	13.8 (4-7)	14.1
TETRA1				
Nitrogen	26	19.1 (5)	13.6 (6-7)	17.5
Nitrogen	24	22.5 (3)	13.7 (4-6)	18.1
Nitrogen	16	20.5 (3)	9.8 (4-10)	13.8
RTF AMPHO				
Nitrogen	40	21.4 (2)	13.1 (3-7)	15.5
Nitrogen	37	21.2 (2)	12.1 (3-4)	16.7
Nitrogen	27	20.3 (3)	8.0 (4)	17.2
Silicon	38	15.5 (1)	8.2 (2)	11.8
Silicon	35	19.2 (2)	5.1 (3-4)	12.2

Biomass is nutrient sufficient until depletion of nutrient from medium.
* (Number of days of nutrient sufficient growth)
** (Day of change to nutrient deficient growth - last day of exp't.)

CONCLUSIONS

The use of the equations for uniform flow in open channels in the design of large raceways (Weissman, Goebel, and Benemann 1988) is justified and practical when adjustments are made for head losses not associated with channel roughness. For the 0.1-hectare raceways, these other losses were just as significant as those due to the channels. Even for larger raceways, the design of the slope and the mixing system must be modified to accommodate increased losses due to bends and sumps. The overall mixing system efficiencies were low, making it evident that before a larger pond system is built, the design mixing velocity must be specified rather closely. Otherwise, power consumed for mixing will be much greater than actually needed to satisfy the hydraulic power comsumption. In terms of operating large raceways, the data indicate that hydraulics and maintenance will be improved, and operation will be more economical, if the design depth is larger than the operating depth of 14 cm used here. During most of 1989, the operating depth will be increased to 18-20 cm. If lower depths are desired, then grading costs will certainly increase greatly for large pond construction.

In order to increase yearly average biomass production, yields during the transition months of March and April must be improved. During these months insolation is very high, but temperatures are still near freezing at night. Assiduous monitoring will be required to push productivity without causing instability of the cultures. More cold-tolerant, high-productivity strains of algae are needed.

Acknowledgements

This work was supported by subcontract number Xk-7-06113-1 from the Solar Energy Research Institute and from funds contributed by the New Mexico Research and Development Institute.

REFERENCES

Weissman, J.C., Goebel, R.P., and Tillett, D.M. 1988. Design and Operation of an Outdoor Microalgae Test Facility, Final Subcontract Report, Solar Energy Research Institute, XK-7-06113-1, 1-112.

Weissman, J.C. and R.P. Goebel 1988. "Production of Liquid Fuels and Chemicals by Microalgae", Final Report, Solar Energy Research Institute, #XK-3-030135-1, Golden, CO.

Weissman, J.C., Goebel, R.P., and Benemann, J.R. 1988, "Photobioreactor Design: Mixing, Carbon Utilization, and Oxygen Accumulation," Biotechnol Bioeng, 31: 336-344.

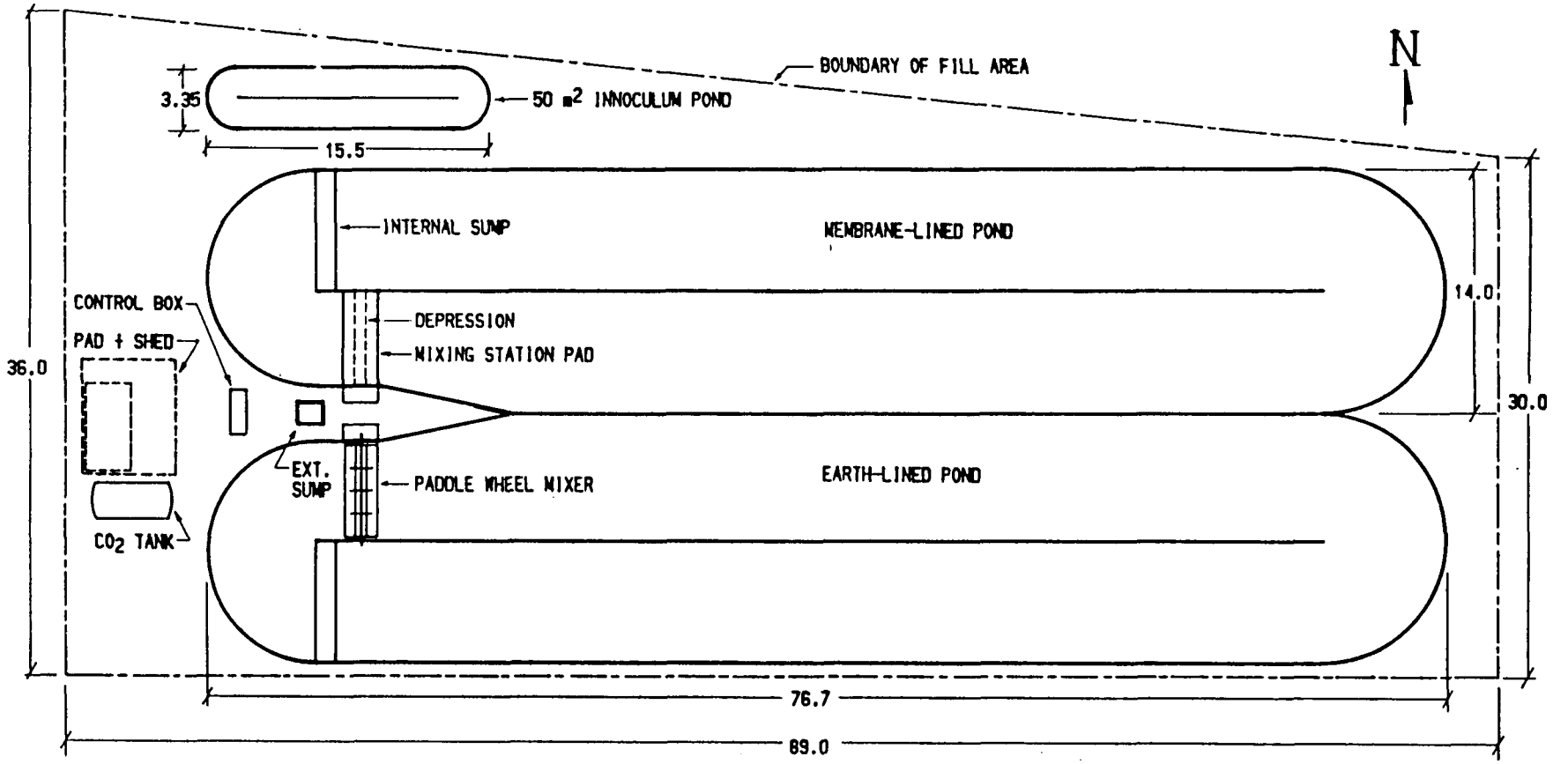

Figure 1. Large-scale system pond layout.

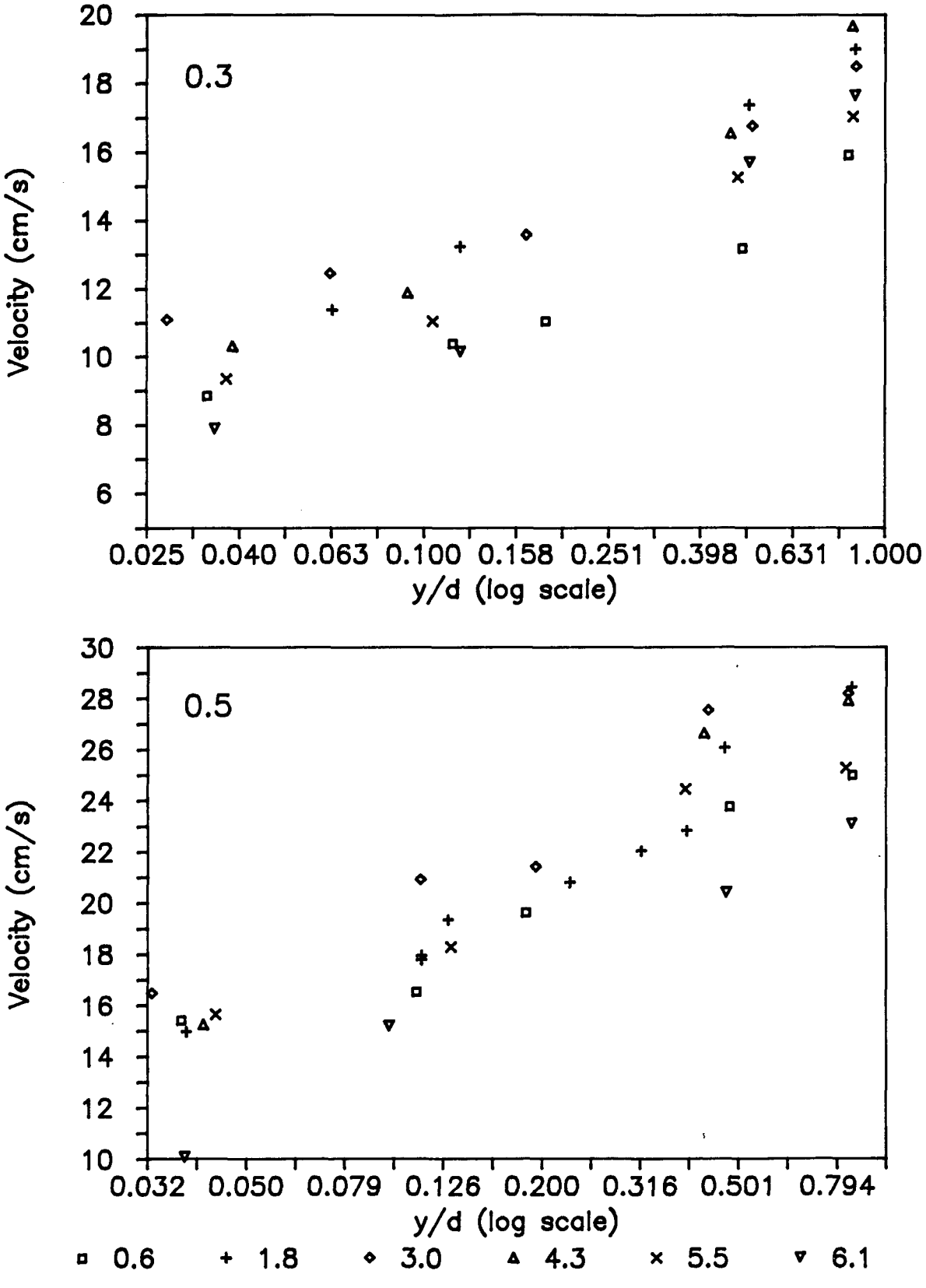

Figure 2. Typical velocity-depth profile in 0.1-hectare raceway. Unlined pond at paddle wheel rotation settings of 0.3 (2.7 rpm) and 0.5 (4.4 rpm). Symbols indicate distance of measuring station from center wall.

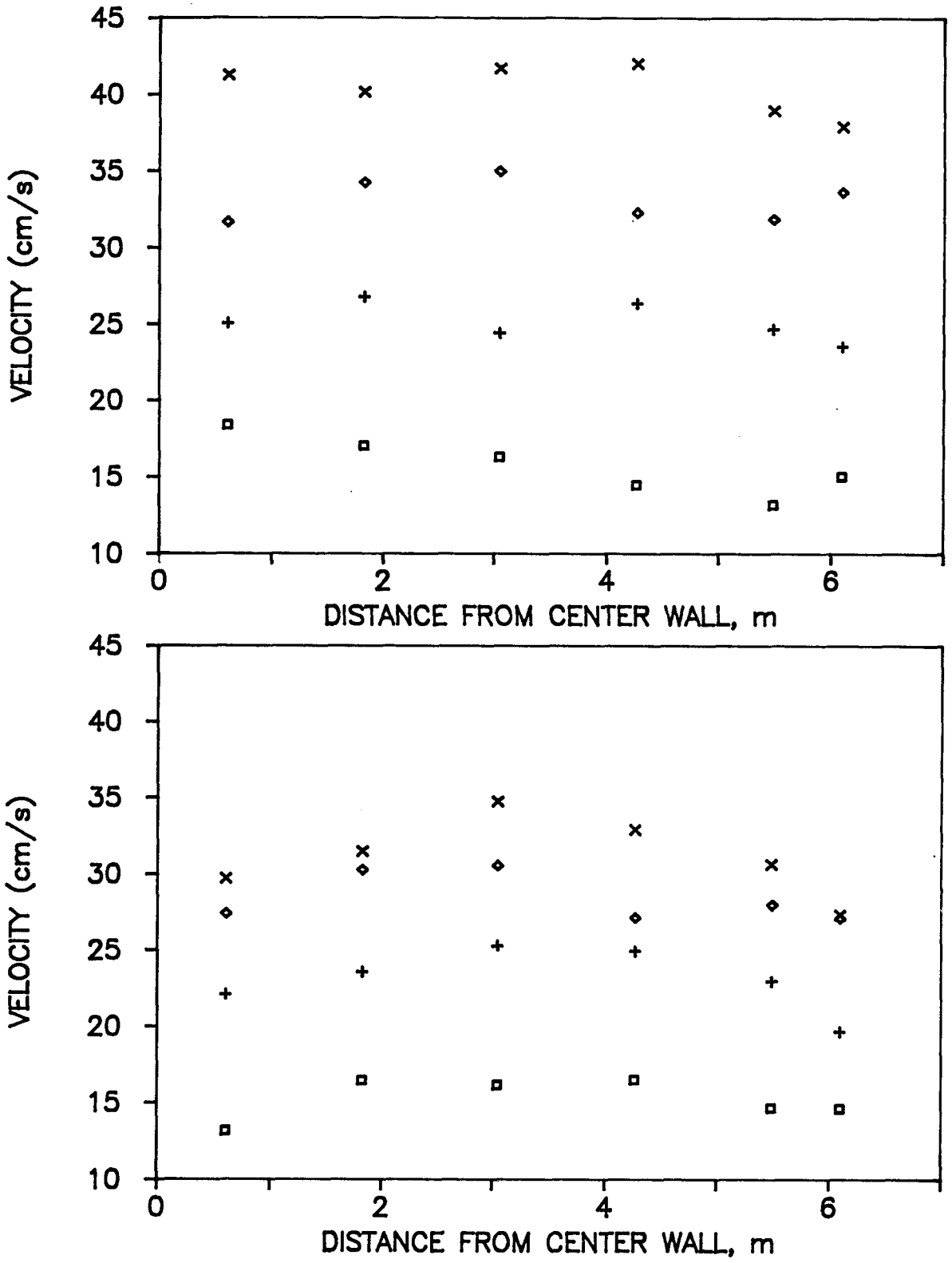

Figure 3. Profiles of depth-averaged velocity across the return channel (1.4 m upstream of sump) in each 0.1 hectare raceway. Symbols indicate paddle wheel rpm: boxes, 2.7; +, 4.4; diamonds, 6.1; and x, 7.8.

Culture Collection Status

Lewis M. Brown

Biotechnology Research Branch
Solar Fuels Research Divison
Solar Energy Research Institute
1617 Cole Boulevard
Golden CO 80401

Abstract

A total of 2367 strains representing the significant strains collected by the program have been screened. This brings the collection and screening phase of the Aquatics Species Subprogram to a close. Further efforts will be directed to the application of genetic engineering techniques to improve lipid yield in rapidly growing strains. This approach is a proven strategy for yield improvement which is widely used in industrial microbiology.

Introduction

The efforts to develop a slate of highly efficient microalgae for outdoor mass culture and fuel production have yielded much information since they were initiated in 1983 (Johansen et al. 1987). This report summarizes the results of this effort which is now complete.

Results and Discussion

A total 3164 strains of microalgae were collected in the Aquatic Species Program by a variety of investigators both from the group at SERI as well as a large group of subcontractors (Table 1). A total 2367 strains were screened for the growth rate and lipid content over the past seven years by a variety of investigators. This exceeds the milestone requirement of screening of 1500 strains. There remain a total 332 which have not been examined in any way, the bulk of these in the clone collection (253) strains which is dominated by a single genus (Chaetoceros - 128 strains). There is no indication that the remaining 332 strains are a program priority for additional screening work as most of the data thus far collected indicate that these clones subcultured from the parent strains which have been studied extensively, are no different from the parents. Thus, the collection and screening efforts of the Aquatic Species Program are now complete. Another significant advance relating to this work is the development of a computer database and associated printout of all data on strains collected in the program. This database is still being edited and updated as gaps become apparent. However, it has already yielded interesting information, which is presented here. Some of this information was only available previously in handwritten notes or subcontractor final reports which are not generally available.

Table 1 demonstrates the collaborative nature of this work between SERI researchers and a variety of subcontractors. A total of 1431 strains still exist in the program. Most of those no longer cultured were discarded long ago by subcontractors early in the program who discarded poor performers, and sent their best strains to SERI. These best strains are still in the SERI collection. Also, one expects some culture die-off in a collection the size of this one, particularly when one is dealing with newly-isolated strains.

One of the advantages of developing this database is that one can start to do detailed analysis of research results and use these as a guide to future program priorities. The most obvious result from all of these work is the large proportion of diatoms in the collection, comprising 65 % of the total (Table 2). However, as a proportion of the most rapidly growing strains green and blue-green algae are occupy a disproportionately large share of the top ranks in growth performance (Table 2). This is also true to some extent for lipid content as well where green algae are a minor component of the total collection, but comprise 44 % of the top lipid producers (Table 3). The predominance of diatoms it the screening program is not altogether surprising, as it is well known diatoms can be aggressive competitors in aquatic environments when silicon is not limiting in the spring (Wetzel 1983). The green algae and blue-green algae are also important. This is as reflected in the ecological data. It is also well known that green algae are effective competitors after silica runs out, but before nitrogen is depleted in the summer when the nitrogen-fixing blue greens predominate (Wetzel 1983). In a sense the screening program is biased towards diatoms in the provision of copious silica during the initial enrichment culture ("screening") protocol. If we had not provided silica, green algae and blue green algae would comprise most of the collection. If we had not provided silica and nitrogen, blue green algae would have dominated alone.

As is stands presently, silica adds to the cost and difficulty of outdoor culture, as it is both expensive and poorly soluble. However, some of the diatoms have been among the most rapidly growing strains. Certainly, good performers in outdoor culture have come out of the screening program, such as MONOR1 and MONOR2 (green algae) and CYCLO1 (diatom). The collection and screening program from this view has been a success. One may quibble about whether certain details of the protocol should have been change earlier or a nitrogen and or silicon limited screen should have been run as well. Nevertheless, we are left with a good cross-section of strains with the properties useful to the program. These being high productivity, potential for high lipid production, tolerance to high salinity, high and low temperatures and high light intensities.

One is struck in examining the list that certain genera seem to predominate. The diatom genus Chaetoceros comprises fully 29 % of the entire collection. However, as with other

diatoms, it is not particularly prominent when considered on the basis of growth rate (Table 4). It is also surprising that among the top 107 strains at Arizona State University, not one strain of Chaetoceros was found. Perhaps some of the investigators in the program tended to go to sites where Chaetoceros was found, used culture methods which favored this genus, or were particularly interested in this genu for non-programmatic reasons. The fact that this genus represents 54 % of the clone collection (136 strains) (Table 5) argues for fact that some of these strains might be good candidates for culling from the collection in favor of more taxonomic and gene pool diversity among various strains which might be in the hands of some former subcontractors.

The gene pool that we currently have is solid. No further collection and screening is necessary. Results from other areas of industrial microbiology have proven this point. Attempts to improve penicillin production by the Penicillium fungus are an excellent example. A total of 60,000 strains of Penicillium fungus were collected and screened by Stanford University, with no improvement in yield over already existing strains (Elander and Chang 1979). Only genetic improvement resulted in improved product yield.

The present collection is sufficient to provide a gene pool for future improvements.

References

Elander, R. P. and L. T. Chang. 1979. Microbial Culture Selection. In Microbial Technology, Vol. II. Edited by H. J. Peppler and D. Perlman. Academic Press, New York. pp. 243-302.

Johansen, J. 1987. Collection, Screeening and Characterization of Lipid Producing Microalgae: Progress During Fiscal Year 1987. FY 1987 Aquatic Species Program. SERI/SP-231-2306 pp. 27-42.

Wetzel, R. G. 1983. Limnology. W. B. Saunders Co. Philadelphia. 767 pp.

Table 1. Screening data for microalgal strains of the Aquatic Species Program.

Current Location	Collector	Collected	Screened	Unscreened	Extant
SERI					
	SERI	498	100	136	236
	U. Britton	1	0	1	1
	D. Chapman	1	1	0	1
	K. Cooksey	18	18	0	0
	R. Fall	14	0	14	14
	Harbor Branch Foundation	110	110	0	40
	E. Laws	1	1	0	1
	J. Lewin	7	0	7	7
	R. Lewin	129	56	73	86
	C. Pienaar	3	0	0	3
	S. Rushforth	110	15	95	110
	J. Ryther	1	1	0	1
	Scripps Institute	2	0	2	2
	M. Sommerfeld	6	6	0	6
	M. Tadros	230	230	0	15
	W. Thomas	304	304	0	45
	D. Thompson	1	0	1	1
	O. Umebayashi	1	0	1	1
	J. Weissman	1	0	1	1
	R. York	125	125	0	52
	unattributed	8	0	8	8
Site Totals		1564	967	332	631

Arizona State University				
M. Sommerfeld	1600	1400	0	800*
Site Totals	1600	1400	0	800*
Program Totals	3164	2367	332	1431

*Approximate total - awaiting exact total from subcontractor.

Table 2. Class distribution data (percentage of for microalgal strains) still existing in the Aquatic Species Program. Also summarized are rank data for growth rates on this basis of class for the top 50 and top 100 growth rates. The data demonstrate that while the initial enrichment protocols favored diatoms, the green algae and blue green algae did better than one would predict based solely on their proportion of the total collection. This table summarizes data for 738 out of 1431 existing strains.

Class	Common name	Percentage of Collection		
		All Strains	Top 50	Top 100
Bacillariophyceae	Diatoms	65	40	34
Chlorophyceae	Greens	13	22	28
Chrysophyceae	Goldens	2	1	3
Cryptophyceae	Cryptomonads	0.4	0	0
Cyanophyceae	Blue-greens	2	12	9
Eustigmatophyceae	Eustigs	4	0	0
Prasinophyceae	Scaly-green monads	0.6	2	1
Prymnesiophyceae	Haptophytes	2	6	6
unattributed	-	11	16	19

Table 3. Rank data for lipid contents on the basis of class for the top 25 lipid contents. The data demonstrate that while the initial enrichment protocols favored diatoms, the green algae did better than one would predict based solely on their proportion of the total collection.

Class	Common name	Percentage of Collection	
		All Strains	Top 25
Bacillariophyceae	Diatoms	65	48
Chlorophyceae	Greens	13	44
Chrysophyceae	Goldens	2	0
Cryptophyceae	Cryptomonads	0.4	0
Cyanophyceae	Blue-greens	2	0
Eustigmatophyceae	Eustigs	4	8
Prasinophyceae	Scaly-green monads	0.6	0
Prymnesiophyceae	Haptophytes	2	0
unattributed	-	11	0

Table 4. Growth data for Chaetoceros, a major diatom genus as a function of the total collection. The data demonstrate that while the genus Chaetoceros is represented in the collection by some rapidly growing strains, it does not dominate the top 50 or 100 strains on the basis of growth rate.

Class	Percentage of Collection		
	All Strains	Top 50	Top 100
Chaetoceros	29	14	8
Other diatoms	36	26	26
Total: Chaetoceros and other diatoms	65	40	34

Table 5. Class distribution data for clones of microalgal strains still existing in the Aquatic Species Program. Summarizes data for the 253 clones in the collection.

Class	Common name	
Bacillariophyceae	Diatoms	237
Chlorophyceae	Greens	10
Prymnesiophyceae	Haptophytes	4
unattributed	-	2

CHARACTERIZATION OF GROWTH AND LIPID YIELD IN MICROALGAE FROM THE SOUTHWEST USING HIGH SALINITY MEDIA

S.B. Ellingson, P.L. Tyler and M.R. Sommerfeld
Department of Botany
Arizona State University
Tempe, Arizona 85287-1601 U.S.A.

ABSTRACT

A screening and characterization protocol incorporating high salinity (55 mS/cm) and temperature (30°C) developed by SERI in collaboration with investigators from Arizona State University was employed to rapidly reduce the number of microalgal strains collected in the Aquatic Species Program to those with the greatest potential as lipid producers.

Initial screening using a RCD (Rotary Culture Device) and Nile Red staining originally isolated procedure successfully reduced the approximately 1400 strains in the culture collection to approximately 800. Of the 800 strains selectively screened, only 102 survived the protocol. Forty strains were capable of growth in both types of media. The average growth rate in SERI Type I Medium was significantly greater than in Type II Medium, averaging 1.04 doublings/day compared to 0.83 doublings/day, respectively.

Intracellular lipid accumulations were evaluated fluorometrically using the dye Nile Red during logarithmic growth. Lipid yield for the microalgae were similar in the two media. After culturing the microalgae for two additional days in nitrogen deficient media, lipid accumulation increased in about 80% of the strains. In these strains the mean lipid yield in SERI Type II Medium was significantly greater (nearly two-fold) than observed in Type I Medium. When yield was evaluated by algal division, each division also showed greater lipid accumulation in Type II Medium.

Lists of the 10 best strains based on growth characteristics, lipid yield and a combination of these factors were prepared. When the strains were compared, the microalgae that accumulated the greatest quantity of lipids were not the most rapidly growing, but those typically growing at between one and two doublings/day. However, a comparison of total lipid yield from logarithmically-growing cultures with yield from stressed cultures suggests that the ability to accumulate substantial lipid during relatively rapid growth may be as desirable as accumulating much larger lipid reserves under stress. The screening protocol used enabled us to evaluate both aspects.

CHARACTERIZATION OF GROWTH AND LIPID YIELD IN MICROALGAE FROM THE SOUTHWEST USING HIGH SALINITY MEDIA

INTRODUCTION

Since 1983 the Aquatic Species Program of SERI has coordinated and sponsored efforts to develop a collection of lipid-producing microalgae that could serve as a renewable source of liquid fuel. Microalgae were initially collected from diverse warm saline habitats, including thermal springs, ephemeral pools, ponds, lakes and tropical and subtropical coastal waters (Barclay 1984; Barclay et al. 1985, 87; Lewin 1985; Lewin et al. 1987; Ryther et al. 1987; Sommerfeld & Ellingson 1987, Tadros 1985, 1987; Thomas 1983, 1984, 1985; York 1987). In 1986, collection efforts were expanded to also include some cold-water saline habitats (Johansen et al. 1987). From these activities, it has been estimated that approximately 3,000 strains of microalgae were in various culture collections, with most still awaiting characterization (Johansen et al. 1987). Characterization of large numbers of strains for growth and neutral lipid yield has turned out to be an extremely laborious task. With the large numbers of strains in culture collections, and the anticipated time required for characterization, program reviewers and SERI investigators realized the need to more rapidly characterize the strains and to standardize procedures among laboratories so that results could be readily compared.

A standardized screening and characterization protocol was developed by SERI in collaboration with investigators at Arizona State University that was designed specifically to identify the most desirable strains in the collections. Establishment of the protocol followed discussions held at Arizona State University and at SERI, and a two-week visitation to the SERI Laboratory by two investigators from Arizona State University. The purpose of this report is to (1) detail the protocol used, (2) describe the results obtained when the protocol was used in characterizing over 800 strains in the culture collection at Arizona State University, and (3) specifically identify the more salinity tolerant and best lipid-producing strains in the ASU collection.

MATERIALS and METHODS

Culture Maintenance

Strains of microalgae were maintained in filter-sterilized (0.22 um pore size) SERI Type I or II Media at 25 mS/cm enriched with modified F/1 medium (Guillard & Ryther 1962) without thiamine, biotin, or cyanocobalamin. Nitrate, phosphate, and silica were also added (Sommerfeld & Ellingson 1987). Cultures were kept in a growth chamber at 25°C with 200 uE/m^2/sec of illumination provided by "cool white" fluorescent tubes. A 12 hour light and 12 hour dark (12L:12D) photoperiod was used.

High Salinity Screening

To duplicate conditions used by researchers at SERI, cultures were enriched with PII trace elements as follows: H_3BO_3, 31.93 mg/L; Na_2EDTA, 28.01 mg/L; $MnCl_2 \cdot H_2O$, 4.01 mg/L; $FeCl_3 \cdot 6H_2O$, 1.35 mg/L; $ZnCl_2$, 280.10 ug/L; $NiSO_4 \cdot 6H_2O$, 242.75 ug/L; $CoCl2 \cdot 6H_2O$, 121.38 ug/L; $NaMoO_4 \cdot 2H_2O$, 232.40 ug/L; $CuSO_4 \cdot 5H_2O$, 9.34 ug/L. Vitamins were added to give a final concentration of 1.87 ug/L biotin; 0.93 ug/L cyanocobalamin; 0.93 ug/L thiamine. An Fe-EDTA solution was prepared with 5.46 mg/L Na_2EDTA and 5.20 mg/L $FeSO_4 \cdot 7H_2O$. The additions of PII trace elements and Fe-EDTA solution brought the final Na_2EDTA concentration to 33.41 mg/L. Cultures were enriched with macronutrients as follows: $CO(NH_2)_2$, 16.74 mg/L; KH_2PO_4, 3.72 mg/L; $Na_2SiO_3 \cdot 9H_2O$, 139.50 mg/L (Johansen et al. 1987). Cultures were placed in a growth chamber under conditions previously described.

A multiple step procedure using small volume test tubes (16 x 150 mm) was used to acclimate microalgae to higher salinity media. Cells were initially grown for two days in SERI Type I or II Media at 25 mS/cm, transferred to SERI Type I or II Media at 40 mS/cm for two days, and finally grown in SERI Type I or II Media at 55 mS/cm for two days. On the sixth day cultures were transferred to large rimmed culture tubes (25 x 150 mm) containing SERI Type I or II Media at 55 mS/cm. The large tubes were placed in a specially constructed plywood screening apparatus. This apparatus consisted of two pieces of 1/2-inch plywood (20 x 27") with 60 holes (2 1/2" on center) in each piece to receive the tubes. The plywood pieces were mounted in an environmental chamber (National Appliance Co., Portland, OR) about 18 inches above seven pairs of 40-watt cool white fluorescent tubes (Philips cat. no. F40CW). Mirrors were placed at the periphery of the lights to achieve a uniform intensity of 200 $uE/m^2/sec$. Light intensity was measured with a LiCor Model LI-185 meter and LI-192S quantum sensor.

Tubes were capped with silicone stoppers containing two holes which held microbore tubing (I.D. 0.032", O.D. 0.064"; Cole-Palmer cat. no. J 6417-31) for air input and exit. Cells were agitated and aerated with filter-sterilized (Gelman Acro 50; Amer. Sci., cat. no. F3059-1) air following humidification.

Cultures were grown at 30°C in a 12L:12D photoperiod. Temperature was monitored continuously with a Model 594 hygro-thermograph (Bendix Corp.; Baltimore, MD). Optical density was read daily. Growth rates were determined by directly inserting the large tubes into a Perkins-Elmer Model 54 spectrophotometer and recording optical density values at 750 nm (2.2 cm path length). Values were transformed to logarithm base two and growth rates calculated from the slope of a linear regression of time (total light and dark period) and optical density (Sorokin, 1973).

During the second or third day 4 mL aliquots were removed to evaluate intracellular lipid accumulation. The algal suspension was placed in a small test tube (12 x 75 mm) and 50 uL of Nile Red (Kodak cat. no. 180 7973, 10 mg/100 mL acetone) added. The mixture was agitated and allowed to react for three to five minutes before quantifying fluorescence with a modified Turner Model 110 fluorometer. The fluorometer held a blue lamp (cat. no. 110-853), lamp adapter (cat. no. 110-856) without metal screen, and a high sensitivity

door (cat.no., 110-865). A Ditric Optics, Inc. three cavity excitation filter (cat. no. 15-30240; center 480.0 ± 2.0 nm, band width 7.1 ± 1.5 nm) was used and emission monitored with a wide band interference filter (cat. no. 15-31150; center 550.0 ± 6.0 nm, band width 40.0 ± 8.0 nm). Standard lipid curves were prepared using appropriate dilutions of triolein (Sigma Chem. Co., cat. no. 405-10) assayed like the algal suspensions. The relative fluorometric units from the nutrient-replete microalgal samples were then converted to normal triolein-equivalents of lipids (NTE).

Following four days growth, cultures were poured into 15 mL sterile centrifuge tubes (Amer. Sci., cat. no. C3973-156) and pelleted at 1500 x g. The supernatant was decanted and cells washed by re-suspension in 15 mL of nitrogen-free media. The washing procedure was repeated and the washed cell suspensions reintroduced into clean large rimmed tubes and grown on the plywood screening apparatus for two days. Following this growth period in nitrogen-free media a 4 mL aliquot was removed for Nile Red staining. Relative fluorometric units were converted to stress triolein-equivalent lipids (STE). Dry weight was found by concentrating 10 mL of algal suspension onto a tared pre-combusted Whatman GF/C filter (2.5 cm diam.) and drying at 105°C to a constant weight measured with a Cahn Model 4400 electrobalance. Ash-free dry weight was obtained by igniting the filter to 500°C for one hour. The filter was cooled, wetted with distilled water, and brought to a constant weight after drying at 105°C.

Lipid Production

To determine whether logarithmically growing strains or nutrient-stressed strains produced more lipids a series of computations were made. It was assumed that stressed cells were grown in nutrient-replete media for four days and then transferred to nitrogen-deficient media for two days. The final lipid production was equal to the STE generated during the screening protocol. Alternatively, lipid production in the rapidly growing strains was calculated as the product of growth rate (doub/d) and NTE over six days. With the rapidly growing strains a continuous culture and negligible initial lag time was assumed.

Statistical Analyses

Statistical manipulations were completed using version 3.0 of SYSTAT (Evanston, IL) run on a Compag Deskpro 386 personal computer with a 8286 math coprocessor. Natural logarithmic transformations (ln) were routinely used to generate similar sample variances, limit the adverse impact of small sample sizes and results which ranged over several orders of magnitude. Slight reductions in sample size occurred during logarithmic transformation because zero values were occasionally generated for NTE and STE. Independent t-tests (ind. t-Test) were generally used to compare growth rates and lipid yields. Dependent (i.e., paired) t-tests (dep. t-Test) were used to compare increases or decreases in lipid levels with SERI Type I or Type II Media. Conservative probability values (p-values) were taken from the separate variances category, when available, since the degrees of freedom were smaller.

RESULTS AND DISCUSSION

Only a small proportion of the total strains collected and isolated from the Southwest were able to withstand the step-wise increase in salinity from 25 to 55 mS/cm. Only 102 strains withstood the shift to higher salinities. A reduction in the excessive number of stenohaline strains, which is a major SERI objective, was definitely achieved. These strains are the hardiest with respect to elevated salinity and should thrive in mass culture conditions. Tolerance to high salinity will allow mass culture facilities to operate more efficiently by reducing the additions of relatively low salinity groundwater or allowing the use of agriculturally unusable high salinity water. Growth rates and lipid yield from these tolerant strains were examined.

Growth Rates

During the first four days, when microalgae were grown on the screening apparatus at 55 mS/cm, optical density measurements were recorded daily. From these measurements growth rates were calculated. Of the 102 strains, 40 demonstrated growth in both SERI Type I and Type II Media, with 42 growing only in SERI Type I Medium, and 19 growing only in Type II Medium. Following logarithmic (ln) transformation mean growth rates for the 102 strains were compared in SERI Type I and Type II Medium. The growth rates were transformed to produce similar variances (Type I, 0.45 doub/d; Type II 0.48 doub/d). When all strains were considered, differences in untransformed variances were large (Type I, 0.63 doub/d; Type II 0.36 doub/d) necessitating the transformations. Growth in SERI Type I Medium (mean = 1.04 doub/d) was significantly faster than in SERI Type II Medium (mean = 0.83 doub/d; ind. t-Test, $p = 0.05$).

When the growth rates were compared for the three algal divisions no preference for media type was observed for the chrysophytes and cyanophytes (Table 1). The chlorophytes on the other hand grew significantly better in SERI Type II Medium. Because only about half of the strains have been identified these results should be considered tentative. Once all the strains have been taxonomically identified the comparison will be repeated.

Four strains grew at a rate of more than 3 doub/d and a strain of Oscillatoria (ASU0050) grew at 4.23 doub/d (Table 2). Eight of the ten fastest growth rates were in SERI Type I Medium. The 10 fastest growing strains were representative of three algal divisions. Eremsphaera (ASU0048), which demonstrated rapid growth (3.26 doub/d) during earlier screening activities (Sommerfeld et al. 1987), also showed rapid growth in high salinity media.

Lipid Yield

Intracellular lipid accumulation was evaluated on the second (or third) day of logarithmic growth in nitrogen-replete media. These NTE values provided an indication of lipid levels during logarithmic growth. Following four days of growth, transfer of cells to nitrogen-free media and incubation for two additional days, Nile Red fluorescence provided an estimate of STE lipid accumulation. Comparisons of lipid accumulation by microalgae in SERI Type I

Table 1. Growth rates (mean doub/d ± standard deviation) of microalgae by division in SERI Type I and Type II Media.

Division	I/55	N	II/55	N	t-test p value
Chlorophyta	1.38 ± 0.86	17	0.87 ± 0.42	13	0.04
Chrysophyta	1.22 ± 0.78	9	1.12 ± 0.46	9	0.75
Cyanophyta	1.39 ± 0.93	14	1.30 ± 0.48	12	0.78

N = number of samples; I/55 = SERI Type I Medium of 55 mS/cm; II/55 = SERI Type II Medium of 55 mS/cm; t-test = independent t-test.

Table 2. List of the ten microalgal strains and the culture medium used to obtain the greatest growth rate in the screening protocol.

Iso.	Genus	Run	Media	Doub/d
0050	Oscillatoria	3	I/55	4.23
0606	Oscillatoria	9	I/55	3.50
0048	Eremosphaera	3	I/55	3.47
3027	Synechococcus	7	II/55	3.25
0735	Oscillatoria	3	I/55	3.06
3010	Amphora	8	I/55	2.81
0972	Nannochloris	3	I/55	2.78
0327	Synechococcus	8	I/55	2.73
0973	Chlorella	3	I/55	2.66
3021	Synechococcus	5	II/55	2.51

I/55 = SERI Type I Medium of 55 mS/cm conductance; II/55 = SERI Type II Medium of 55 mS/cm conductance; Run = experiment number.

and Type II Media were made during logarithmic growth and following nitrogen deprivation (Fig. 1). The transformed NTE values in the two SERI media (Type I, 6.36 mg/L; Type II, 7.94 mg/L) were similar (ind. t-Test, $p = 0.28$). The ratio of STE:NTE was then used to divide strains into four groups demonstrating an increase or decrease in lipid levels following nitrogen deficiency in each SERI media. In SERI Type I Medium 49 strains accumulated lipids (i.e., STE:NTE > 1) while 13 showed no change or a decrease (i.e., STE:NTE < 1). A similar proportion of strains increased their intracellular

lipid levels (n = 42) whereas seven decreased or remained constant in SERI Type II Medium. Four comparisons (Type I NTE vs. increased STE, Type I vs. decreased STE, Type II NTE vs. increased STE, Type II NTE vs. decreased STE) were made to determine if STE differed from NTE. The STE in SERI Type I and Type II Media were significantly different from the NTE levels in SERI Type I and Type II Media (dep. t-Tests, p = 0.00 to 0.01). When the decreased STE levels were compared between SERI Type I and II Media no difference was apparent (ind. t-Test, p = 0.12). SERI Type II Medium seems to promote a significantly greater accumulation of lipids than SERI Type I Medium (ind. t-Test, p = 0.03). The mean lipid concentration in SERI Type II Medium (28.81 mg/L) was nearly twice that observed in SERI Type I Medium (15.38 mg/L).

This pattern of greater lipid accumulation in SERI Type II Medium was apparent when the strains were divided among the three divisions (Table 3). Relatively low levels of STE were found in the chlorophytes and cyanophytes but a significant preference for lipid accumulation was demonstrated in SERI Type II Medium (ind. t-Test, p = 0.01 and 0.03). The diatoms showed much higher levels of STE, ranging from ten to 22-fold that observed in the other divisions.

The substantial accumulation of lipids by diatoms is readily apparent when the ten highest STE levels are ranked (Table 4). Eight of the ten are diatoms, with four of the diatoms accumulating more than 900 mg STE/L. The association of SERI Type II Medium with greater lipid accumulation is again revealed by the fact that seven of the top ten lipid accumulations occurred in this medium.

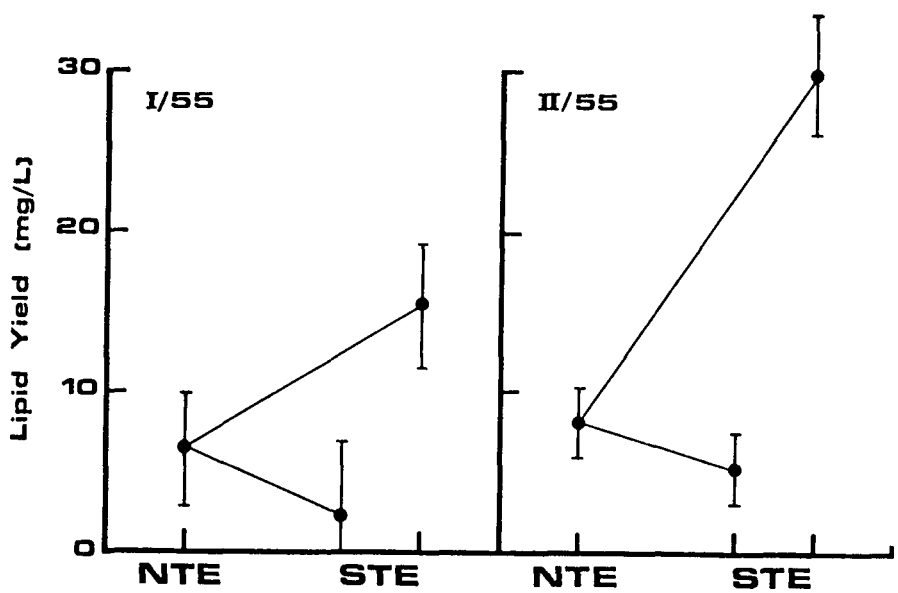

Figure 1. Comparison of lipid yield (mean ± Std. Dev.) in SERI Type I and Type II Media at 55 mS/cm. NTE = normal triolein equivalents; STE = stressed triolein equivalents.

Table 3. Mean lipid yield (mg STE/L ± standard deviation) of microalgae by division in SERI Type I or Type II Media. Only strains demonstrating an increase (i.e., STE:NTE > 1) are given.

Division	I/55	N	II/55	N	t-test p value
Chlorophyta	4.11 ± 2.02	7	11.40 ± 1.70	11	0.01
Chrysophyta	86.92 ± 3.26	9	238.17 ± 1.73	9	0.03
Cyanophyta	8.70 ± 1.75	9	19.32 ± 1.73	9	0.08

N = number of samples; I/55 = SERI Type I Medium of 55 mS/cm; II/55 = SERI Type II Medium of 55 mS/cm; t-test = independent t-test.

Table 4. List of the ten microalgal strains demonstrating the greatest lipid yield in the screening protocol.

Iso.	Genus	Run	Media	Doub/d	NTE (mg/L)	STE (mg/L)	AFDW (ug/L)	STE/NTE Ratio
0613	Nitzschia	5	I/55	0.78	8.14	1002.50	428.4	123.16
0510	Nitzschia	2	II/55	1.22	17.20	934.25	540.0	54.32
3013	Nitzschia	5	II/55	1.15	37.36	907.86	740.5	24.30
3004	Amphora	2	II/55	1.66	8.82	592.56	238.4	86.89
0749	Nitzschia	3	I/55	0.74	61.07	578.80	48.4	9.44
3002	Amphora	8	II/55	1.66	38.50	308.00	--	8.00
0626	Fragilaria	2	I/55	1.71	5.50	303.54	565.5	55.19
3013	Nitzschia	5	I/55	2.07	6.82	256.61	903.8	37.63
0032	Amphora	5	II/55	1.14	38.03	234.70	367.8	6.17
0268	Nitzschia	8	I/55	0.81	23.65	233.85	215.2	9.89

I/55 = SERI Type I Medium of 55 mS/cm; II/55 = SERI Type II Medium of 55 mS/cm; NTE = Triolein equivalent lipid during logarithmic growth; STE = Triolein equivalent lipids after stress (nitrogen deprivation); AFDW = ash free dry weight.

A few taxa not only grew exceptionally well but also accumulated appreciable lipid reserves during logarithmic growth. The ten best strains are listed in Table 5. If the potential lipid yield of these strains is calculated on a daily or six-day basis, the amount of lipid produced may either exceed or be similar to that produced by the best lipid accumulating strains by the end of the four-day growth and two-day nitrogen stress protocol as shown in

Table 4. Strain ASU 0032 Amphora, for example, accumulated 202 mg/l lipid during logarithmic growth which represents a theoretical yield of 345 mg/l of lipid per day or almost 2,100 mg/L over six days. In contrast, the best lipid accumulating strain from the six day screening protocol (Nitzschia, ASU0613) yielded 1,002 mg/l over six days.

Table 5. Estimates of lipid production (mg/L) by logarithmic growth phase cultures of the ten most productive microalgal strains.

Iso.	Genus	Run	Media	doub/d	NTE (mg/L)	NTE (mg/day)	NTE (mg/L/6 days)
0032	Amphora	3	I/55	1.73	201.8	345	2094
0048	Eremosphaera	3	I/55	3.47	33.8	117	704
3027	Synechococcus	7	II/55	3.25	26.7	86	520
3010	Amphora	8	I/55	2.81	25.5	71	430
3022	Synechococcus	7	II/55	2.26	28.7	64	389
3022	Synechococcus	7	I/55	2.14	29.9	64	384
3002	Amphora	8	II/55	1.66	38.5	63	383
3013	Nitzschia	2	II/55	1.53	31.9	48	292
0263	Oocystis	7	I/55	1.25	37.6	46	281
0268	Nitzschia	7	I/55	1.08	42.0	49	272

I/55 = SERI Type I Medium of 55 mS/cm; II/55 = SERI Type II Medium of 55 mS/cm; NTE = Triolein equivalent lipids during logarithmic growth.

The results again illustrate the need to continue to mesh growth rate and lipid accumulation data. The screening and characterization protocol used in this study allows one to obtain both types of data. The operational costs of production and harvesting in a bioculture facility may ultimately dictate which traits are the most desirable in microalgal strains that will be used as the feedstock.

REFERENCES

Barclay, W.R. 1984. Species collection and characterization. In: McIntosh, R.P. (ed.), Aquatic Species Program Review, Proceedings of the April 1984 Principal Investigators Meeting, pp. 152-159. SERI, Golden, CO.

Barclay, B., Nagle, N., Terry, K. and Roessler, P. 1985. Collecting and screening microalgae from shallow, inland saline habitats. In: McIntosh, R.P. (ed.), Aquatic Species Program Review, Proceedings of the March 1985 Principal Investigators Meeting, pp. 52-67. SERI, Golden, CO.

Barclay, B., Nagle, N. and Terry, K. 1987. Screening microalgae for biomass production potential: protocol modification and evaluation. In: Johnson, D.A. (ed.), FY 1986 Aquatic Species Program, Annual Report, pp. 23-40. SERI, Golden, CO.

Guillard, R.R.L. and Ryther, J.H. 1982. Studies of marine planktonic diatoms. I. Cyclotella nana Hustedt and Detonula confervarea (Cleve) Gran. Can. J. Microbiol. 8:229-39.

Johansen, J., Lemke, P.R., Nagle, N., Chelf, P., Roessler, P., Galloway R. and Toon, S. 1987. Addendum to Microalgae Culture Collection 1986-87, Publ. No. SERI/SP-232-3079A, Solar Energy Research Institute, Golden, CO, 23 pp.

Johansen, J.R., Lemke, P.R., Barclay, W.R. and Nagle, N.J. 1987. Collection, screening and characterization of lipid producing microalgae: progress during fiscal year 1987. In: Johnson, D.A. and Sprague, S. (eds.), FY 1987 Aquatic Species Program, Annual Report, pp. 27-45, SERI, Golden, CO.

Lewin, R.A. 1985. Production of hydrocarbons by micro-algae; isolation and characterization of new and potentially useful algal stains. In: McIntosh, R.P. (ed.), Aquatic Species Program Review, Proceedings of the March 1985 Principal Investigators Meeting, pp. 43-51. SERI, Golden, CO.

Lewin, R.A., Cheng, L. and Burrascano, C. 1987. Some picopleuston algae from the Caribbean region. FY 1986 Aquatic Species Program, Annual Report, pp. 105-121. SERI, Golden, CO.

Ryther, R.H., Carlson, R.D., Pendoley, P.D. and Jensen, P.R. 1987. Collection and characterization of saline microalgae from South Florida. In: Johnson, D.A. (ed.), FY 1986 Aquatic Species Program, Annual Report, pp. 122-136. SERI, Golden, CO.

Sommerfeld, M.R. and Ellingson, S.B. 1987. Collection of High Energy Yielding Strains of Saline Microalgae from Southwestern States, Final Report, Department of Botany/Microbiology, Arizona State University, Tempe, AZ, 40 pp. + appen.

Sommerfeld, M.R. and Ellingson, S.B. 1987. Collection of high energy yielding strains of saline microalgae from southwestern states. In: Johnson, D.A. (ed.), FY 1986 Aquatic Species Program, Annual Report, pp. 53-66. SERI, Golden, CO.

Sommerfeld, M., Ellingson, S. and Tyler, P. 1987. Screening microalgae isolated from the Southwest from growth potential and lipid yield. In: Johnson, D.A. and Sprague, S. (eds.), FY 1987 Aquatic Species Program, Annual Report, pp. 43-57. SERI, Golden, CO.

Sorokin, C. 1973. Dry weight, packed cell volume and optical density. In: Stein, J.R. (ed.), Handbook of Phycological Methods: Culture Methods and Growth Measurements, Cambridge Univ. Press, Cambridge, pp. 321-343.

Tadros, M.G. 1985. Screening and characterizing oleaginous microalgal species from the southeastern United States. In: McIntosh, R.P. (ed.), Aquatic Species Program Review, Proceedings of the March 1985 Principal Investigators Meeting, pp. 28-42. SERI, Golden, CO.

Tadros, M.G. 1987. Screening and characterizing oleaginous microalgal species from the southeastern United States. In: Johnson, D.A. (ed.), FY 1986 Aquatic Species Program, Annual Report, pp. 67-89. SERI, Golden, CO.

Tadros, M.G. 1987. Conclusion of the warm water algae collection and screening efforts conducted in the southeastern United States. In: Johnson, D.A. and Sprague, S. (eds.), FY 1987 Aquatic Species Program, Annual Report, pp. 58-74. SERI, Golden, CO.

Thomas, W.H., Seibert, D.L.R., Alden, M., Eldridge, P., Neori, A. and Gaines, S. 1983. Selection of high-yielding microalgae from desert saline environments. In: Lowenstein, M.Z. (ed.), Aquatic Species Program Review, Proceedings of the March 1983 Principal Investigators Meeting, pp. 97-122. SERI, Golden, CO.

Thomas, W.H., Seibert, D.L.R., Alden, M. and Eldridge, P. 1984. Cultural requirements, yields, and light utilization efficiencies of some desert saline microalgae. In: McIntosh, R.P. (ed.), Aquatic Species Program Review, Proceedings of the April 1984 Principal Investigators Meeting, pp. 7-63. SERI, Golden, CO.

Thomas, W.H., Seibert, D.L.R., Alden, M. and Eldridge, P. 1985. Selection of desert saline microalgae for high yields at elevated temperatures and light intensities and in SERI standard artificial media. In: McIntosh, R.P. (ed.), Aquatic Species Program Review, Proceedings of the March 1985 Principal Investigators Meeting, pp. 5-27. SERI, Golden, CO.

York, R.H., Jr. 1987. Collection of high energy yielding strains of saline microalgae from the Hawaiian Islands. In: Johnson, D.A. (ed.), FY 1986 Aquatic Species Program, Annual Report, pp. 90-104. SERI, Golden, CO.

Strategies for Genetic Improvement of Microalgae with Ability to Grow in Outdoor Mass Culture

Lewis M. Brown, Terri G. Dunahay and Eric E. Jarvis

Biotechnology Research Branch
Solar Fuels Research Division
Solar Energy Research Institute
1617 Cole Boulevard
Golden CO 80401

Abstract

There are many strains of microalgae in the SERI Culture Collection with proven ability for rapid growth in outdoor culture. Also, most of these strains can be induced to accumulate large quantities of lipid under nutrient stress. The goal of genetics research at SERI is to be able to control more easily the accumulation of lipids by microalgae and thus achieve higher lipid contents in outdoor mass culture. The tools of modern molecular biology are being applied to this work in order to clone some of the key genes which regulate lipid biosynthesis and to find ways to introduce genetic material into the microalgae and have these genes expressed.

Overall Strategy

The overall strategy is outlined in Figure 1, where the integrated elements of the research program at SERI are shown. The key features of this work are the application of recombinant DNA technology, as well as standard techniques of mutagenesis and selection for microalgae with potential for outdoor mass culture and fuel production.

Industrial Microalgae vs. Model Systems

We have decided to focus our research efforts on microalgal strains with proven ability for growth in outdoor culture rather than using a standard microalgal model system such as Chlamydomonas reinhardtii. Workers in other fields have shown that even closely related organisms can have substantially different genetic structures, which makes it impossible for techniques and genetic constructs developed for one organism to be used in others. This principle is exemplified by studies of the yeasts Schizosaccharomyces pombe and Saccharomyces cerevisiae; although these two species share many features, they have significant differences at the molecular level that prevent easy application of techniques developed for one yeast to be

applied to the other (Russell and Nurse 1986). It is likely that an analogous situation will exist between laboratory strains of Chlamydomonas and microalgae with industrial potential such as the green alga Monoraphidium or the diatom Chaetoceros. In fact our own work is beginning to show that most of the microalgae that we work with have substantially different properties from Chlamydomonas (Brown et al. 1989, unpublished).

Mutagenesis and Selection

One method we plan to use to obtain algae with altered lipid metabolism is mutagenesis and selection of mutants with desired traits, (i.e. increased lipid yields). This approach has been the standard for industrial microbiology and has resulted in many successes over the years. An example of this approach was demonstrated for penicillin production (Elander and Chang 1979). Successive rounds of mutagenesis and selection resulted in a 55-fold increase in production over the standard Fleming strain. These methods have not been applied to microalgal lipid production, but have tremendous potential, not only to produce improved strains, but also to generate aberrant strains with interesting properties for study of lipid biochemistry and genetic structure.

Recombinant DNA Strategies

A second approach will be to utilize recombinant DNA technology to obtain algae with desired lipid-accumulating properties. A key issue here is the introduction of genetic material into the cell through protoplast production, particle bombardment, electroporation or other methods. Several of these approaches are being customized at SERI for the introduction of genetic material into microalgae with proven ability for growth in outdoor mass culture.

Selectable genetic marker for industrial microalgae

A prerequisite to the development of genetic systems such as these is the application of a dominant selectable marker which can be used to assess efficiency of transformation and as a marker for following the fate of foreign DNA. A widely used marker in eukaryotic systems is the kan^r/neo^r gene which codes for resistance to the antibiotics kanamycin/neomycin/G418. This gene, isolated from the Tn5 transposon of Klebsiella (Berg et al. 1975), has been successfully expressed in a variety of species, including mammalian cells (Southern and Berg 1982), plants (Barton et al. 1983, Negruitu et al. 1987, Jongsma et al. 1987, Hayford et al. 1988), Dictyostelium discoideum (Hirth et al. 1982, Barclay and Meller 1983, Nellen et al. 1984, Early and Williams 1987), filamentous fungi (Reveulta and Jayaram 1986, Stahl et al. 1987, Suarez and Eslava 1988, Arnau et al. 1988), yeasts (Sakai et al. 1984, Ascenzioni and Lipps

1986, Sakai and Yamamoto 1986), protozoa (Ascenzioni and Lipps 1986, Hughes and Simpson 1986, Meyers and Helftenbein 1988) and Chlamydomonas reinhardtii (Hasnain et al. 1985). Preliminary tests of several strains in the SERI microalgae collection indicate that they are sensitive to low levels of G418 (Brown et al. 1989, unpublished).

Exploitation of DNA sequences which promote autonomous replication in industrial microalgae

The stability of genetic material introduced into microalgae requires that there be a mechanism for replication. This can be achieved by integration of the plasmid into the host genome; alternatively the plasmid can be maintained via a specific sequence that confers autonomous replication to the plasmid. Such an autonomously replicating sequence (ARS) was first described in yeast (Stinchcomb et al. 1979). This sequence represents genomic DNA that allows autonomous replication and has been used to provide high levels of plasmid in yeast cells.

In addition to the sequences derived from yeast genetic material, sequences from an extensive variety of eukaryotic genomic sources promote autonomous replication in yeast (e. g. Williamson 1985, Katayose et al. 1986, Gold et al. 1987). ARSs derived from DNA of a variety of eukaryotes will sometimes function to promote autonomous replication in the both donor organism and S. cerevisiae. Examples of this behavior include sequences from D. discoideum (Hirth et al. 1982), C. reinhardtii (Rochaix et al. 1984, Hasnain et al. 1985), Phycomyces blakesleeanus (Revuelta and Jayaram 1986, Suarez and Eslava 1988), Canadida maltosa (Kawai et al. 1987) and Penicillium chrysogenum (Stahl et al. 1987).

From all of this work it is clear that eukaryote/prokaryote shuttle plasmids with replicative ability based on ARSs can be constructed in a wide variety of lower eukaryotes including yeasts, filamentous fungi, protozoans and algae. There is an excellent chance that such a shuttle plasmid can be constructed for industrially relevant microalgae. The starting material will be a plasmid which we will demonstrate can express the kan^r gene in the these algae. ARS sequences, derived either from yeast or microalgae, will then be inserted into this plasmid.

Plasmid vector - strategy using integrative vectors

Another mechanism for stabilizing introduced genetic material is integration of the DNA into the host genome, resulting in higher stability and lower copy number than for autonomous plasmids. In S. cerevisiae, plasmids can sometimes integrate stably (Larimer et al. 1983). In addition, integration can be directed by homology between sequences on the plasmid and the host chromosome (Zhu et al. 1986).

References

Arnau, J., Murillo, F. J. and Torres-Martinez, S. 1988. Mol. Gen. Genet. 212: 375-377.

Ascenzioni, F. and H. J. Lipps 1986. Gene 46: 123-126.

Barclay, S. L. and E. Meller. 1983. Molec. Cell Biol. 3: 2117-2130.

Barton, K. A., A. N. Binns, A. J. M. Matzke, and M.-D. Chilton. 1983. Cell 32: 1033-1043.

Berg, D., J. Davies, B. Allet, J. D. Rochaix. 1975. Proc. Natl. Acad. Sci. 72: 3628-3632.

Early, A. E. and J. G. Williams. 1987. Gene 59: 99-106.

Gold, B. N. Carrillo, K. Tewari and L. Bogorad. 1987. Proc. Natl. Acad. Sci. 84: 194-198.

Elander, R. P. and L. T. Chang. 1979. Microbial Culture Selection. In Microbial Technology, Vol. II. Edited by H. J. Peppler and D. Perlman. Academic Press, New York. pp. 243-302.

Hasnain, S. E., E. K. Manavathu, and W.-C. Leung. 1985. Mol. Cell. Biol. 5: 3647-3650.

Hayford, M. B., J. I. Medford, N. L. Hoffmann, S. G. Rogers, and H. J. Klee. 1988. Plant Physiol. 86: 1216-1222.

Hirth, K.-P., C. A. Edwards, and R. A. Firtel. 1982. Proc. Natl. Acad. Sci. 79: 7356-7360.

Hughes, D. E. and L. Simpson. 1986. Proc. Natl. Acad. Sci. 83: 6058-6062.

Jongsma, M., M. Koorneef, P. Zabel, and J. Hille. 1987. Plant Mol. Biol. 8:383-394.

Katayose, Y., K. Shishido, M. Ohmasa. 1986. Biochem. Biophys. Res. Commun. 138:1110-1115.

Kawai, S., C. W. Hwang, M. Sugimoto, M. Tagaki and K. Yano. 1987. Agric. Biol. Chem. 51: 1587-1591.

Larimer, F. W., C. C. Morse, A. K. Beck, K. W. Cole and F. H. Gaertner. 1983. Molec. Cell Biol. 3: 1609-1614.

Meyers, G. and E. Helftenbein. 1988. Gene 63: 31-40.

Negruitu, I., R. Shillito, I. Potrykus, G. Biasini and F. Sala. Plant Molec. Biol. 8: 363-373.

Nellen, W., C. Silan and R. A. Firtel. 1984. Mol. Cell. Biol. 4: 2890-2898.

Neumann, E., M. Schaefer-Ridder, Hofschneider, P. H. 1982. EMBO J. 1: 841-845.

Revuelta, J. L. and M. Jayaram. 1986. Proc. Natl. Acad. Sci. 83: 7344-7347.

Rochaix, J.-D., J. van Dillewijn and M. Rahire. 1984. Cell 36: 925-931.

Russell, P. and P. Nurse. 1986. Cell 45:781-782.

Sakai, K., J. Sakaguchi and M. Yamamoto. 1984. Molec. Cell. Biol. 4: 651-656.

Sakai, K. and M. Yamamoto. 1986. Agric. Biol. Chem. 50: 1177-1182.

Southern, P. J. and P. Berg 1982. J. Mol. Appl. Genet. 1: 327-341.

Stahl, U., E. Leitner, and K. Esser. 1987. Appl. Microbiol. Biotechnol. 26:237-241.

Stinchcomb, D. T., K. Struhl, and R. W. Davis. 1979. Nature 282:39-43.

Suarez, T. and A. P. Eslava. 1988. Mol. Gen. Genet. 212: 120-123

Williamson, D. H. 1985. Yeast 1: 1-4.

Zhu, J., R. Conttreras, and W. Fiers. 1986. Gene 50: 225-237.

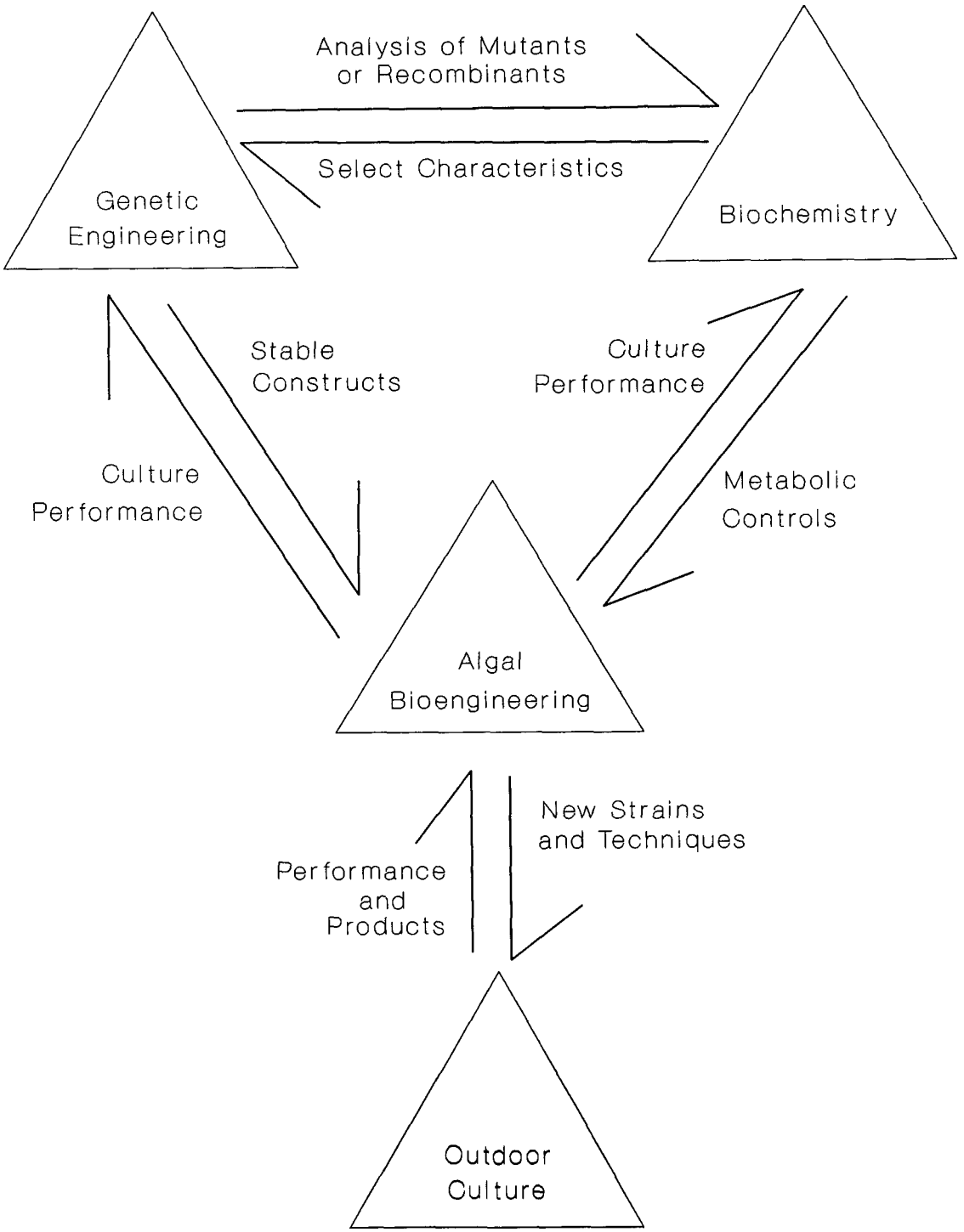

Figure 1. The relation of genetics to other aspects of the industrial microalgal research program at SERI.

THE MITOCHONDRIAL GENOME OF THE EXSYMBIOTIC CHLORELLA-LIKE GREEN ALGA N1A

James A. Waddle, Anne M. Schuster[1], Kit W. Lee, and Russel H. Meints[1,2]

School of Biological Sciences
University of Nebraska-Lincoln
Lincoln, Nebraska 68588-0118
U.S.A.

[1]Present Address: Department of Botany and Plant Pathology
Oregon State University
Corvallis, OR 97331-2902
U.S.A.

[2]Author for Offprints

[2]To whom all correspondence should be addressed:

Summary

Mitochondrial (mt) DNA from the unicellular, exsymbiotic Chlorella-like green alga, strain N1a was isolated and cloned. The mtDNA has a buoyant density of 1.6919 g/cc in CsCl and an apparent G/C base composition of 32.5%. The genome contains approximately 76 kbp of DNA based on restriction fragment summation and electron microscopic measurements. A map using four site-specific endonucleases was generated. From mapping studies the genome is presented as a circular molecule and appears as such under the electron microscope. Eight genes were assigned to the map as demonstrated by heterologous hybridization using mt encoded specific probes. These include the genes for subunits 6, 9, and alpha of the F_o-F_1 ATPase complex, the large and small subunit rRNAs, cytochrome oxidase subunits I and II, and apocytochrome b.

Keywords: Chlorella, mitochondria, genome, map

INTRODUCTION

The mitochondrial (mt) genomes of photosynthetic, single-celled eukaryotic green algae have been little studied. These algae typically possess a cell wall recalcitrant to wall lytic enzymes precluding the easy purification of intact organelles. In addition, these organelles often exist as a reticulated network within the cell, varying in size and shape over the course of the cell cycle (Pellegrini 1980).

Unlike that of other chlorophyte algae, Chlamydomonas mitochondria have been prepared from a cell wall-less mutant (Ryan et al. 1978; Grant and Chiang 1980). The small, linear ca. 16 kilobase pair (kbp) mitochondrial (mt) genome of Chlamydomonas reinhardtii has been characterized (Vahrenholz et al. 1985; Boer and Gray 1986). The results suggest a closer evolutionary link between Chlamydomonas and higher plant mtDNA than to animal or fungal mtDNA (Boer et al. 1985). Aside from Chlamydomonas, all other reports of algal mtDNA structure and organization have been concerned with renaturation studies and sedimentation properties in CsCl density gradients (Bayen and Rode 1973; Talen et al. 1974; Aldrich et al. 1982; Bohnert et al. 1982).

We have initiated a study of mt gene organization in a Chlorella-like green algae originally isolated from a hereditary symbiotic endocellular relationship with Paramecium bursaria. The detailed study of this alga is of interest since the discovery of a group of dsDNA containing, plaque-forming viruses which synchronously infect and replicate uniquely within them (reviewed in Meints et al. 1985; 1986; 1987; Van Etten et al. 1986; 1987; 1988). The present paper describes the characterization of the mt genome of the exsymbiotic Chlorella-like green alga, strain N1a.

MATERIALS AND METHODS

Maintenance of algal cultures. Chlorella N1a, colony purified (Meints et al. 1986) from a mass algal isolate from a Paramecium bursaria culture was grown on modified liquid Bold's basal medium (BBM) (Nichols and Bold 1965) containing 0.25% sucrose and 1.0% proteose peptone (KBBM). Tetracycline (25 µg/ml) was added to deter bacterial growth. Cultures were maintained at 25° C under constant fluorescent light (45 µEi) with moderate shaking. Freshly subcultured cells in mid-log phase (4 X 10^8 cells/ml) were used for isolating nucleic acids.

Isolation of mitochondrial DNA. DNA was isolated by a modified procedure originally developed by Yelton et al. (1984) and Van Etten et al. (1984). A pellet containing 1.5 X 10^{11} algal cells was ground in a mortar under liquid nitrogen with 20 g of sand. The mixture was transferred to tubes containing 20 ml of suspension buffer (50 mM Tris-HCl pH 8.0, 50 mM EDTA, 0.2% SDS) at room temperature. The cell debris was removed by centrifuging at 8,700 x g for 15 min at 4° C. Membranous elements were precipitated from the supernatant by the addition of potassium acetate to 0.5 M and removed by a 25,000 x g spin at 4° C. Nucleic acids in the supernatant were precipitated with 2 volumes of ethanol, resuspended in TE (10 mM Tris-HCl pH 8.0, 1 mM EDTA), digested with 10 µg/ml RNase A, and precipitated with 2 volumes of ethanol at -20° C. The dried pellet was resuspended in TE containing 0.3 µg/ml protease K and incubated for 60 minutes at room temperature. This mixture was adjusted to 56% (w/w) CsCl, centrifuged at 38,000 rpm in a Ti50 rotor for 70 hours at 25° C and fractionated (ISCO model 185 Density Gradient Fractionator coupled to a UA-5 Absorbance Monitor). The region of the gradient corresponding to 1.685 - 1.695 g/cc

was pooled, dialysed against TE, and again centrifuged on CsCl to reduce the amount of contaminating chloroplast DNA (1.697 g/cc). The mitochondrial DNA was dialysed at 4° C against TE and precipitated with 0.3 M sodium acetate and 2 volumes of ethanol at -20° C overnight.

Isolation of RNA. RNA was isolated by the method of Schuster et al. (1986). Pellets of 2.5 X 10^{11} cells were ground in liquid nitrogen as above but were transferred immediately to 5 ml of cold extraction buffer (50 mM Tris-HCl pH 8.0, 1 mM EDTA, and 0.1% SDS), extracted twice with an equal volume of phenol-chloroform-isoamyl alcohol (25:24:1), twice with chloroform-isoamyl alcohol (24:1) and precipitated with 0.2 M sodium acetate pH 6.0 and two volumes of ethanol at -20° C. The pellet was resuspended in 10 mM Tris-HCl, 1 mM EDTA, 10 mM $MgCl_2$ containing 20 units of RNase-free DNase (Boerhinger Mannheim Biochemicals) and incubated on ice for 1 hour. The reaction was extracted twice with chloroform-isoamyl alcohol (24:1) and precipitated as above. The RNAs were resuspended in TE and stored at -80° C until use.

Cloning of mitochondrial DNA. Plasmids pBR322 and pUC19 served as cloning vectors. *E. coli* strain HB101 was used to propagate pBR322 derived clones and strain DH5/alpha for pUC19 derived recombinants. Restriction endonucleases and T4 DNA ligase were obtained from Bethesda Research Laboratories. Calf intestinal alkaline phosphatase and X-gal (5-bromo-4-chloro-3-indolyl β-D galactoside) were purchased from Boeringher Mannheim Biochemicals.

Mitochondrial DNA was digested with BamHI or SstI and ligated into BamHI digested pBR322 or SstI digested pUC19, respectively. Prior to

ligation, all vectors were dephosphorylated with calf intestinal alkaline phosphatase according to the directions of the supplier. The ligation products were then introduced into competent E. coli cells as described by Hanahan (1985).

Gel electrophoresis of nucleic acids. DNA was digested with restriction endonucleases and the products were electrophoresed on 0.8% agarose gels in TPE buffer (0.08 M Tris-phosphate, 0.008 M EDTA, pH 8.5), stained with ethidium bromide (0.5 µg/ml) and photographed under UV light.

RNAs were heated to 65° C in Hepes/EDTA (0.02 M HEPES 0.001 M EDTA, pH 7.8), 50% formamide, 6% formaldehyde, quenched on ice and electrophoresed on 1.2% agarose, 6% formaldehyde denaturing gels (Rave et al. 1979) in HEPES/EDTA, 6% formaldehyde buffer. Molecular weight standards and the cytoplasmic and plastid ribosomal RNAs were visualized by transferring the RNA to nylon and staining with methylene blue as described by Monroy (1988).

Nick translation. Plasmids or gel purified DNA fragments were radioactively labelled using a nick translation kit (Bethesda Research Laboratories) as directed containing 10 - 20 µCi of alpha ^{32}P dATP (800 or 3000 Ci/mmol) per reaction. Unincorporated nucleotides were removed by the spun column method described in Maniatis et al. (1982) using Sephadex G-50 (Sigma Chemical Corp.).

Heterologous probes. All mitochondrial gene probes were kindly provided by Dr. Charles S. Levings III (North Carolina State University, Raleigh, N.C.). Specific clones used in heterologous hybridizations are given in

Table II. Prior to radioactive labelling, 5 - 10 µg of each vector containing a gene probe was digested with appropriate restriction endonuclease(s), electrophoresed on a 0.4% low melting point agarose gel (Sea Plaque, FMC) in TAE buffer (0.04 M Tris-acetate, 0.001 M EDTA pH 8.0), stained with ethidium bromide (0.5 µg/ml), and the desired band excised. The gel bands were melted at 65° C in 14 volumes of 0.2 M NaCl, 0.02 M Tris-HCl pH 7.3 - 7.5, 0.001 M EDTA for 15 minutes and the DNA was recovered using Elutip-d columns (Schleicher & Schuell) according to the manufacturer's instructions.

Southern transfer and hybridization to probes. Southern transfers of DNA to nylon supports (Amersham) were performed as described by Wahl et al. (1979). After transfer, the nucleic acids were covalently fixed to the nylon by a 5 min UV treatment and baked at 80° C for 10 min.

Hybridization of boiled ^{32}P labelled heterologous probes (> 10^6 cpm) was performed in 20 ml of hybridization solution (5X SSC, 0.075 M Na_2HPO_4, 200 µg/ml denatured salmon sperm DNA (Sigma), 15% formamide (v/v) and 1X Denhardts solution) at 37 or 41° C for 24 hours. Following hybridization, the filters were washed 3 times in 5X SSC, 0.1% SDS for 20 minutes each at 37 or 41° C. Restriction mapping studies employing homologous probes were hybridized in the same manner except 50% formamide was used and hybridization was carried out at 45° C. Similarly, stringent wash conditions (0.1X SSC, 0.1% SDS, 50° C) were employed. Autoradiography was carried out at -80° C using Kodak XAR-5 film with Cronex intensifying screens (DuPont).

Northern transfer and hybridization. After electrophoresis in denaturing formaldehyde gels, RNAs were transferred to nylon without further treatment according to Thomas (1980). Hybridizations were carried out using the conditions described above.

Electron microscopic analysis of mtDNA. Samples of mtDNA were spread according to the method of Kleinschmidt (1968). Briefly, DNA was resuspended in hyperphase solution (0.5 M ammonium acetate pH 7.5, 0.001 M EDTA, 0.1 mg/ml cytochrome C) and applied to the surface of a talc-dusted hypophase (0.25 M ammonium acetate). After the monolayer formed, a carbon coated grid was touched to the surface and lifted away vertically. The prepared grid was stained in 0.05 M uranyl acetate and shadowed with platinum-tungsten. Specimens were examined and photographed with a Philips 201 electron microscope operated at 60 kV. Contour distances of the DNA molecules were measured using a digitizing pad driven by an ERDAS-GIS software package. Use of this system was provided by Dick Ehrman of the Nebraska Department of Environmental Control (Lincoln, Nebraska). Bacillus subtillus plasmid pUB110 was used as a size standard.

RESULTS

Cellular morphology

Exsymbiotic Chlorella-like N1a is similar in morphology to other members of the genus (Fig.1). Observation of numerous thin sections indicates the presence of a single large cup-shaped chloroplast and suggests that a single mitochondrion, closely appressed to the chloroplast, is present. Well organized Golgi is typically seen and a distinct nuclear

envelope is visible. The cell wall is a trilaminar structure.

Isolation of Chlorella N1a mtDNA and cloning of restriction fragments

The buoyant density of the N1a mitochondrial DNA (1.6919 g/cc) is sufficiently different from the chloroplast (1.6974 g/cc) and nuclear (1.7191 g/cc) fractions allowing an enriched mtDNA fraction to be isolated after two rounds of CsCl density gradient centrifugation. The restriction patterns of N1a mtDNA cleaved by BamHI, SalI, SstI, XhoI are designated numerically in order of decreasing size (Fig. 2, Table I). The lightly staining bands (Fig. 2) are contaminating chloroplast DNA fragments (see accompanying paper). Subgenomic DNAs were not detected in unrestricted preparations. The genome size determined by restriction fragment summation was approximately 76 kbp. This is similar to the calculated value of 77 kbp based on contour lengths of N1a mtDNA molecules as viewed on electron micrographs (Fig. 3). The DNA does not appear to be methylated since it was restricted by all enzymes we tried. In addition, the cleavage patterns of the methylation sensitive isoschizomers HpaII and MspI, and MboI and Sau3AI, were identical (data not shown).

Screening a library of BamHI fragments in pBR322 yielded five BamHI mtDNA fragments, B2-B6 (Table I). Four Sst I fragments, Ss2 - Ss5, were also recovered from a gene bank in pUC19. Collectively, these nine clones span the entire length of the N1a mt genome.

Physical mapping of Chlorella N1a mtDNA

Two strategies were used to derive the N1a mtDNA restriction map: (i)

Southern hybridization of cloned probe DNAs to single and double digests of total mtDNA, and (ii) fine point restriction mapping of overlapping mitochondrial DNA clones. Any ambiguities in hybridization to closely migrating fragments were resolved by probing appropriate digests of cloned DNAs.

The resulting map is shown in Fig. 4. Although represented linearly, the genome maps as a 76 kbp circular molecule and appears as such under the electron microscope (Fig. 3).

Ribosomal RNA gene arrangement in Chlorella N1a mtDNA

The 26S and 18S rRNA probes from Zea mays and Zea diploperennis, respectively, hybridize to different regions of N1a mtDNA (Fig. 4). The 26S rRNA homology has been further localized (data not shown) to the 6.5 kbp BamHI-SalI region of mt clone B3 (Fig. 4). The two XhoI fragments (X2 and X4) which hybridize to the 18S rRNA probe are adjacent on the Chlorella N1a mtDNA map (Fig. 4). These results suggest a single gene copy for both large and small subunit rRNAs separated by at least 8 kbp.

Homology of ATPase subunits 9 and alpha in Chlorella N1a mtDNA

Fig. 5 depicts a Southern transfer of Chlorella N1a mtDNA probed with the genes for mitochondrial-encoded ATPase subunits 9 and alpha from maize. Both probes show homology to N1a mtDNA as evidenced by the hybridizion to fragments B3 and B5 (Fig. 5A and 5B, respectively). While these Southern transfers contain contaminating chloroplast DNAs, no chloroplast-related hybridization signals were detected with these two probes. In addition,

N1a nuclear DNA was probed with the same ATPase subunit genes and did not hybridize (data not shown). Thus, these regions of homology are unique to Chlorella N1a mtDNA.

Four other mitochondrial genes were localized to the map: cytochrome oxidase subunits I and II, ATPase subunit 6, and apocytochrome b. Their boundaries are summarized on the map in Fig. 4B.

Northern analysis of Chlorella N1a mt ribosomal RNAs

The sizes of the Chlorella N1a mt large and small subunit ribosomal RNAs were determined by probing Northerns blots of total N1a RNA with the heterologous rRNA genes from corn (e.g,. 26S and 18S). The 26S rRNA probe hybridized with several bands (Fig. 6). The large subunit transcript (3.1 kb) is smaller than would be expected for the comparable gene 26S in higher land plants. A strong cross-hybridization to the chloroplast small (16S) subunit is also noted.

The 18S rRNA-specific probe identified a strongly hybridizing 1.46 kb transcript and also cross-hybridizes with the chloroplast small subunit rRNA (Fig. 6, lane C).

DISCUSSION

Two rounds of CsCl density gradient centrifugation resulted in an enriched fraction of DNA sedimenting at 1.6919 g/cc. The identification of this component as mitochondrial DNA is based on heterologous mt-specific gene probes which identify restriction fragments derived from this fraction of DNA but no other Chlorella N1a DNAs (see accompanying paper). The DNA

fraction with a buoyant density of 1.6974 g/cc, sedimenting close to the mtDNA fraction, has been cloned, restriction mapped and identified as the chloroplast genome (see accompanying paper).

The copy number of the Chlorella N1a mt genome was calculated to be ca. 10 genomes per cell (accompanying paper). This value represents about two percent of the total cellular DNA as compared to one percent in animal and higher plant mtDNAs (Leaver and Gray 1982). Chlorella N1a probably contains a single mitochondrion (Fig. 1 and unpublished observations), thus all 10 genomes are confined to a single organelle. The size of the N1a mt genome based on physical mapping studies is 76 kbp. This value agrees with that determined from electron microscopic measurements (ca. 77 kbp). The apparent base composition of N1a mtDNA, calculated from sedimentation values, is 32.5% guanine plus cytosine. This value is much lower than that for higher plants (range 46 - 51 %; Clayton 1984) or Chlamydomonas reinhardtii (47.5%; Ryan et al. 1978).

Bayen and Rode (1973) have previously described characteristics of a mitochondrion-like satellite DNA from a free-living strain of Chlorella pyrenoidosa sedimenting at 1.700 g/cc. Interestingly, this component shares similar physiochemical traits with those described here for Chlorella N1a: (i) 40% G+C versus 32.5% for N1a, (ii) a kinetic complexity of ca. 80 kbp compared to 76 kbp for N1a and (iii) it comprises 1.5% total cellular DNA and is present at 9 copies per cell as opposed to our estimates of 2.0% and 10 copies per cell for N1a. In agreement with the higher mtDNA G+C content described for the free-living C. pyrenoidosa, the CsCl density gradient profiles of DNA from several free-living species of Chlorella in our laboratory do not show three distinct CsCl fractions (i.e., mitochondria, chloroplast and nuclear) suggesting co-sedimentation

of the mt and chloroplast DNAs in these organisms (A. Schuster, unpublished observations).

The organization of mt ribosomal RNA genes in higher angiosperms is highly conserved (Huh and Gray 1982). The large and small subunit mt rRNA structural genes of six species of angiosperms are about 16 kbp apart (Huh and Gray 1982). This is in contrast to animal mtDNAs where these genes are separated by a single tRNA gene and are often co-transcribed (Eperon et al. 1980). Chlorella N1a mt rRNA structural genes are separated by at least 8 kbp (Fig. 4B). The Chlorella N1a mt large and small subunit rRNAs (3.1 and 1.46 kb) are smaller than their counterparts in maize by about 10 and 25%, respectively. The lengths are similar to the corresponding rRNAs in fungi (Dams et al. 1988; Gutell and Fox 1988).

The gene content of higher plant mtDNA differs from that of animal mtDNA by encoding at least 2 additional components of the F_1-F_o ATPase complex. In animals, the structural genes for F_o-ATPase subunit 9 (DCCD-binding protein) and subunit alpha of the F_1-ATPase complex are encoded in the nucleus (Yaffe and Schatz 1984). In contrast, these are mitochondrial translation products in maize and soybean (Dewey et al. 1985b, Braun and Levings 1985). Yeast mtDNA is intermediate to these two kingdoms as it encodes subunit 9 but not subunit alpha (Schatz and Mason 1974). In Neurospora crassa, both subunits 9 and alpha are nuclear encoded but a pseudogene for subunit 9 occurs in the mt genome (van den Boogart et al. 1982). We have demonstrated the presence of both ATPase subunits 9 and alpha sequences in N1a mtDNA (Fig 6, A and B). We predict that these sequences are transcriptionally active since the two probes do not hybridize to N1a chloroplast or nuclear DNAs (data not shown).

An analysis of ribosomal RNA (rRNA) sequences has raised the possibility that mt genomes arose at different times during evolution, i.e., are polyphyletic (Spencer et al. 1984). Using 5S rRNA sequence comparisons between the nuclear genomes of algae and higher plants, Dayhoff and Schwartz (1981), and Kuntzel et al. (1983) have postulated that mitochondria of green algae and vascular plants had an origin separate from mitochondria of fungi and animals. Based on findings reported here Chlorella N1a share at least two unique mt DNA gene organizational features with higher plant mtDNA i.e., distant physical separation of the large and small subunit rRNA structural genes and the presence of ATPase 9 and alpha sequences exclusively in the mtDNA. These findings support the postulation of Dayhoff and Schwartz (1981) that mitochondria in green algae and higher plants have evolved from a different endosymbiotic event than did the mitochondria in animals and fungi. Sequence analysis of the regions of ATPase subunits 9 and alpha homology in N1a mtDNA, as well as a comparison of the Chlorella mt large and small rRNA gene sequences with those of higher plant and Chlamydomonas mtDNAs, will provide additional evidence regarding polyphyletic origins of mitochondria.

ACKNOWLEDGEMENTS

We thank Marcia Ziegelbein for her excellent technical assistance. Thanks to James Van Etten and Philip Kelley for helpful discussions. This investigation was supported in part by grant DCB-8417373 from The National Science Foundation, grant 85-CRCR-1-1613 from The United States Department of Agriculture and contract XK-5-05073-2 from the Solar Energy Research Institute.

REFERENCES

Aldrich J, Gelvin S, Cattalico RA (1982) Extranuclear DNA of a marine chromophytic alga: Restriction endonuclease analysis. Plant Physiol 69:1189-1195

Bayen M, Rode A (1973) The 1.700 DNA of Chlorella pyrenoidosa: Heterogeneity and complexity. Plant Sci Lett 1:385-389

Boer P, Bonen L, Lee W, Gray MW (1985) Genes for respiratory chain proteins and ribosomal RNAs are present on a 16-kilobase-pair DNA species from Chlamydomonas reinhardtii mitochondria. Proc Natl Acad Sci USA 82:3340-3344

Boer PH, Gray MW (1986) The URF5 gene of Chlamydomonas reinhardtii mitochondria: DNA sequence and mode of transcription. EMBO J 5:21-28

Bohnert HJ, Crouse EJ, Pouyet J, Mucke H, Loffelhardt W (1982) The subcellular localization of DNA components from Cyanophora paradoxa, a flagellate containing endosymbiotic cyanelles. Eur J Biochem 126:381-388

Braun CJ, Levings CS III (1985) Nucleotide sequence of the F1-ATPase alpha subunit gene from maize mitochondria. Plant Physiol 79:571-577

Clayton DA (1984) Transcription of the mammalian mitochondrial genome. Ann Rev Biochem 53:573-594

Dale RMK, Mendu N, Ginsburg H, Kridl JC (1984) Sequence analysis of the maize mitochondrial 26S rRNA gene and flanking regions. Plasmid 11:141-150

Dams E, Hendriks L, Van de Peer Y, Neefs J-M, Smits G, Vandenbempt I, De Wachter R (1988) Compilation of small ribosomal subunit RNA sequences. Nucleic Acids Res 16:r87-r99

Dawson AJ, Jones VP, Leaver CJ (1984) The apocytochrome b gene in maize mitochondria does not contain introns and is preceded by a potential ribosome binding site. EMBO J 3:2107-2113

Dayhoff MO, Schwartz RM (1981) Evidence on the origin of eukaryotic mitochondria from protein and nucleic acid sequences. Ann NY Acad Sci 361:92-103

Dewey RE, Levings CS III, Timothy DH (1985a) Nucleotide sequence of ATPase subunit 6 gene of maize mitochondria. Plant Physiol 79:914-919

Dewey RE, Schuster AM, Levings CS III, Timothy DH (1985b) Nucleotide sequence of Fo-ATPase proteolipid (subunit 9) gene of maize mitochondria. Proc Natl Acad Sci USA 82:1015-1019

Eperon IC, Anderson S, Nierlich DP (1980) Distinctive sequence of human mitochondrial ribosomal RNA genes. Nature (London) 286:460-467

Fox TD, Leaver CJ (1981) The Zea mays mitochondrial gene coding cytochrome oxidase subunit II has an intervening sequence and does not contain TGA codons. Cell 26:315-323

Grant D, Chiang K-S (1980) Physical mapping and characterization of Chlamydomonas mitochondrial DNA molecules: Their unique ends, sequence homogeneity and conservation. Plasmid 4:82-96

Gray MW, Doolittle WF (1982) Has the endosymbiont hypothesis been proven? Microbiol Rev 46:1-42

Gwynn B, Dewey RE, Sederoff RR, Timothy DH, Levings CS III (1987) Sequence of the 18S-5S ribosomal gene region and the cytochrome oxidase II gene from mtDNA of Zea diploperennis. Theor Appl Genet 74:781-788

Gutell RR, Fox GE (1988) A compilation of large subunit RNA sequences presented in a structural format. Nucleic Acids Res 16:r175-r183

Hanahan D: Techniques for transformation of E. coli. In: Glover DM (ed) DNA cloning volume I: a practical approach. IRL Press, Oxford, 1985, pp. 109-135

Huh TY, Gray MW (1982) Conservation of ribosomal RNA gene arrangements in the mitochondria of angiosperms. Plant Mol Biol 1:245-249

Isaac PG, Jones VP, Leaver CJ (1985) The maize cytochrome c oxidase subunit I gene: sequence, expression and rearrangement in cytoplasmic male sterile plants. EMBO J 4:1617-1623

Kleinschmidt AK (1968) Monolayer technique in electron microscopy of nucleic acid molecules. Meth Enzymol 12:361-377

Kuntzel H, Diechulla B, Hahn U (1983) Consensus structure and evolution of 5S rRNA. Nucleic Acids Res 11:893-900

Leaver CJ, Gray MW (1982) Mitochondrial genome organization and expression in higher plants. Ann Rev Plant Physiol 33:373-402

Maniatis T, Fritsch EF, Sambrook J (1982) Molecular cloning. A laboratory manual. Cold Spring Harbor Laboratory. Cold Spring Harbor, New York

Meints RH, Schuster AM, Van Etten JL (1985) Chlorella viruses. Plant Mol Biol Rep 3:180-187

Meints RH, Lee K, Van Etten JL (1986) Assembly site of the virus PBCV-1 in a Chlorella-like green alga: Ultrastructural studies. Virology 154:240-245

Meints RH, Burbank DE, Van Etten JL, Lamport DTA (1988) Properties of the Chlorella receptor for the virus PBCV-1. Virology 164:15-21

Monroy AF: Staining immobilized RNA ladder. Focus 10:14, 1988, Bethesda Research Laboratories, Inc.

Nichols HW, Bold MC (1965) Trichosarchina polymorpha gen. et. sp. nov. J Phycol 1:34-38

Pellegrini M (1980) Three-dimensional reconstruction of organelles in Euglena gracilis Z. J Cell Sci 43:137-166

Pring DR, Lonsdale DM (1985) Molecular biology of higher plant mitochondrial DNA. Int Rev Cytol 97:1-46

Rave N, Crkvenjakov R, Boedtker H (1979) Identification of procollagen mRNAs transferred to diazobenzyloxymethyl paper from formaldehyde agarose gels. Nucleic Acids Res 6:3559-3568

Ryan R, Grant D, Chiang K-S, Swift H (1978) Isolation and characterization of mitochondrial DNA from Chlamydomonas reinhardtii. Proc Natl Acad Sci USA 75:3268-3272

Schatz G, Mason TL (1974) The biosynthesis of mitochondrial proteins. Ann Rev Biochem 43:51-87

Schuster AM, Girton L, Burbank DE, Van Etten JL (1986) Infection of a Chlorella-like alga with the virus PBCV-1: Transcriptional studies. Virology 148:181-189

Spencer DF, Schnare MN, Gray MW (1984) Pronounced structural similarities between the small subunit ribosomal RNA genes of wheat mitochondria and Escherichia coli. Proc Natl Acad Sci USA 81:493-497

Talen JL, Sanders JPM, Flavell RA (1974) Genetic complexity of mitochondrial DNA from Euglena gracilis. Biochim Biophys Acta 374:129-135

Thomas PS (1980) Hybridization of denatured RNA and small DNA fragments transferred to nitrocellulose. Proc Natl Acad Sci USA 77:5201-5205

Vahrenholz C, Pratje E, Michaelis G, Dujon B (1985) Mitochondrial DNA of Chlamydomonas reinhardtii: sequence and arrangement of URF5 and the gene for cytochrome oxidase subunit I. Mol Gen Genet 201:213-224

van den Boogart P, Samallo J, van Dijk S, Agsteribbe E (1982) In: Slonimski P, Borst P, Attardi G (eds) Mitochondrial genes. Cold Spring Harbor Laboratory, Cold Spring Harbor, N.Y. pp 375-380

Van Etten JL, Burbank DE, Joshi J, Meints RH (1984) DNA synthesis in a Chlorella-like alga following infection with the virus PBCV-1. Virology 134:443-449

Van Etten JL, Schuster AM, Girton L, Burbank DE, Swinton D, Hattman S (1985) DNA methylation of viruses infecting a eukaryotic Chlorella-like green alga. Nucleic Acids Res 13:3471-3478

Van Etten JL, Xia Y, Narva KE, Meints RH (1986) Chlorella algal viruses. In: Extrachromosomal elements in lower eukaryotes. Wickner CRB, Hinnebusch A, Lambowitz AM, Gunselau IC, Hollaender A (eds) Plenum, New York, pp 337-347

Van Etten JL, Xia Y, Meints RH (1987) Viruses of a Chlorella-like green alga. In: Plant-microbe interactions II. Kosuge T, Nester EW (eds) Macmillan Publishing Co.

Van Etten JL, Schuster AM, Meints RH (1988) Viruses of fungi and simple eukaryotes. Yigal K, Leibowitz MJ (eds) Marcel Dekker, Inc. New York pp 411-428

Wahl GM, Stern M, Stark GR (1979) Efficient transfer of large DNA fragments from agarose gels to diazobenzyloxymethyl paper and rapid hybridization by using dextran sulfate. Proc Natl Acad Sci USA 76:3683-3687

Yaffe M, Schatz, G (1984) The future of mitochondrial research. TIBS 9:179-181

Yelton MM, Hamer JE, Timberlake WE (1984) Transformation of Aspergillus nidulans by using a trpC plasmid. Proc Natl Acad Sci USA 81:1470-1474

Table I: Restriction fragment lengths (kbp) and designations (in parenthesis) of Nla mitochondrial DNA.

	BamHI	SalI	SstI	XhoI
	26.8 (B1)	37.0 (Sa1)	38.8 (Ss1)	41.2 (X1)
	15.0 (B2)	29.6 (Sa2)	14.5 (Ss2)	11.2 (X2)
	11.6 (B3)	5.8 (Sa3)	12.4 (Ss3)	10.4 (X3)
	8.8 (B4)	3.7 (Sa4)	7.0 (Ss4)	5.5 (X4)
	7.5 (B5)		3.8 (Ss5)	5.3 (X5)
	6.5 (B6)			3.2 (X6)
Totals:	76.2	76.1	76.5	76.8

Table II: Heterologous gene probes.

Gene	Product	Species	Fragment	Reference
coxI	(a)	Maize	3.9 kb BamHI/EcoRI	Isaac et al. 1985
coxII	(b)	Maize	2.0 kb EcoRI/HindIII	Fox and Leaver 1981
atp6	(c)	Maize	0.8 kb EcoRI/HindIII	Dewey et al. 1985a
atp9	(d)	Maize	1.2 kb XhoI/XbaI	Dewey et al. 1985b
atpA	(e)	Maize	23 kb EcoRI/HindIII	Braun and Levings 1985
cob	(f)	Maize	0.7 kb EcoRI/HindIII	Dawson et al. 1984
26S rRNA		Maize	4.9 kb PvuII/PvuII	Dale et al. 1984
18S rRNA		Teosinte	2.4 kb PstI/HindIII	Gwynn et al. 1987

(a) Cytochrome Oxidase Subunit I

(b) Cytochrome Oxidase Subunit II

(c) Subunit 6 of F_o-ATPase

(d) Subunit 9 of F_o ATPase

(e) Subunit alpha of F_1-ATPase Complex

(f) Apocytochrome b of Subunit II

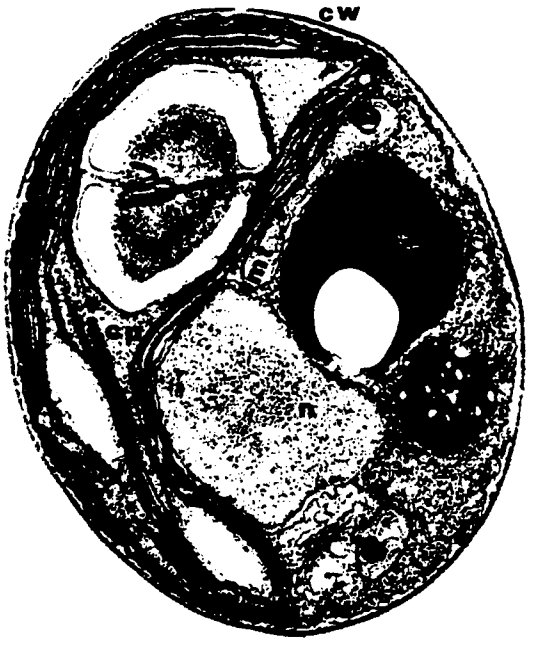

Fig.1. Electron micrograph of Chlorella N1a cell. The single mitochondrion (mt), chloroplast (cp), nucleus and Golgi (g) all lie within a trilaminar cell wall (cw).

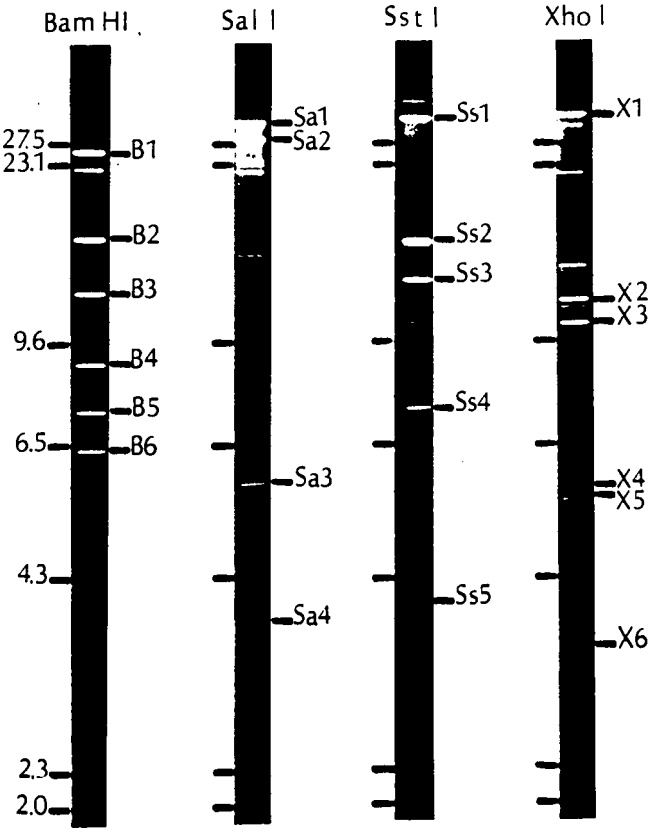

Fig.2. Nla mtDNA restriction fragments: Nla mtDNA (0.5 µg) was digested with BamHI, SalI, SstI or XhoI and electrophoresed on a 20 cm, 0.8% agarose gel in TPE buffer at 40 V for 22 hours. Lambda DNA cut with HindIII served as size markers. Sizes of the standards in kbp are given to the left of each lane and are identical for each digest.

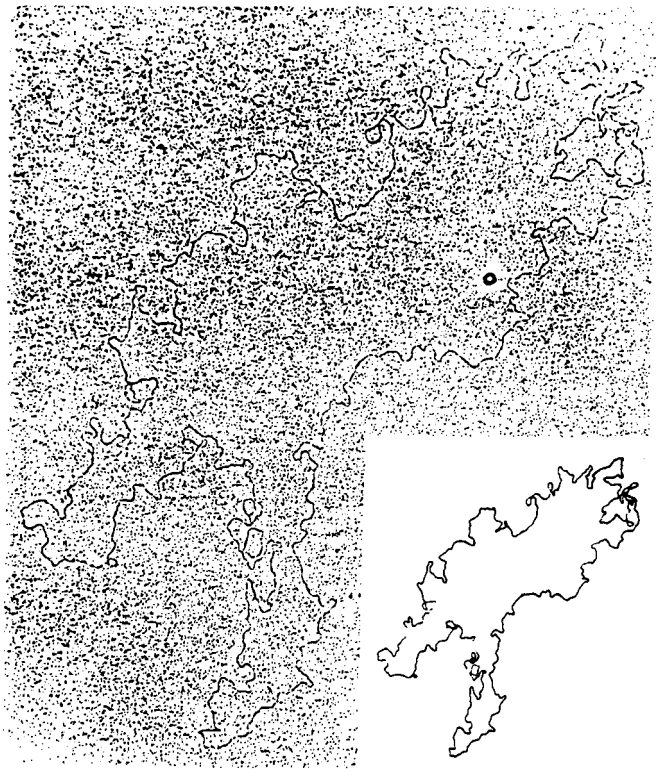

Fig.3. Electron micrograph of N1a mt DNA. Intact mt DNA (0.5 µg) was spread according to the method of Kleinschmidt (1968). The specimen was photographed at 51,300 magnification at 60 kV. Inset lower right: Hand trace of micrograph.

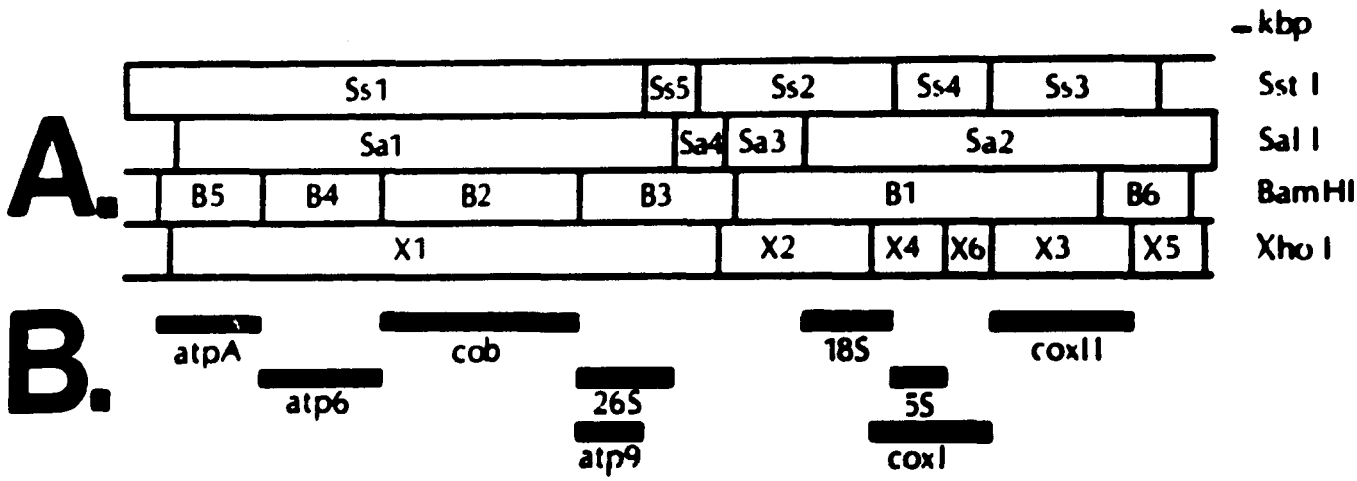

Fig.4. Restriction site (A) and gene map (B) of N1a mtDNA: End boundaries of the above genes were determined as described in the text. (A) Restriction sites are denoted by vertical bars. Fragment designations are as in Table I. (B) Bold lines represent regions of homology between the indicated probe and N1a mtDNA. Abbreviations used: coxI, cytochrome oxidase subunit I; coxII, cytochrome oxidase subunit II; atp6, ATPase subunit 6; atp9, ATPase subunit 9; atpA, ATPase alpha subunit; 26S, 26S rRNA; 18S, 18S rRNA; cob, apocytochrome b.

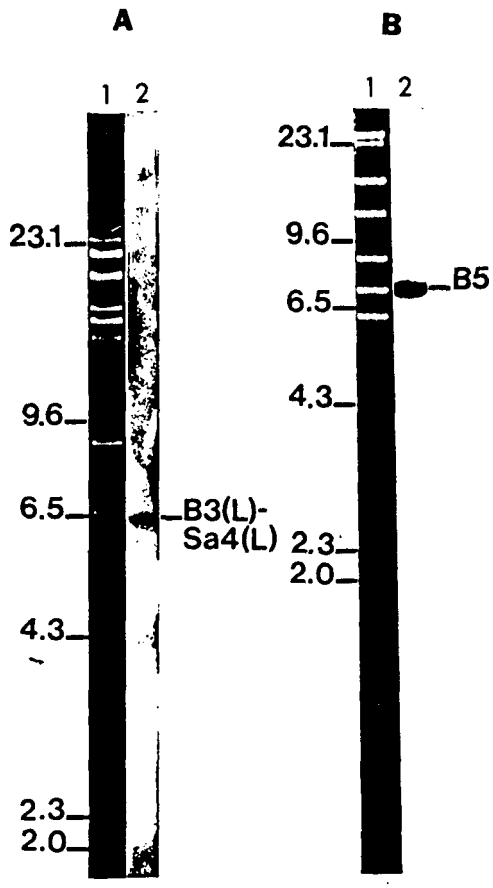

Fig.5. ATPase subunits 9 and alpha sequence homology in N1a mtDNA: N1a mtDNA digested with both BamHI and SalI (A) or BamHI alone (B) was separated on 0.8% agarose gels and stained with ethidium bromide (A1, B1). Southern transfers of these gels (A2, B2) were hybridized with ATPase subunit 9 (A) or subunit alpha (B) probes and autoradiographed. The designation B3(L) - Sa4(L) denotes homology covering the region between the left border of Bam fragment 3 and the left border of Sal fragment 4 on the N1a mt map. All other fragment designations are as in Table I. Lambda HindIII fragments served as size standards. Sizes are given in kbp.

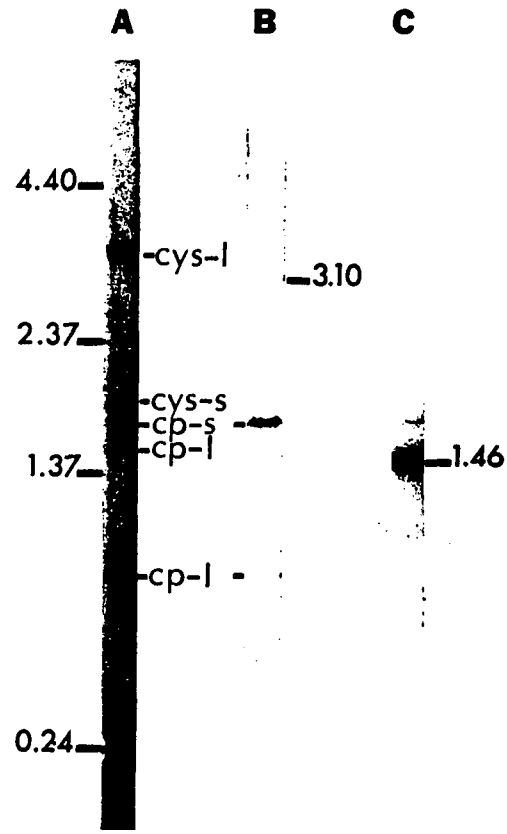

Fig.6. Northern analysis of Nla mt rRNAs. Ten micrograms of Nla total RNA was subjected to electrophoresis in 1.2% agarose, 6% formaldehyde denaturing gels in HEPES/EDTA buffer for 22 hours at 40 V. The RNAs were transferred to a nylon support and a single lane (A) was cut off and stained with methylene blue as described (Monroy 1988). The filters were probed with radiolabelled probes specific for the 26S rRNA (B) or 18S rRNA (C) genes. Lengths of hybridizing species are given in kilobases to the right. MW_r standards are indicated on the left. Cys-l and Cys-s are the large and small cytoplasmic subunits of rRNA. Cp-s is the chloroplast small subunit of rRNA. The cp large subunit is always nicked during preparation and both fragments are labeled.

PURIFICATION AND CHARACTERIZATION OF ACETYL-CoA CARBOXYLASE FROM THE DIATOM CYCLOTELLA CRYPTICA

Paul G. Roessler
Biotechnology Research Branch
Solar Energy Research Institute
Golden, CO 80401

ABSTRACT

Malonyl-CoA, the precursor used for the biosynthesis of fatty acids, is produced via the action of the enzyme acetyl-CoA carboxylase. Since previous research has suggested that this enzyme plays a key role in the regulation of lipid biosynthetic rates in the diatom Cyclotella cryptica, it was of interest to investigate the physical, chemical, and kinetic properties of acetyl-CoA carboxylase from this species. The results from this and similar studies will be necessary before microalgal species can be genetically engineered for higher lipid production rates in outdoor mass culture.

C. cryptica acetyl-CoA carboxylase has been purified to near homogeneity by the use of ammonium sulfate fractionation, gel filtration chromatography, and monomeric avidin affinity chromatography. The specific activity of the final preparation was as high as 8.9 μmoles malonyl-CoA formed/mg protein/min, indicating that the enzyme had been purified 300 to 400-fold. The enzyme has maximal activity at pH 8.5, but enzyme stability is greater at pH 6.5.

Gel filtration chromatography of the enzyme indicated that the molecular weight of native acetyl-CoA carboxylase is approximately 740 kD. SDS-PAGE of the purified enzyme revealed only one major band with a molecular weight of 185 kD. Western blot analysis of this peptide using an avidin-horseradish peroxidase probe indicated that this peptide contains biotin. Therefore, it appears that acetyl-CoA carboxylase from this alga may be composed of four identical subunits.

K_m values for MgATP, acetyl-CoA, and HCO_3^- were determined to be 65, 233, and 750 μM, respectively. The purified enzyme was strongly inhibited by palmitoyl-CoA, and was inhibited to a lesser extent by malonyl-CoA, ADP, and phosphate. Acetyl-CoA carboxylase from Cyclotella cryptica was not inhibited by cyclohexanedione or aryloxyphenoxypropionic acid herbicides as strongly as monocot acetyl-CoA carboxylases; 50% and 0% inhibition was observed in the presence of 23 μM clethodim and 100 μM haloxyfop, respectively.

PURIFICATION AND CHARACTERIZATION OF ACETYL-CoA CARBOXYLASE FROM THE DIATOM CYCLOTELLA CRYPTICA

INTRODUCTION

Acetyl-CoA carboxylase (ACC) catalyzes an early step in the biosynthesis of fatty acids. Previous research has indicated that changes in the activity of this enzyme may play a role in the accumulation of lipids when the diatom Cyclotella cryptica is grown under silicon-limiting conditions (19). It was therefore of interest to investigate the properties of ACC from this alga. Although ACC has been purified from several higher plants, the enzyme has not previously been purified from an alga.

ACCs from higher plants have several characteristics in common, including an alkaline pH optimum and an absolute requirement for ATP and divalent metal cations. Although early studies indicated that plant ACCs had complex subunit structures (three to six peptides having different molecular weights), more recent studies suggest that these earlier attempts to characterize ACC were subject to error due to the effects of endogenous proteolytic activity. Recent studies have suggested simpler subunit structures. High molecular weight (200 kD to 240 kD), biotin-containing subunits are commonly observed, leading several investigators to suggest that plant ACCs are multifunctional proteins able to catalyze both steps of the reaction (biotin carboxylation and carboxylase transfer to acetyl-CoA) (8).

Little is known about the allosteric regulation of ACC activity in higher plants. Adenylate nucleotides (AMP, ADP, and free ATP) have been shown to inhibit the enzyme from several higher plants (2,3,15,20). ACC from maize is also inhibited by malonyl-CoA and palmitoyl-CoA (15). Free coenzyme A has been shown to both inhibit and stimulate the activity of ACC from higher plants (11,15). Citrate, free Mg^{2+}, K^{+}, and glycine have also been reported to stimulate ACC from various plant sources (6,12,13,14,15).

The research described in this report was carried out in order to further our understanding of ACCs from eukaryotic microalgae, and to compare the properties of ACC from the diatom Cyclotella cryptica with those of higher plant ACCs.

MATERIALS AND METHODS

Organism and growth conditions. Cyclotella cryptica Reimann, Lewin, and Guillard strain T13L was obtained from the Culture Collection of Marine Phytoplankton at the Bigelow Laboratory for Ocean Sciences (W. Boothbay Harbor, Maine). Cells were cultured in 2 L polycarbonate bottles as described previously (18). Cultures were bubbled with 0.5% CO_2 in air (500 mL/min) and maintained at 25°C under constant illumination from fluorescent lamps (photon flux density at the vessel surface averaged over 360° = 85 μmol quanta$\cdot m^{-2}\cdot s^{-1}$).

Materials. Analytical grade haloxyfop and clethodim were kindly provided by J. Secor (Dow Chemical Co., Walnut Creek, CA) and A. Rendina (Chevron Chemical Co., Richmond, CA), respectively.

Analytical Methods. Protein was quantified by the Coomassie blue dye-binding method (Biorad), using bovine gamma globulin as a standard. Radioactivity was determined by liquid scintillation counting in a Beckman Model LS9000 scintillation counter, using the H# routine for quench correction. Biofluor (Dupont/New England Nuclear) or Optifluor (Packard) was used as the scintillation cocktail for all isotope studies.

Electrophoresis. SDS-PAGE was performed using the buffer system of Laemmli (10) with a 7.5% acrylamide/2.7% bis-acrylamide separating slab gel. Proteins were transferred to nitrocellulose membranes with a semi-dry electroblotting apparatus (American Bionetics) using the buffer system of Svendsen and Shafer-Nielsen (23). Proteins were detected by the Biorad Biotin-Blot procedure, using the manufacturer's protocol. Biotin-containing proteins were detected by the same procedure, except that the protein biotinylation step was omitted.

Assay for ACC activity. ACC activity was measured by the incorporation of [^{14}C]bicarbonate into acid and heat stable material (malonyl-CoA). The reaction mixture (final volume = 0.3 mL) contained 100 mM Tricine buffer (pH 8.2), 0.5 mM acetyl-CoA, 1 mM ATP, 2 mM $MgCl_2$, 10 mM KCl and 10 mM $NaH^{14}CO_3$ (specific activity = 11.1 MBq/mmol). The reaction was initiated by the addition of enzyme and terminated after 10 min at 30°C by the addition of 0.3 mL of 2 N HCl. A portion (0.5 mL) of the acidified solution was transferred to a scintillation vial and heated at 70°C until dry (approx. 3 h). The residue was dissolved in 0.3 mL of 0.2 N HCl prior to the addition of scintillation cocktail. Control assays were carried out in the absence of acetyl-CoA in order to correct for non-specific radioactivity, which was typically less than 5% of the acetyl-CoA-dependent ^{14}C incorporation. This is a modification of the procedure of Sauer and Heise (20). One unit of activity is defined as the amount of enzyme required to catalyze the formation of one μmol of malonyl-CoA per minute under standard assay conditions.

The reaction product was analyzed by the procedure described by Thomson and Zalik (24), which includes an alkaline hydrolysis step to cleave the thioester linkage to coenzyme A. The reaction product co-migrated with authentic [^{14}C]malonate on silica gel thin-layer chromatography plates (J.T. Baker Co., Si250) developed in water-saturated diethyl ether:formic acid (7:1, v:v) (24) and on Whatman No. 1 paper developed in isobutyric acid:NH_4OH:H_2O (66:1:33, v:v:v) (25).

Preparation of cell-free extracts. Cells were harvested by centrifugation at 5000 x g for 5 min and washed with MCD buffer (100 mM MES containing 10 mM K-citrate and 2 mM dithiothreitol (DTT), pH 6.5). The cells were then suspended in 10 to 25 mL of MCD buffer and passed through a French Pressure cell at 15000 psi. The pressate was centrifuged at 37000 x g for 20 min. The supernatant was diluted with MCD buffer so that the total protein concentration was below 5 mg/mL; this is referred to as the crude extract.

Purification procedure:

$(NH_4)_2SO_4$ fractionation - A saturated solution of $(NH_4)_2SO_4$ was added to the crude

extract with stirring to yield a 30% saturated solution, which was then centrifuged at 8000 x g for 5 min. The precipitate was discarded and the supernatant solution was subjected to further fractionation by the addition of $(NH_4)_2SO_4$ to 43%, 50%, and 60% saturation. All precipitates were discarded except for the one obtained at 60% saturation, which was dissolved in 5 to 10 mL of MCD buffer and used for the gel filtration chromatography step.

Gel filtration chromatography - The solution obtained after $(NH_4)_2SO_4$ fractionation was loaded onto a 90 x 2.2 cm column of Biogel A-1.5m (Biorad) and eluted with MCD buffer at a flow rate of 20 mL/h. Fractions 41-57 (4 mL each) were combined and used for monomeric avidin affinity chromatography.

Monomeric avidin affinity chromatography - Monomeric avidin-agarose was prepared by covalent attachment of tetrameric chicken egg avidin (Calbiochem) to Affi-gel 10 (Biorad), followed by treatment of the gel with 6 M guanidine-HCl (pH 2.15) for 16 h at 20°C. Non-covalently attached avidin subunits were removed from the column by washing with several column volumes of 6 M guanidine-HCl. The column was prepared for use by passing four column volumes of MKD buffer (100 mM MES buffer with 100 mM KCl and 2 mM DTT) containing 0.5 mg biotin/ml through the column to saturate the biotin-binding sites followed by ten column volumes of 0.1 M glycine (pH 2) to remove exchangeable biotin (9). Portions of the gel filtration-purified solution were passed through a two mL column of monomeric avidin-agarose followed by washing with 15 mL of MKD buffer. ACC was eluted from the column with MKD buffer containing 0.5 mg/mL biotin.

RESULTS

Acetyl-CoA carboxylase (ACC) was purified from Cyclotella cryptica by a simple procedure utilizing $(NH_4)_2SO_4$ precipitation, gel filtration chromatography, and affinity chromatography with monomeric avidin-agarose. This procedure resulted in a nearly homogeneous preparation having a specific activity of up to 8.9 μmoles malonyl-CoA formed/mg protein/min, which typically represented an increase in specific activity of approximately 300-fold. The results from a typical purification are shown in Table I.

Gel filtration chromatography of C. cryptica ACC resulted in a single peak of activity (Fig. 1). Based on this chromatographic analysis, the molecular weight of native ACC was estimated to be 740 kD. When analyzed by SDS-polyacrylamide gel electrophoresis, affinity-purified ACC migrated as a single major band having an apparent molecular weight of 185 kD (Fig. 2). This peptide was shown to contain biotin, based on its ability to specifically bind an avidin-horseradish peroxidase conjugate (avidin-HRP) after transfer to a nitrocellulose membrane (Fig. 2). Some lightly stained peptides that migrated slightly ahead of the 185 kD peptide were typically observed. These peptides also appeared to contain biotin since they were detected by avidin-HRP, and thus probably represent products of limited ACC proteolysis.

ACC from C. cryptica had a slightly alkaline pH optimum (pH 8.2), which is typical for ACCs from many sources (Fig. 3). Enzyme stability, on the other hand, was maximal at pH 6.5. When ACC purified through the $(NH_4)_2SO_4$ fractionation step was stored at 4°C at pH 6.5, 97% of the activity was retained

after 48 h, while only 15% and 4% of the initial activity remained after 48 h when stored at pH 7.5 and pH 5.5, respectively. ACC also lost activity rapidly in the absence of a sulfhydryl reductant, and therefore DTT was included in all buffers. Citrate had a slight stabilizing effect on the enzyme, and was therefore routinely included in all buffers up to the affinity chromatography step. Partially purified ACC from C. cryptica could be stored frozen for at least three weeks with little loss in activity. However, affinity-purified ACC was unstable upon freezing, and lost a substantial portion (30%) of the inititial activity after 24 h at 4°C.

The activity of the enzyme was dependent upon the presence of divalent metal cations, with Mg^{2+} being the most active species. When ATP was included at a concentration of 1 mM, maximal ACC activity was observed at a Mg^{2+} concentration of 2 mM (Fig. 4). Above this concentration, enzyme activity declined to a slight extent. Mn^{2+} was able to partially replace the Mg^{2+} requirement, but 2 mM $MnCl_2$ yielded only 20% of the activity observed in the presence of 2 mM $MgCl_2$. The enzyme was inactive when Co^{2+} (2 mM) was the only divalent metal cation present.

Purified ACC from C. cryptica exhibited Michaelis-Menten kinetics with respect to MgATP, acetyl-CoA, and $NaHCO_3^-$ (Fig. 5). The apparent K_m values for these substrates were determined to be 65, 233, and 750 μM, respectively. Citrate (1 mM) did not affect the K_m of the enzyme for acetyl-CoA or the V_{max} of the reaction using different concentrations of acetyl-CoA as substrate (data not shown). Propionyl-CoA was a poor substrate for C. cryptica ACC; 0.5 mM propionyl-CoA was carboxylated at only one-tenth the rate of 0.5 mM acetyl-CoA.

The effects of various cellular metabolites on the activity of purified ACC are shown in Table II. Malonyl-CoA, ADP, and orthophosphate, which are all products of the reaction, substantially inhibited ACC activity. The inclusion of 1 mM ADP and 1 mM $NaHPO_4$ at the same time resulted in a 64% reduction in ACC activity, while 1 mM malonyl-CoA inhibited the reaction by 84%. Palmitoyl-CoA was a strong inhibitor, decreasing enzymatic activity by 78% when included at a concentration of 100 μM. Free palmitate was also quite inhibitory; 100 μM palmitate (which is approximately three times higher than the solubility limit of palmitate in water) inhibited malonyl-CoA formation by 44%. The photosynthetic/glycolytic intermediates 3-phosphoglycerate, phosphoenolpyruvate, fructose-1,6-bisphosphate, glucose-1-phosphate, glucose-6-phosphate, and fructose-6-phosphate had little effect on ACC activity, but 1 mM pyruvate was shown to consistently stimulate enzymatic activity to a small extent. Coenzyme A, which has been shown to both stimulate and inhibit the activity of various higher plant ACCs (11,15), had no effect on the enzyme from C. cryptica. Citrate, acetate, AMP, NADH, NADPH, NAD^+ and $NADP^+$ (1 mM) likewise did not alter ACC activity substantially.

Since ACC has recently been shown to be the site of action of monocot-specific aryloxyphenoxypropionic acid and cyclohexanedione herbicides (1,16,21), it was of interest to determine the effects of these herbicides on the activity of purified C. cryptica ACC. The cyclohexanedione herbicide clethodim inhibited C. cryptica ACC activity in a dose-dependent manner, with 50% inhibition occurring at a clethodim concentration of 23 μM (Fig. 6). On the other hand, the aryloxyphenoxypropionic acid herbicide haloxyfop did not affect enzymatic activity at concentrations up to 100 μM.

DISCUSSION

Many properties of acetyl-CoA carboxylase (ACC) from the diatom Cyclotella cryptica are similar to those of ACCs isolated from various higher plants. Like the enzyme from higher plants, C. cryptica ACC is a large (740 kD) protein composed of several subunits. The molecular weight of ACC from wheat germ (4), avocado (12), castor seed (6), maize (15), and cultured parsley cells (5) was reported to be 700 kD, 650 kD, 528 kD, 500 kD, and 420 kD, respectively. C. cryptica ACC appears to be a tetrameric protein composed of four identical biotin-containing subunits, each having a molecular weight of 185 kD. This suggests that the subunits are multifunctional peptides containing domains responsible for both biotin carboxylation and subsequent carboxyl transfer to acetyl-CoA. ACC from maize is also composed of multiple identical subunits (15) but in this case the subunits are only 60-61 kD. ACC from cultured parsley cells is composed of two equal subunits, each having a molecular weight of 220 kD (5). Oilseed rape ACC is also composed of only one type of subunit with a molecular weight of 220 kD (8). The enzyme from one variety of soybean (variety "9686") is composed of identical subunits having a molecular weight of 240 kD, although another variety of soybean ("Wayne") exhibited a more complex subunit structure (2). ACC from C. cryptica and the majority of ACCs from higher plants therefore appear to be similar in that they are composed of multiple, but identical, subunits. The number of subunits in the holoenzyme can vary substantially, however. It is rather surprising that so much diversity in the structure of this ubiquitous enzyme exists among different plants. It is interesting to note that the subunit structure of C. cryptica ACC is more similar to ACC from brewer's yeast (which is composed of four identical 150 kD subunits (22)) than to the ACCs described thus far from higher plants.

The activity of all ACCs thus far described has been shown to be dependent upon the presence of divalent metal cations. C. cryptica ACC also exhibited this characteristic (Fig. 4). It has been demonstrated on several occasions (6,12,13,20) that MgATP is the actual substrate for ACC, and it is assumed that this is also the case for ACC from C. cryptica. In addition, free Mg^{2+} stimulates ACC activity in several higher plants (6,12,13,20). Based on the increase in activity of C. cryptica ACC due to concentrations of Mg^{2+} that exceeded the ATP concentration in the assay mixture (Fig. 4), it appears that free Mg^{2+} also stimulates the activity of the C. cryptica enzyme.

The K_m values obtained for C. cryptica ACC for acetyl-CoA, MgATP, and bicarbonate (233, 65, and 750 μM, respectively) are similar to the K_m values reported for higher plant ACCs. A survey of K_m values for ACCs from several higher plants, (including spinach (12,20), avocado (12), maize (15), wheat (7), parsley (5), soybean (2), barley (16), and castor seed (6)) yielded ranges of 26 to 320 μM for acetyl-CoA, 21 to 460 μM for MgATP, and 0.86 to 8 mM for bicarbonate. Unlike the case for ACC from avocado and spinach (12), citrate did not affect the V_{max} of the reaction when supplying the enzyme with different concentrations of acetyl-CoA.

The activity of C. cryptica ACC can be modulated by several metabolites. As is the case with ACC from several higher plants (2,3,15,20), the diatom enzyme is inhibited by ADP. For the higher plants examined, this inhibition appears to be competitive with respect to ATP. C. cryptica ACC is also inhibited by orthophosphate and malonyl-CoA. It is not clear whether the inhibitory effects

of ADP, phosphate and malonyl-CoA are due to true allosteric mechanisms or simply to shifts in the thermodynamic equilibrium of the reaction. Nonetheless, it is clear that ACC activity would be higher during periods of photosynthesis due to the combined effects of increased pH and Mg^{2+} levels and decreased ADP and orthophosphate levels within the chloroplast (the presumed location of the enzyme).

The strongest inhibitor of C. cryptica ACC activity tested was palmitoyl-CoA, which inhibited the reaction by 35% and 78% when included at concentrations of 10 μM and 100 μM, respectively. It appears that the acyl component is at least partially responsible for this inhibition since free palmitate also inhibited enzymatic activity quite strongly. Palmitoyl-CoA was also reported to inhibit maize leaf ACC activity (15), with nearly complete inhibition occurring at a concentration of 37.5 μM. The low concentration of acyl-CoA (or free fatty acids) required to inhibit ACC suggests that this inhibition may be physiologically relevant under conditions when acyl chains are not incorporated into membrane lipids or exported from the chloroplast at rates comparable to their rates of synthesis.

The only metabolite tested that stimulated the activity of C. cryptica ACC was pyruvate, which increased the rate of malonyl-CoA formation by nearly 50% when included at a concentration of 1 mM. It is not known whether this slight stimulation has physiological significance. It should be noted, however, that the acetyl-CoA used in this reaction may be derived from pyruvate within the chloroplast, as appears to be the case with many higher plants.

ACC from C. cryptica is much less sensitive to inhibition by cyclohexanedione and aryloxyphenoxypropionic acid herbicides than monocot ACCs. Although clethodim inhibited C. cryptica ACC quite substantially, the I_{50} value determined (23 μM) is one to two orders of magnitude higher than the values reported when monocot ACCs were treated with cyclohexanedione herbicides (1,16). Likewise, haloxyfop inhibits several monocot ACCs by 50% at concentratiuons less than 1 μM (1,17), and yet 100 μM haloxyfop had no effect on C. cryptica ACC activity. The structures of the C. cryptica ACC active sites apparently differ greatly from those of monocot ACCs.

The results of this investigation suggest that ACC from C. cryptica has many properties in common with higher plant ACCs. Current efforts are directed at obtaining an N-terminal amino acid sequence for C. cryptica ACC and producing polyclonal antibodies to the purified enzyme; these items will be necessary for future research involving the genetic engineering of this important enzyme.

REFERENCES

1. **Burton JD, Gronwald JW, Somers DA, Connelly JA, Gengenbach BG, Wyse DL** (1987) Inhibition of plant acetyl-CoA carboxylase by the herbicides sethoxydim and haloxyfop. Biochem Biophys Res Comm **148**: 1039-1044

2. **Charles DJ, Cherry JH** (1986) Purification and characterization of acetyl-CoA carboxylase from developing soybean seeds. Phytochemistry **25**: 1067-1071

3. **Eastwell KC, Stumpf PK** (1983) Regulation of plant acetyl-CoA carboxylase by adenylate nucleotides. Plant Physiol **72**: 50-55

4. **Egin-Buhler B, Loyal R, Ebel J** (1980) Comparison of acetyl-CoA carboxylases from parsley cell cultures and wheat germ. Arch Biochem Biophys **203**: 90-100

5. **Egin-Buhler B, Ebel J** (1983) Improved purification and further characterization of acetyl-CoA carboxylase from cultured cells of parsley (Petroselinum hortense). Eur J Biochem **133**: 335-339

6. **Finlayson SA, Dennis DT** (1983) Acetyl-coenzyme A carboxylase from the developing endosperm of Ricinus communis. I. Isolation and characterization. Arch Biochem Biophys **225**: 576-585

7. **Heinstein PF, Stumpf PK** (1969) Fat metabolism in higher plants. XXXVIII. Properties of wheat germ acetyl coenzyme A carboxylase. J Biol Chem **244**: 5374-5381

8. **Hellyer A, Bambridge HE, Slabas AR** (1986) Plant acetyl-CoA carboxylase. Biochem Soc Trans **14**: 565-568

9. **Henrikson KP, Allen SHG, Maloy WL** (1979) An avidin monomer affinity column for the purification of biotin-containing enzymes. Anal Biochem **94**: 366-370

10. **Laemmli UK** (1970) Cleavage of structural proteins during the assembly of the head of the bacteriophage T4. Nature **227**: 680-685

11. **Laing WA, Roughan PG** (1982) Activation of spinach chloroplast acetyl-coenzyme A carboxylase by coenzyme A. FEBS Lett **144**: 341-344

12. **Mohan SB, Kekwick RGO** (1980) Acetyl-coenzyme A carboxylase from avocado (Persea americana) plastids and spinach (Spinacia oleracea) chloroplasts. Biochem J **187**: 667-676

13. **Nielsen NC, Adee A, Stumpf PK** (1979) Fat metabolism in higher plants. Further characterization of wheat germ acetyl coenzyme A carboxylase. Arch Biochem Biophys **192**: 446-456

14. **Nikolau BJ, Hawke JC, Slack CR** (1981) Acetyl-CoA carboxylase in maize leaves. Arch Biochem Biophys **211**: 605-612

15. **Nikolau BJ, Hawke JC** (1984) Purification and characterization of maize leaf acetyl-coenzyme A carboxylase. Arch Biochem Biophys **228**: 86-96

16. **Rendina AR, Felts JM** (1988) Cyclohexanedione herbicides are selective and potent inhibitors of acetyl-CoA carboxylase from grasses. Plant Physiol **86**: 983-986

17. **Rendina AR, Felts JM, Beaudoin JD, Craig-Kennard AC, Look LL, Paraskos SL, Hagenah JA** (1988) Kinetic characterization, stereoselectivity, and species selectivity of the inhibition of plant acetyl-CoA carboxylase by the aryloxyphenoxypropionic acid grass herbicides. Arch Biochem Biophys **265**: 219-225

18. **Roessler PG** (1988) Effects of silicon deficiency on lipid composition and metabolism in the diatom Cyclotella cryptica. J Phycol **24**: 394-400

19. **Roessler PG** (1988) Changes in the activities of various lipid and carbohydrate biosynthetic enzymes in the diatom Cyclotella cryptica in response to silicon deficiency. Arch Biochem Biophys **267**: 521-528

20. **Sauer A, Heise K-P** (1984) Regulation of acetyl-coenzyme A carboxylase and acetyl-coenzyme A synthetase in spinach chloroplasts. Z Naturforsch **39c**: 268-275

21. **Secor J, Cseke C** (1988) Inhibition of acetyl-CoA carboxylase activity by haloxyfop and tralkoxydim. Plant Physiol **86**: 10-12

22. **Sumper M, Riepertinger C** (1972) Structural relationships of biotin-containing enzymes. Acetyl-CoA carboxylase and pyruvate carboxylase from yeast. Eur J Biochem **29**: 237

23. **Svendsen PJ, Shafer-Nielsen C** (1980) J Biochem Biophys Methods **3**: 97-128

24. **Thomson LW, Zalik S** (1981) Acetyl coenzyme A carboxylase activity in developing seedlings and chloroplasts of barley and its virescens mutant. Plant Physiol **67**: 655-661

25. **Wakil SJ** (1963) Methods Enzymol **6**: 540-544

Table I. Purification of acetyl-CoA carboxylase from the diatom Cyclotella cryptica.

Step	Total Volume	Total Protein	Total Activity	Yield	Specific Activity	Purification
	mL	mg	units	%	units/mg protein	fold
Crude extract	30	78.0	2.43	100.0	0.0311	1.00
$(NH_4)_2SO_4$ fractionation	5	23.2	1.06	43.5	0.0455	1.46
Biogel A-1.5m column	68	4.47	1.05	43.2	0.235	7.54
Monomeric avidin-agarose column	23	0.083	0.74	30.5	8.90	286

Table II. Effects of various compounds on the activity of acetyl-CoA carboxylase purified from Cyclotella cryptica. The values shown are the mean values obtained from two to four separate experiments.

Additions	Relative Activity ± SD
None	100
1 mM malonyl-CoA	16.0 ± 1.3
100 μM malonyl-CoA	59.7 ± 6.7
1 mM $NaHPO_4$	53.0 ± 4.2
1 mM ADP[a]	51.3 ± 2.9
1 mM $NaHPO_4$ + 1 mM ADP[a]	36.2 ± 0.3
1 mM AMP	94.8 ± 1.1
100 μM palmitoyl-CoA	21.8 ± 4.9
10 μM palmitoyl-CoA	64.7 ± 8.7
100 μM CoA	98.1 ± 3.5
1 mM 3-phoshoglycerate	94.4 ± 0.5
1 mM phosphoenolpyruvate	84.1 ± 8.3
1 mM pyruvate	147.3 ± 13.1
1 mM glucose-1-phosphate	103.1 ± 9.1
1 mM glucose-6-phosphate	100.1 ± 8.2
1 mM fructose-6-phosphate	94.6 ± 7.0
1 mM fructose-1,6-bisphosphate	99.7 ± 8.1
1 mM citrate[a]	107.0 ± 8.3
1 mM acetate	94.1 ± 6.2
1 mM NADH	98.3 ± 5.4
1 mM NADPH	87.3 ± 7.5
1 mM NAD^+	100.0 ± 0.8
1 mM $NADP^+$	94.5 ± 5.0

[a]Additional $MgCl_2$ (1 mM) was also included in these assays to overcome the effects of Mg^{2+} chelation.

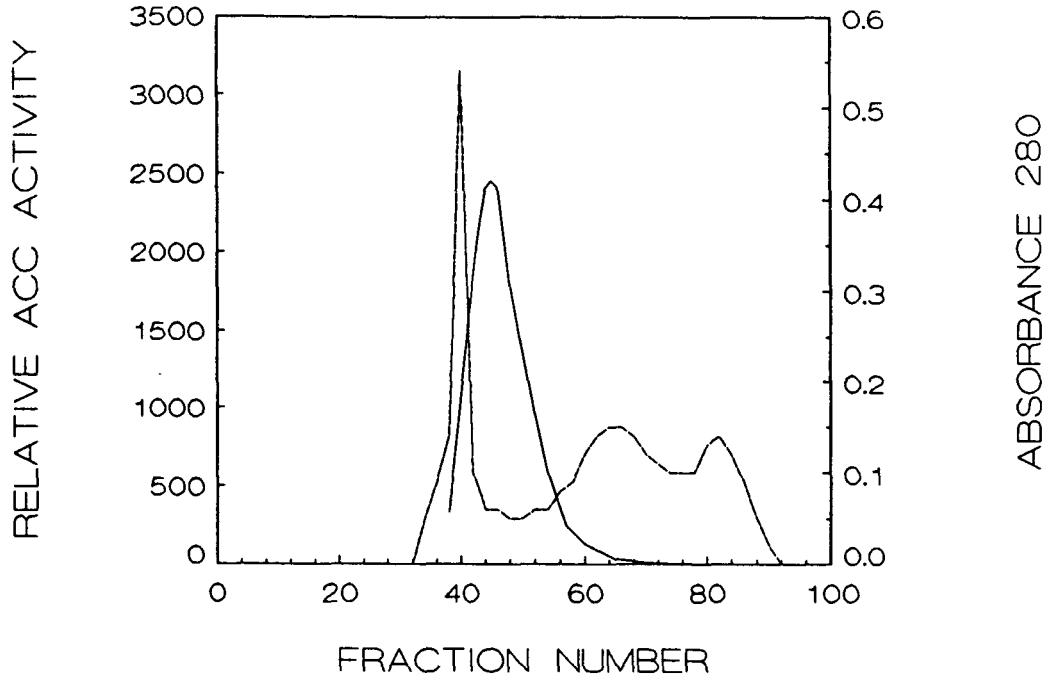

Figure 1. Gel filtration chromatography of Cyclotella cryptica ACC. Relative ACC activity (———); A_{280} (-------).

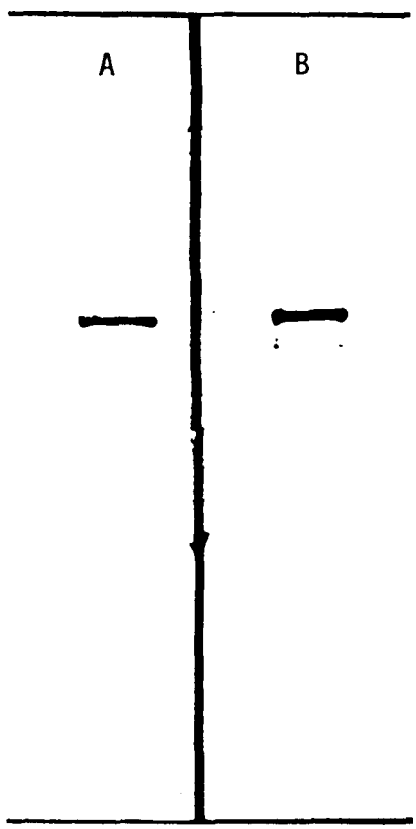

Figure 2. SDS-polyacrylamide gel electrophoresis of affinity-purified ACC from Cyclotella cryptica. A. Avidin-HRP stain. B. Total protein stain.

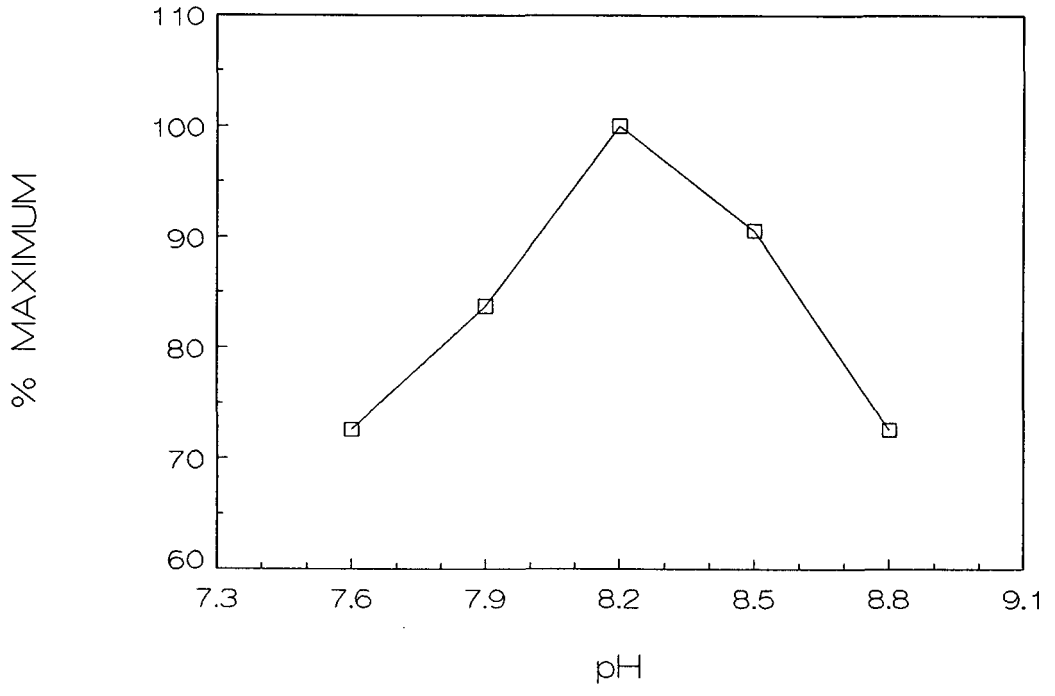

Figure 3. Effect of pH on Cyclotella cryptica ACC activity. 100 mM Tricine buffer was used for all assays.

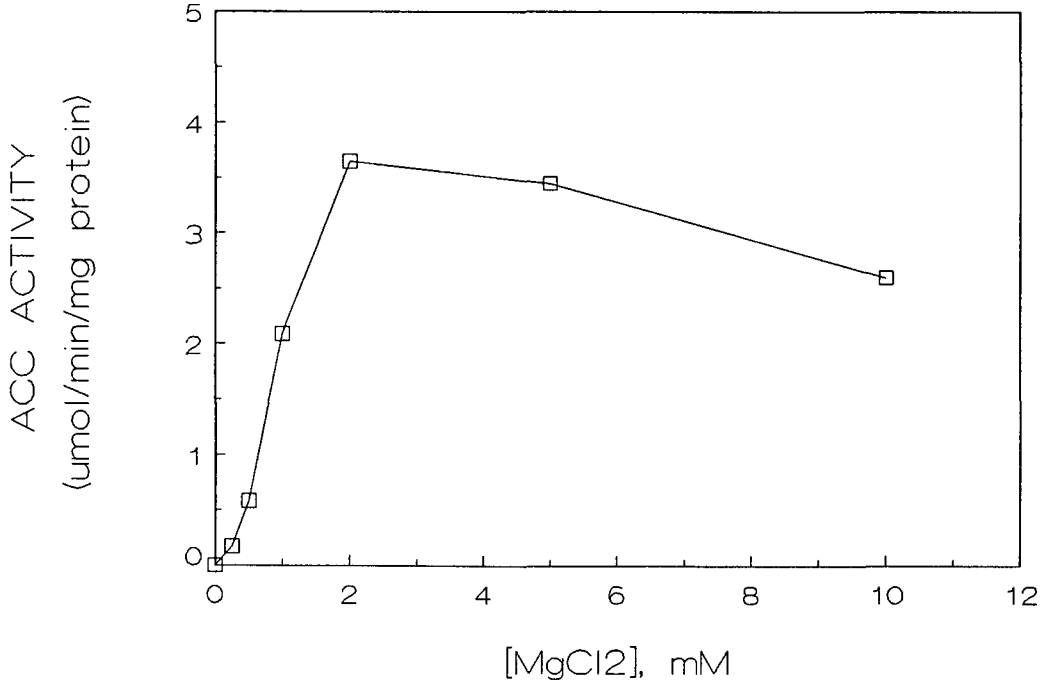

Figure 4. Effect of Mg^{2+} on Cyclotella cryptica ACC activity.

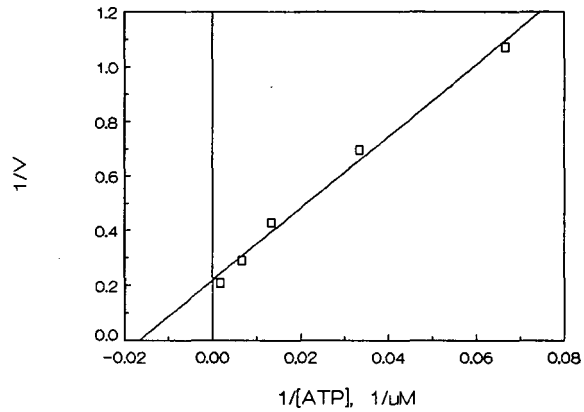

Figure 5. Double-reciprocal plots of ACC activity versus substrate concentration. A. ATP. B. Acetyl-CoA. C. HCO_3^-.

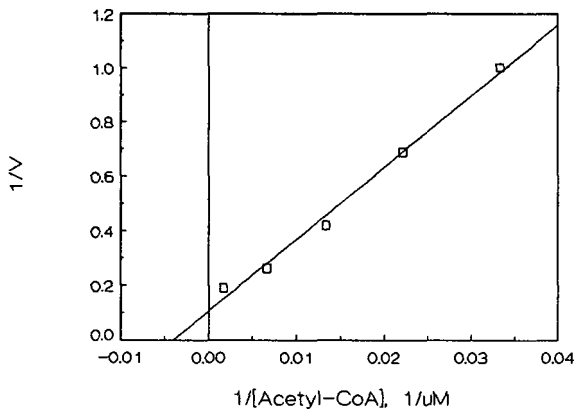

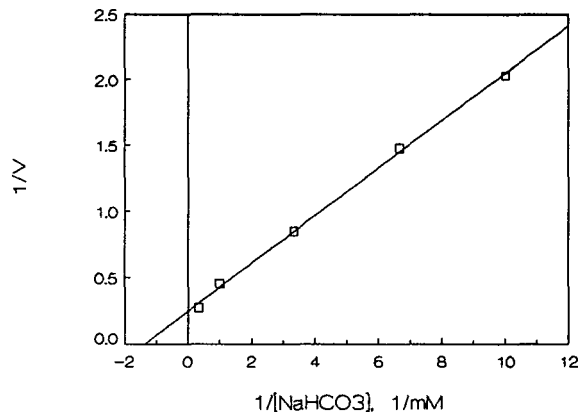

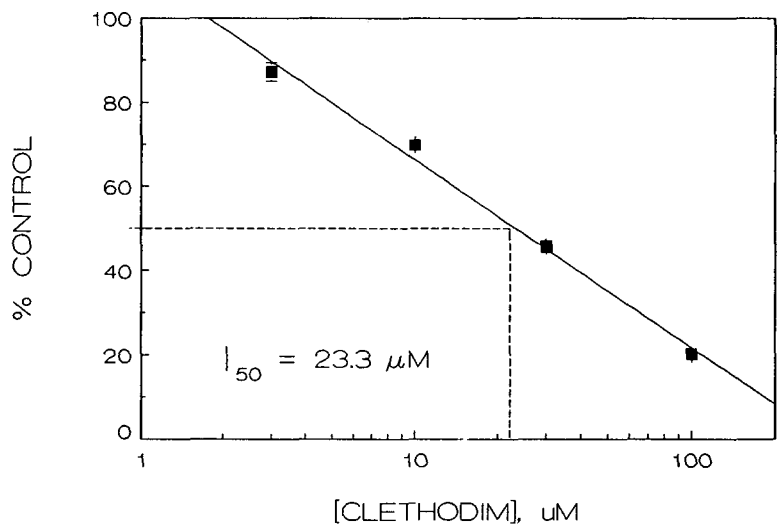

Figure 6. Inhibition of Cyclotella cryptica ACC by clethodim.

TRIGLYCERIDE ACCUMULATION AND THE CELL CYCLE IN MICROALGAE

K.E. Cooksey, J.B. Guckert and R. Thomas
Department of Microbiology
Montana State University
Bozeman, Montana 59717

ABSTRACT

Triglyceride (TG) storage lipid is the only lipid which accumulates in microalgae during exposure to stresses which inhibit algal cell cycles. This inhibition has most often been induced by nutrient limitations such as depletion of nitrogen for green algae and silicate for diatoms. No direct mechanism has been described for low nutrient-induced lipid accumulation. In this work, we report that alkaline pH stress results in triglyceride accumulation. This accumulation was independent of medium nitrogen or carbon levels. Like nutrient deprivation, it is apparent that the high pH has only an indirect effect on lipid accumulation. Based on morphological observations, it is apparent that in Chlorella CHOR-1, alkaline pH inhibits autospore release. We propose that triglyceride accumulation in microalgae could be based on a synthesis/utilization cycle which is constitutive within the cell division cycle, as opposed to a specifically-induced synthesis of triglyceride. The alkaline pH stress effects lipid accumulation by inhibiting the cell division cycle prior to triglyceride utilization and before autospore release. If synthesis continues beyond utilization, the result is an accumulation of triglyceride. Cells inhibited in this manner show a polar and glycolipid fatty acid profile somewhat similar to that of neutral lipid i.e. fatty acids are shorter in chain length and less unsaturated than in polar and glycolipids of control cells.

TRIGLYCERIDE ACCUMULATION AND THE CELL CYCLE IN MICROALGAE

INTRODUCTION

Under optimal conditions of growth, microorganisms synthesize fatty acids principally for esterification into membrane lipids. When microorganisms are stressed by nutrient-limiting conditions which still permit carbon incorporation, lipid biosynthesis patterns change. In microeukaryotic algae, triglyceride (TG)-rich lipid droplets form in the cytoplasm [Cooksey et al., 1988]. Lipid accumulation in microalgae has been reported for limiting concentrations of a variety of medium constituents with the most common being nitrogen [Suen et al., 1987] and in diatoms, silicate [Taguchi, et al., 1987].

Although lipid accumulation during nutrient limitation is well-documented, no direct biochemical mechanism for this change in metabolism has been determined. Nutrient limitations which result in microalgal TG accumulation generally increase the time required to complete the cell cycle [Olson, et al., 1986]. It is possible, therefore, that there is no direct influence of a nutrient limitation on the biochemistry of TG accumulation. Instead, the nutrient-limitation might effect TG accumulation indirectly by inhibiting a specific portion of the microalgal cell cycle. [Fisher and Schwarzenbach, 1978].

The importance of a discussion of microalgal cell cycle stages lies in previous work which has shown that there are sequential synthesis patterns for different lipid classes during cell cycles [Sicko-Goad et al., 1988, Suen et al., 1988]. TG accumulation therefore may be the result of an uncoupling of a synthesis/ utilization cycle within one cell division cycle. Studies of fatty acid dynamics in the diatom Thalassiosira have suggested that storage TG is utilized during cellular energy demand (e.g. in the dark or during cell division) and accumulates when the cell has excess energy available, such as in non-dividing cells in constant light [Fisher and Schwarzenbach, 1978]. This is similar to the findings of Otsuka and Morimura [1966] who reported that synchronous cultures of Chlorella ellipsoidea synthesized TG throughout the photosynthetic growth phase of the cell cycle and utilized it during the process of cell division. Studies which have not reported such cycles have generally quantified total lipid and may have missed the independent cycling of TG during the synthesis of membrane lipids and cell biomass [e.g. Shifrin and Chisholm, 1981].

The following experiments were designed to uncouple changing pH conditions, nutrient utilization and microalgal cell growth from the TG accumulation. Non-metabolizable biological buffers were used to control the pH independently of all other medium conditions to determine if there was a correlation between high pH and TG accumulation. The results indicate that TG accumulates in

Chlorella CHLOR1 independently of nitrogen limitation. Further, changes in lipid metabolism under high pH-stress are coupled to morphological alterations and suggest an indirect influence of high pH on TG accumulation through cell cycle inhibition.

MATERIALS AND METHODS

Microalgae

Experiments utilizing Chlorella CHLOR1 (Solar Energy Research Institute culture collection, Golden, CO.) were done with axenic cultures grown on Bold's basal medium, initial pH 6.7 [Nichols and Bold, 1965], as described previously [Guckert et al., 1987]. This medium was sometimes buffered at a final concentration of 25mM. Buffers used were: Hepes (N-2-hydroxy- ethylpiperazine-N'-2-ethane-sulfonic acid, pKa 7.5), Ches (2-[N- cyclohexylamino]ethane-sulfonic acid, pKa 9.3), and Caps (3-[cyclo-hexylamino]-1-propanesulfonic acid, pKa 10.4) (Sigma Chemical Company). Sodium bicarbonate additions (final concentration 5mM) were made to previously-autoclaved medium. Experiments were conducted with 100 ml cultures in 250 ml flasks shaken at 100 rpm at 26°C under continuous illumination (200 $\mu E/m^2/s$).

Synchronous cultures of Chlorella were achieved by subjecting cells to a 14h:10h light/dark cycle followed by a 24h dark period and then continuous light at 350 $\mu E/m^2/s$. The culture, as judged by the number of cells/ml, remained synchronous through at least two cell divisions.

Determination of DNA/Cell

DNA in cells was determined using the bisbengimide fluor, Hoechst 33258 (Paul and Myers, 1982).

Triglyceride Accumulation Experiments with Chlorella

Comparisons of the cell growth, culture pH, medium nitrate levels and triglyceride accumulation were made for cultures inoculated into the following treatment flasks: unbuffered Bold's medium (Bold's), unbuffered medium + 5mM sodium bicarbonate, (B+c); medium buffered with Hepes (pH 7.0-7.4) either with 5mM sodium bicarbonate (H+c) or without (H); medium buffered with Ches (pH 9.0-9.5) either with 5mM sodium bicarbonate (CH+C) or without (CH), medium buffered with Caps (pH 10.0-10.4) either with 5mM sodium bicarbonate (CA+C) or without (CA), and unbuffered Bold's medium which had 5mM sodium bicarbonate added after 7 days of growth ((B(+C)). Four of these culture treatments were examined with 4 independent replicates in each of three separate experiments. Some treatments were repeated to assess between-experiment variation. At the end of the experiments, cells were harvested by centri-fugation at 3000xg for 15 min. After wet-weight determination, cell pastes were lyophyllized and dry weights determined. Details of the subsequent lipid analyses are given in Guckert et al.,

(1988) and Cooksey et al., (1987). In some cases, preparative thin-layer chromatography was utilized to isolate triglycerides from the neutral lipid fraction obtained from silicic acid chromatography. The molar content of each lipid fraction was obtained from the integrator signal of a gas-chromatograph.

Analysis of Media Components

These were performed as described previously [Guckert et al., 1987].

Lipid Analysis Using Nile Red

Estimation of triglyceride lipid was performed by the method using Nile Red developed by Cooksey et al. (1987). Results are expressed in arbitrary fluorescence units.

Microscopy and Photomicrography

Photomicrographic records were made at every sampling time throughout each 10-day experiment. The algal cells were always viewed at 400x at their undisturbed cell densities and photographed both with phase and epi-fluorescent illumination. The appropriate filters for Nile Red staining of TG droplets were used [Cooksey et al., 1987]. Photomicrographs were taken with a Nikon Optiphot microscope utilizing Ektachrome film (160 ASA, tungsten) exposed at ASA 80. Color slide positives were used to make inter-negatives for black and white illustrations.

RESULTS

Growth Experiments

The buffered media maintained the desired pH during the 10-day experiments (Fig 1) and this Chlorella strain was able to grow under all conditions (data not shown). Cells doubled 3.0-4.4 times during the 10-day experiments in buffered media; however, in unbuffered media, cells grew less well and the pH of the medium remained high, especially where bicarbonate had been added (>pH 11). When 5mM bicarbonate was added to unbuffered Bold's medium after 7 days of growth (FIgure 1A), there was an initial pH rise from 7.9 to 9.2. The following day, the pH had risen to over pH 11 and remained at this level for the balance of the experimental period. In these circumstances, the cells doubled 3.4 times in 10 days.

The accumulation of triglyceride lipid per volume of Chlorella culture for each treatment was measured by the Nile Red technique (Fig. 2). The results of this technique have been verified chromatographically (Fig. 5). Cells in the Hepes-buffered media (with or without bicarbonate) accumulated little TG by the final day of the incubation (9±0.4 to 16±3 units/ml) (Fig. 2C). In unbuffered medium and Ches-buffered medium (with or without

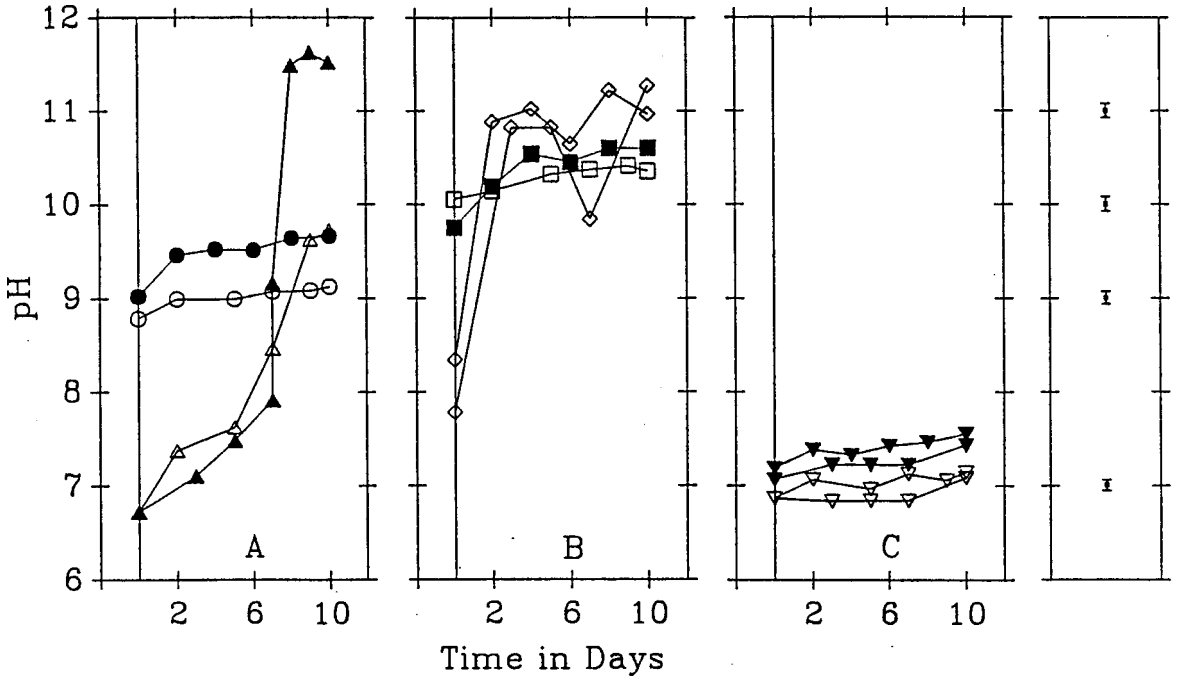

FIGURE 1: Average pH of four independent flasks for each treatment over a ten day incubation. Panel A includes: Ches (open circles), Ches + bicarbonate (filled circles), unbuffered Bold's (open triangles), and unbuffered Bold's to which bicarbonate was added at Day 7 (filled triangles). Panel B includes: Caps (open squares), Caps + bicarbonate (filled squares), and unbuffered Bold's with bicarbonate (open diamonds, 2 separate experiments). Panel C includes: Hepes (open, inverted triangles, 2 separate experiments) and Hepes + bicarbonate (filled, inverted triangles, 2 separate experiments). The panel to the far right gives an indication of the variability of the data by showing the average standard deviation for selected values of pH.

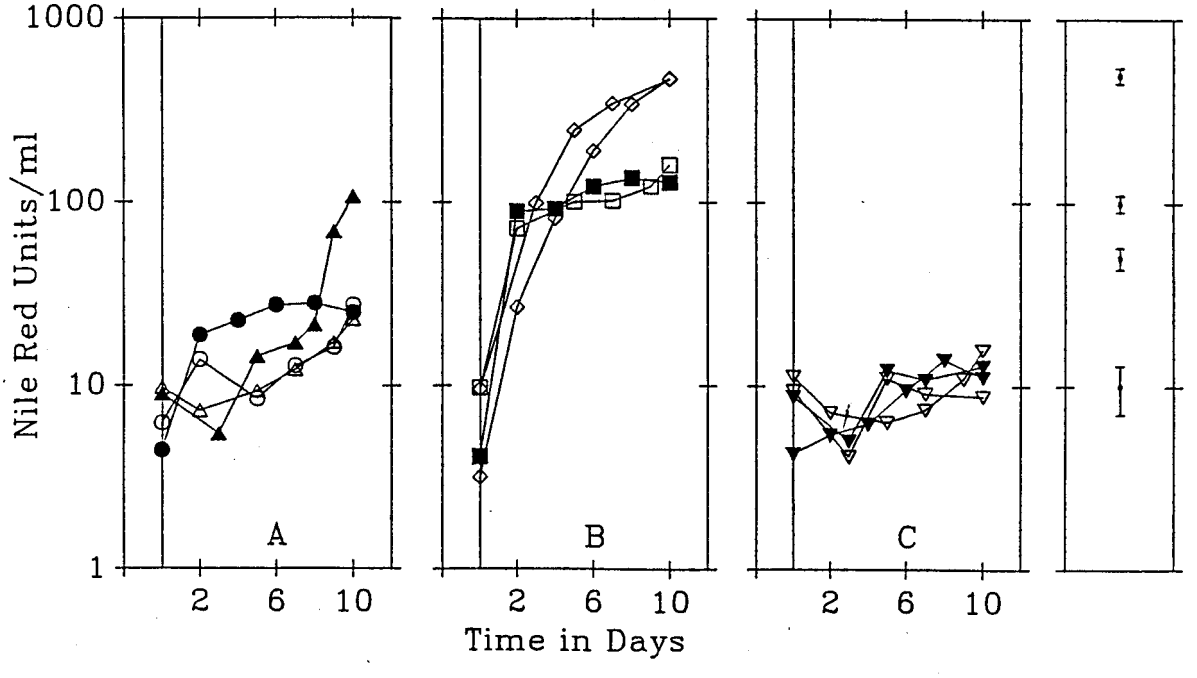

FIGURE 2: Average triglyceride accumulation as measured by Nile Red response (units/ml) of four independent flasks for each treatment over a ten-day incubation. Symbol designations are the same as in Figure 1.

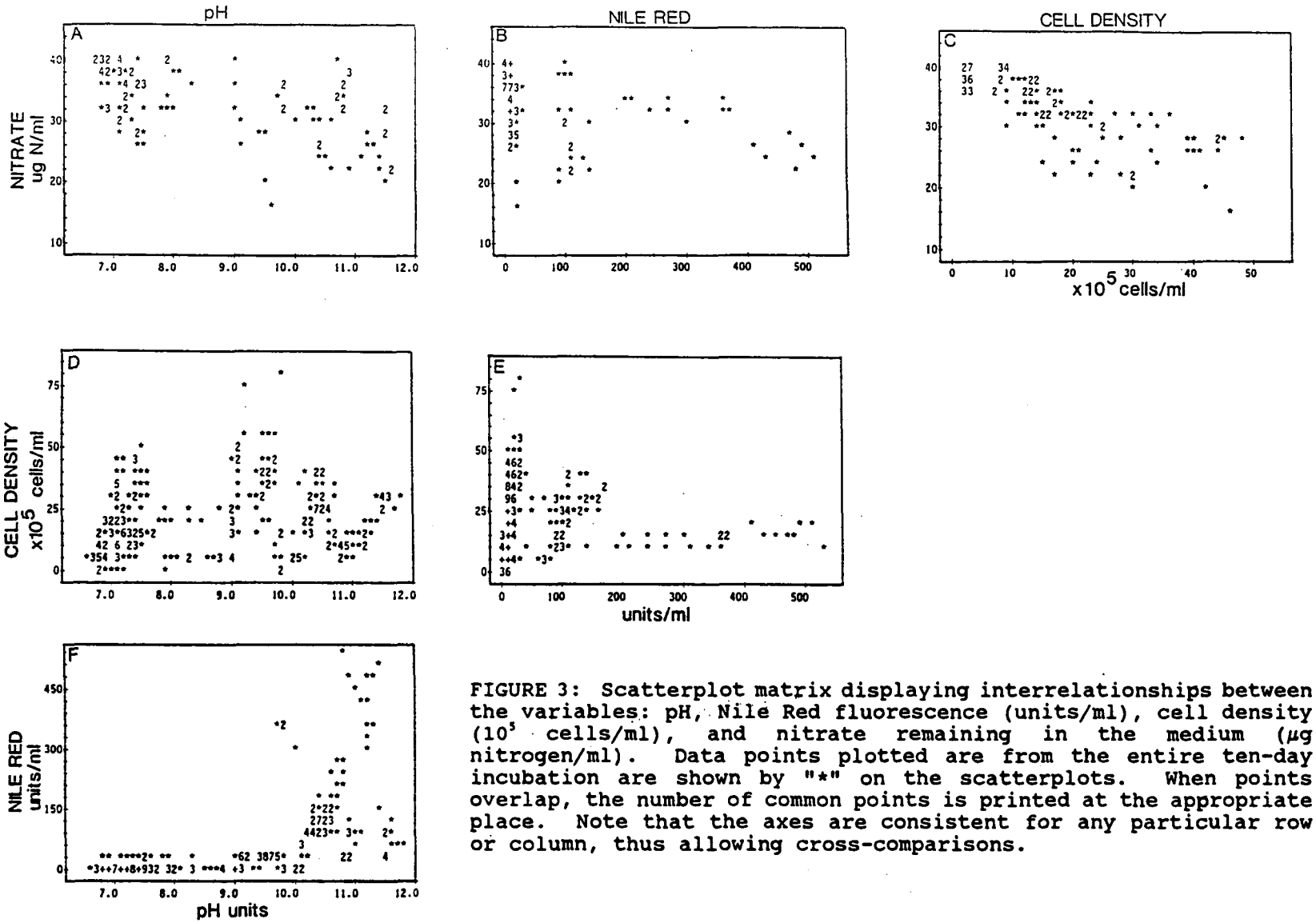

FIGURE 3: Scatterplot matrix displaying interrelationships between the variables: pH, Nile Red fluorescence (units/ml), cell density (10^5 cells/ml), and nitrate remaining in the medium (μg nitrogen/ml). Data points plotted are from the entire ten-day incubation are shown by "*" on the scatterplots. When points overlap, the number of common points is printed at the appropriate place. Note that the axes are consistent for any particular row or column, thus allowing cross-comparisons.

bicarbonate), a Nile Red response twice as great as that for the Hepes-buffered systems was found, i.e. 23±7 and 25±4 to 27±4 units/ml, respectively (Fig. 2A). On the other hand, when cells were inoculated directly into Bold's medium plus 5mM bicarbonate, the Nile Red response rose to approximately 100 units/ml within 3 days and after 10 days had increased to over 470 units/ml (Fig. 2B). When Bold's medium was buffered with Caps (with or without bicarbonate) the response was 71±7 to 89±11 units/ml Nile Red within 2 days, but this value became level at approximately 100 units/ml. When 5mM bicarbonate was added to cells which were growing in unbuffered Bold's medium and thus producing little Nile Red response (17±5 units/ml at day 7, Fig. 2A), the cells responded with an increase to 69±19 units/ml within 2 days of bicarbonate addition, and 108±26 units/ml after 3 days. Note that the data presented for each curve in Figures 1 and 2 are means of 4 independent flasks. Between experiment variation can be judged by the duplicate curves (Figs. 1B,C; 2B,2C). The average sample standard deviation is plotted in the far right panel of each figure for a range of the measured, dependent variables.

The scatterplot matrix shown in Figure 3 is used to display in a concise manner the interrelationships of the relevant medium and cell variables. Figures 3A-C indicate that although nitrate was utilized during algal cell growth (Fig. 3C), only 50% of the initial nitrate concentration of Bold's basal medium was used over the 10-day experiments, leaving approximately 20 μg/ml nitrate nitrogen available. The nitrate/Nile Red scatterplot (Fig. 3B) indicates two clusters of points occurred during nitrate utilization; one cluster did not accumulate TG (as measured by Nile Red response) above 100 units/ml, while another cluster progressively increased its Nile Red response to approximately 500 units/ml as nitrate was utilized.

Algal cell number varied in response to the medium pH (Fig. 3D). The cell density/pH scatterplot (Fig. 3D) indicates a general decline in algal cell density above pH 10 with a possible maximum at pH 9-10 with similar densities at pH 7. The Nile Red/pH scatterplot (Fig 3F) indicates that no culture incubated below pH 9.5 accumulated TG lipid over the 10-day experiment. Generally, all cultures began with equivalent lipid content at Day 0, as measured by the Nile Red technique (Fig. 2). The cultures grown at higher pH accumulated more TG, as indicated by increased Nile Red fluorescence (Fig. 2, Fig. 3F).

The photomicrographs shown in Figure 4 represent differences in morphology when the cells were incubated in medium buffered at different pH values. Cells grown in Hepes (pH 6.8-7.1) or Ches-buffered media (pH 8.8-9.1) were predominantly individual, small cells (Figs. 4A and 4B). Cells grown in media buffered with Caps (pH 10.0-10.4) showed an increased number of autosporangial complexes (Fig. 4C) in which the individual autospores had not yet separated following nuclear division. The cells incubated in the unbuffered medium with 5mM bicarbonate added continued the trend noted for the Caps-buffered cultures to the degree that the

FIGURE 4: Representative photomicrographs of Chlorella cells after 10 days incubation in different media at the undisturbed final cell densities. All micrographs were taken at 400x and are displayed with identical print magnifications. The bar shown in micrograph A is equivalent to 10μm in length. The treatments are: A) Hepes, final pH 7.1; B) Ches, final pH 9.1; C) Caps, final pH 10.3; D) unbuffered Bold's + bicarbonate, final pH 11.1.

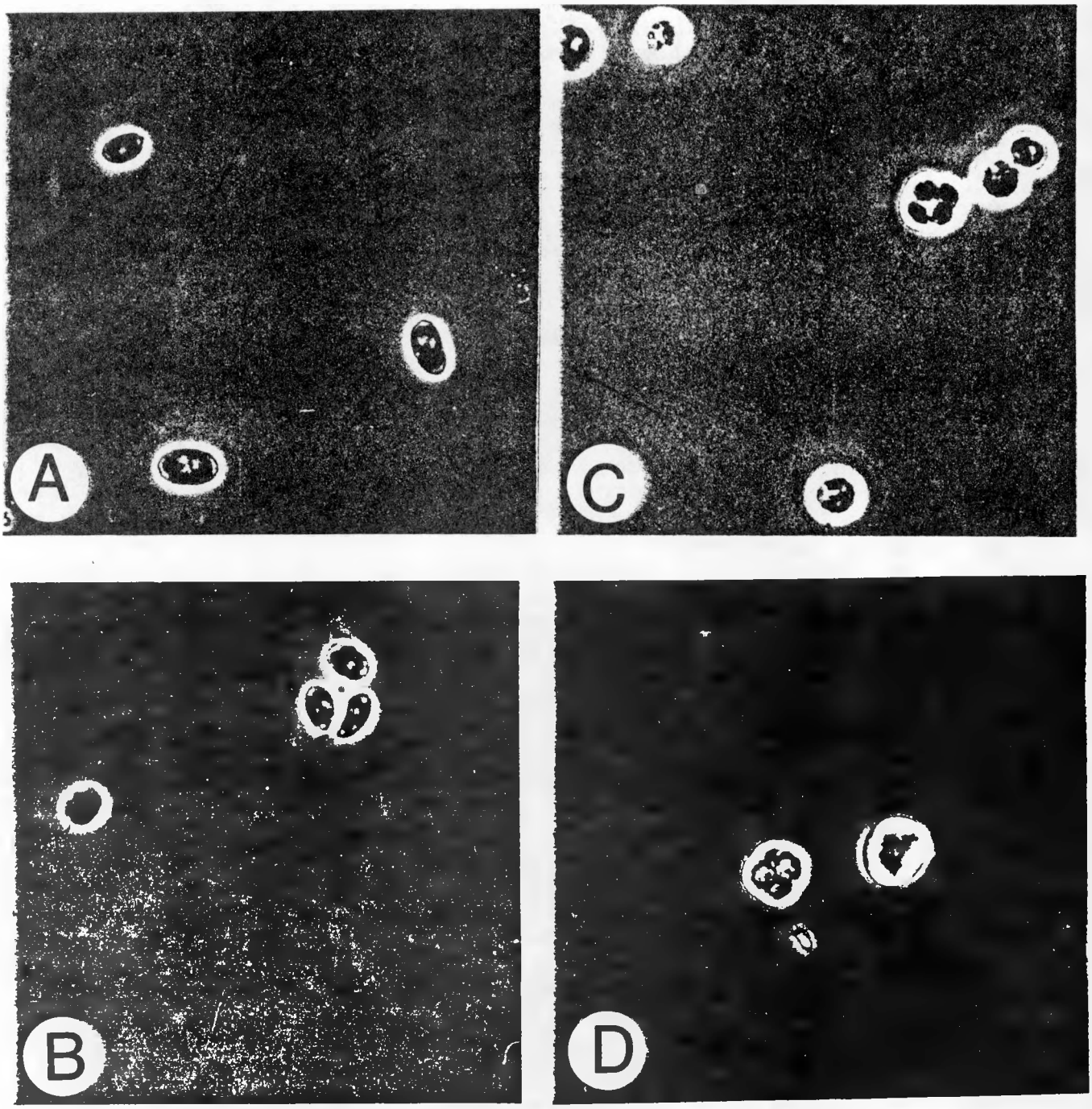

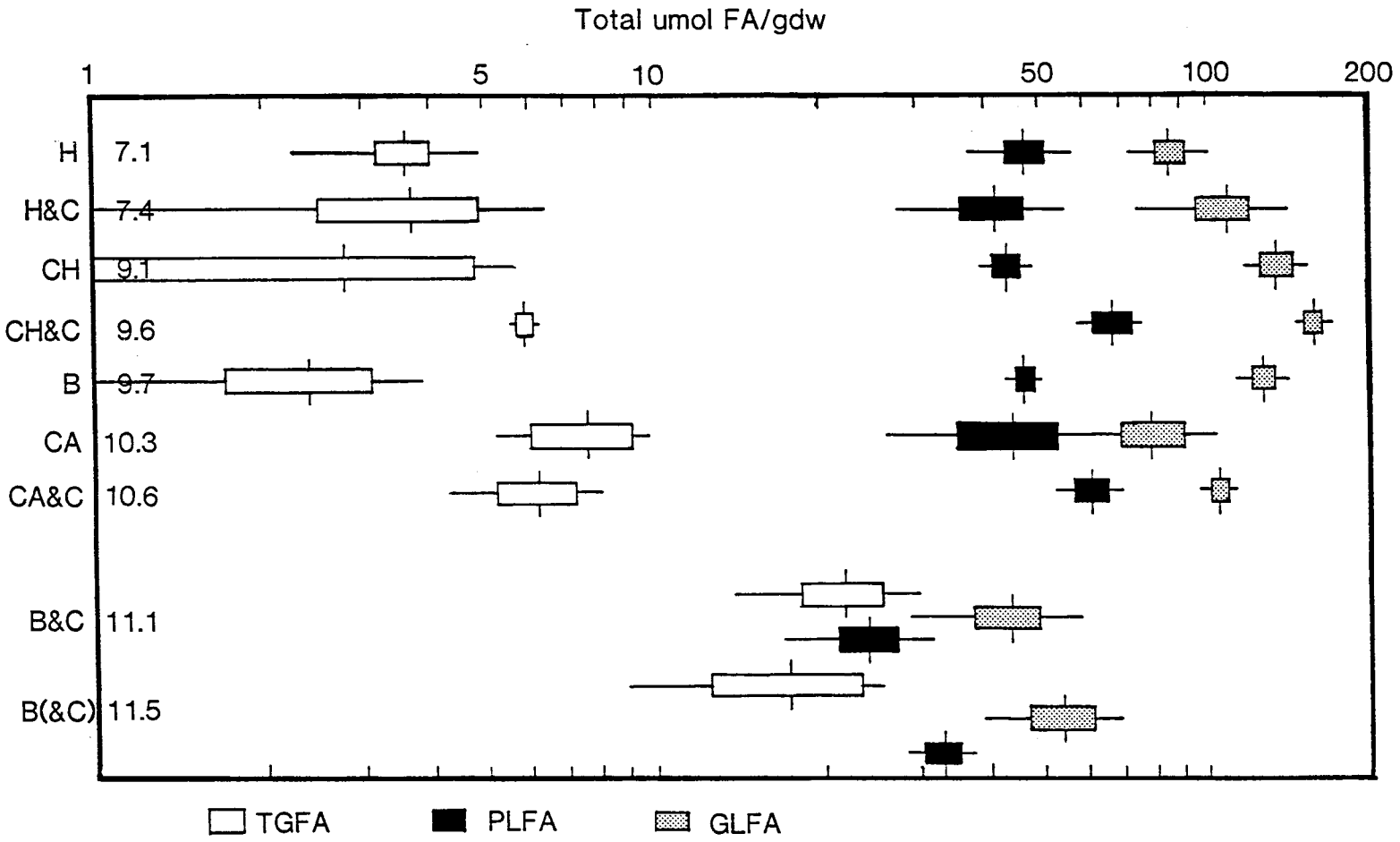

FIGURE 5: Chromatographic analysis results showing triglyceride (open bars), glycolipid (speckled bars) and polar lipid (filled bars) total fatty acids in μmol/gram dry weight. For each media treatment, the average triglyceride fatty acid (TGFA), glycolipid fatty acid (GLFA), and polar lipid fatty acid (PLFA) levels are shown by the vertical line in the approximate middle of the bar. The bar indicates ±1 standard error of the mean while the horizontal line extending from the box indicates ±1 standard deviation. The media treatments are abbreviated as given in the text. The final average pH for each treatment is also given.

TABLE 1: Ratios of fatty acid groups given as the average (±1 standard deviation) of the total fatty acids recovered for each gross lipid type. The treatments were combined into three groups on the basis of the final pH of the medium: final pH<10 (HEPES, H&C, CHES, CH+C, BOLDS), pH 10-11 (CAPS, CAPS+C) and pH>11 (BOLDS+C, BOLDS(+C)).

	Polyunsaturated 18-carbon/ Precursor fatty acids	Unsaturated 16-carbon/ Precursor fatty acids
Triglyceride		
pH<10	0.30 (0.14)	0.04 (0.03)
pH 10-11	0.31 (0.10)	0.06 (0.03)
pH>11	0.21 (0.07)	0.02 (0.01)
Glycolipid		
pH<10	*2.12 (0.41)	*0.91 (0.15)
pH 10-11	*1.67 (0.19)	*0.63 (0.08)
pH>11	*1.08 (0.33)	*0.36 (0.13)
Phospholipids		
pH<10	*0.67 (0.17)	*0.13 (0.03)
pH 10-11	0.62 (0.25)	*0.08 (0.02)
pH>11	*0.41 (0.18)	*0.05 (0.02)

* Averages marked are significantly different from other averages within that group by a two-tailed t-test ($p \leq 0.01$).

FIGURE 6: Analytical Measurements made versus Time on a Synchronous Culture of Chlorella CHLOR1.

a. Relative cell number. Cells begin to divide at the 7h. Division is complete at 26h.
b. Increase in DNA/ml culture. DNA replication begins after about 7-10h, and is complete at 26h.
c. Nile Red Fluorescence/ml culture. Triglyceride (Nile Red fluorescence) increase to 7h when it falls to its original level. This signal rises again as cell number increases.
d. Nile Red/cell. Triglyceride rises from zero time to hour 7, when it falls again to its original level. No further accumulation per cell is seen.
e. DNA replication/cell. DNA replication begins at hour 7 and is complete at 16h. Cytokinesis which takes place after 16h is the reason the amount of DNA/cell falls to its original value. Note DNA replication takes place after accumulation of triglyceride.

FIGURE 6a

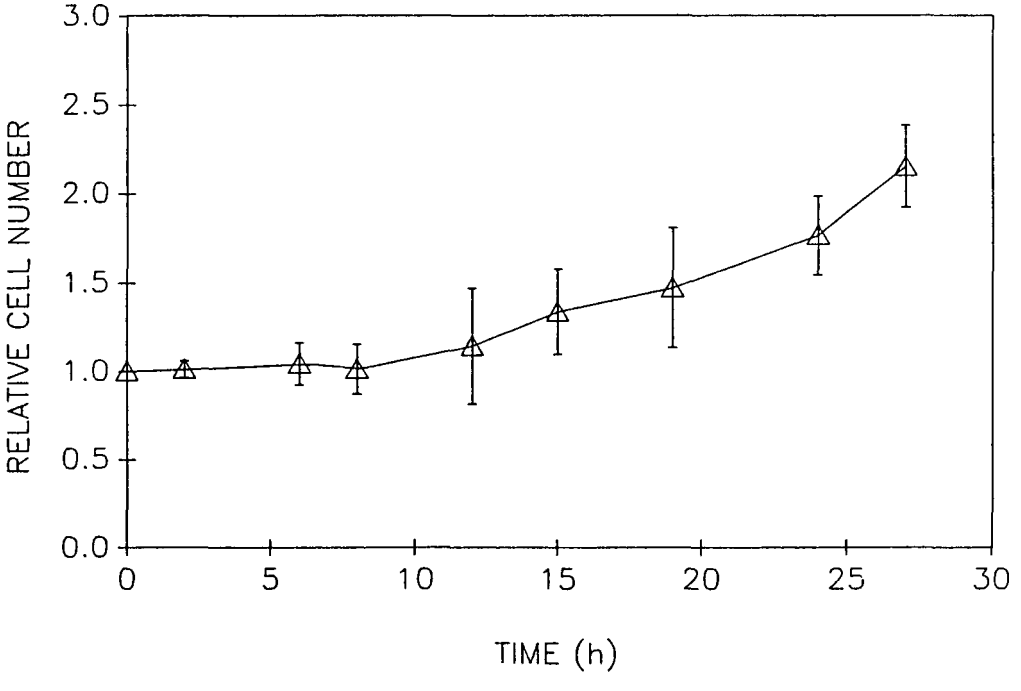

FIGURE 6b

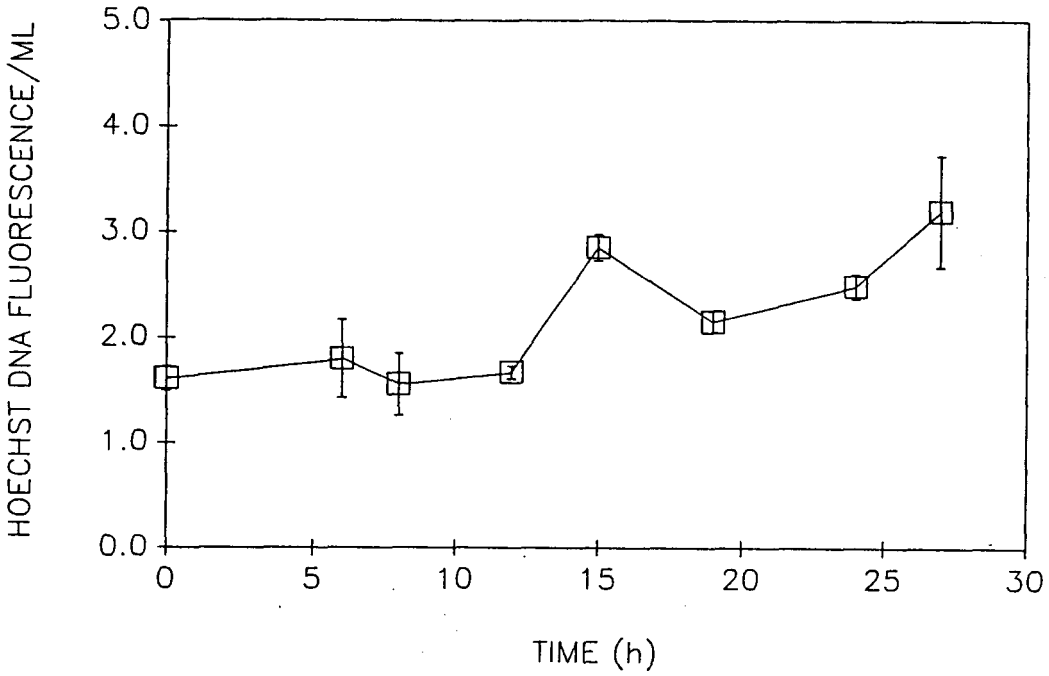

FIGURE 6c

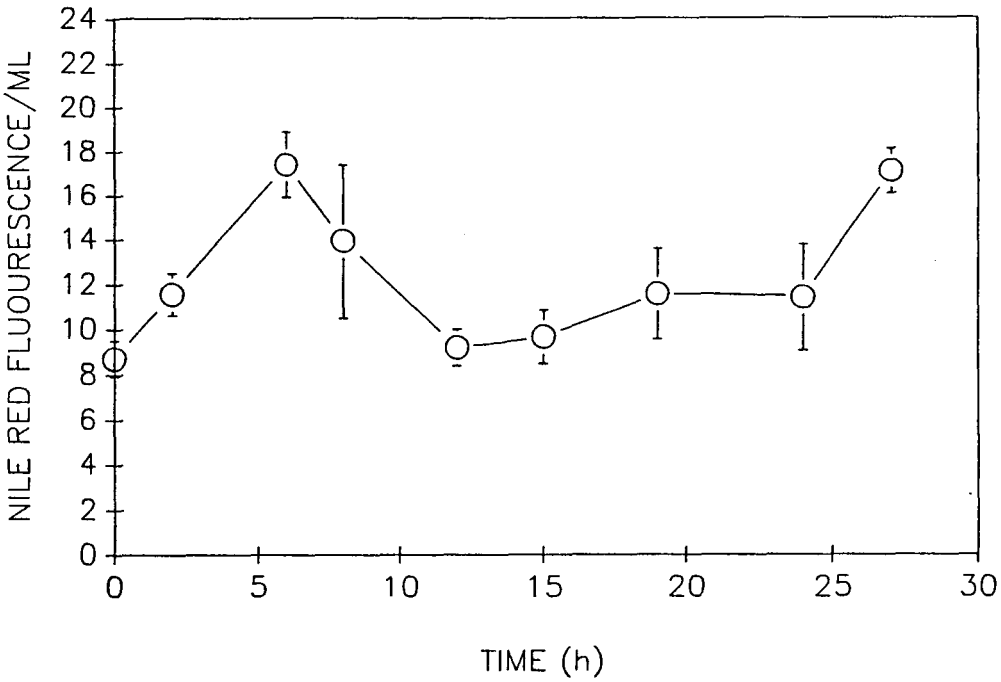

FIGURE 6d

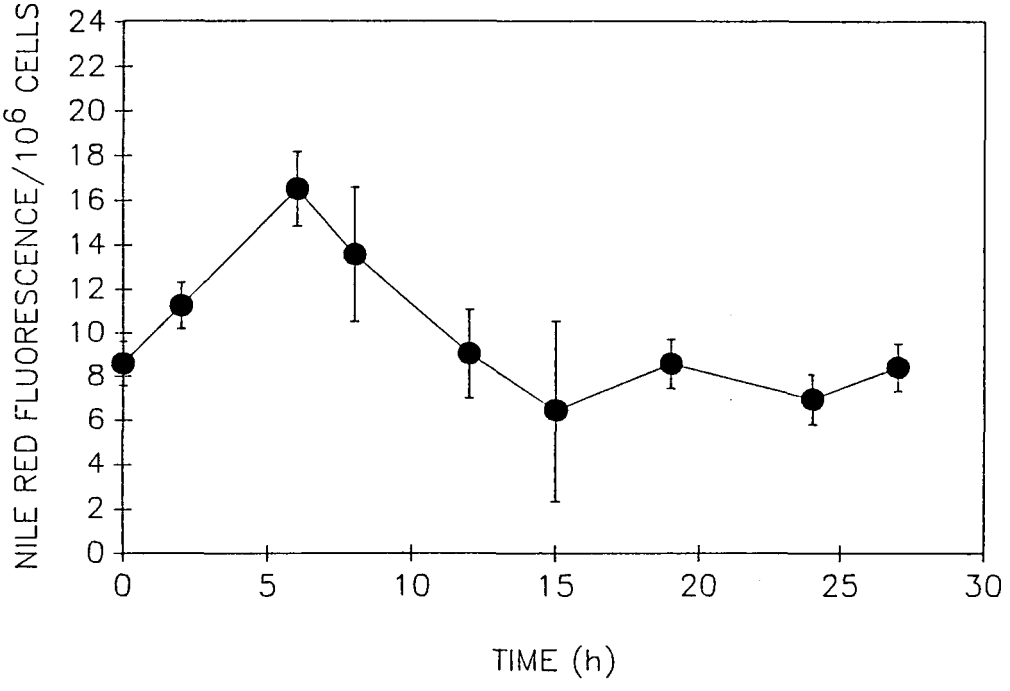

FIGURE 6e

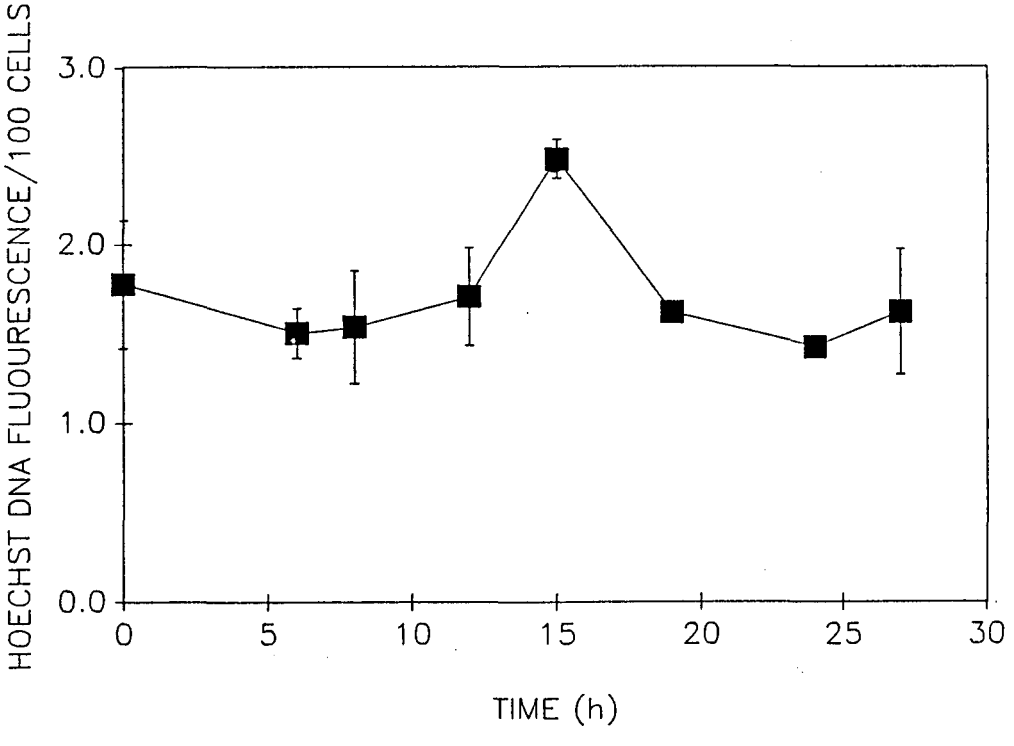

autosporangial complex was the dominant, and sometimes exclusive, morphology noted (Fig. 4D).

Figures 5 presents the 8-fold increase in TG with respect to changes in the other lipid fractions of the cell. Note that the X-axis is a logarithmic scale and that Y-axis is not linear. Besides the increase in TG as a function of final pH, the figure indicates that both the phospholipid and glycolipid content of he cells falls as pH rises. The fatty acid analyses of the individual lipid fractions were examined to determine if merely the total amount of lipid changed, or whether the quality of the lipid altered also. To do this, fatty acids were grouped according to their postulated function in the cells (Frentzen, 1986). Group 1 consisted of precursor fatty acids, Group 2 of unsaturated 16-carbon acids and Group 3 of polyunsaturated 18-carbon acids. As the pH of the incubation medium rose, the proportions of these acids in the triglyceride fraction did not change significantly (Table 1), i.e. the profile was dominated (70%) by the so-called precursor fatty acids. However, this was not the case for the glycolipid and to a lesser extent, the phospholipid fraction. Here, as the pH of the medium rose, these two fractions contained less unsaturated 16-and 18-carbon acids and more precursor fatty acids. These pattern changes were not borne out by analyses of Amphora coffeaeformis grown until silicate-limited in batch culture (results not shown).

Cell-Cycle Experiments

Figures 6a-e show that cell division gave rise to a doubling of the cell number, not a four-fold increase as is usual in Chlorella (6a). During this time, the total DNA in the culture also doubled (6b), but the fluorescence due to Nile Red staining of cellular triglyceride increased and then decreased (6c). When these parameters examined at the cellular rather than the population level, triglyceride content of the cells increased and decreased over the period 0-15h (peak at 7h), whereas DNA/cell replicated during the period 7-18h (peak of 16h), i.e. cycling of triglyceride took place before DNA replication was completed. During the time that triglyceride synthesis took place, no increase in cell number occurred.

DISCUSSION

When Chlorella CHLOR1 was incubated in an unbuffered algal medium, its growth and photosynthetic activity raised the pH of the medium from its initial value of less than 7 to more than 9 within 10 days. The non-metabolizable biological buffers used in these experiments permitted the uncoupling of the rising pH conditions from other media changes that occurred during algal growth. The similar Nile Red responses (fig. 2) as well as the final cell densities (data not shown) and morphology (Fig. 4) for unbuffered and buffered cultures at similar media pH values (Fig. 1) indicated that the buffered media posed few artifacts (if any) and were thus

representative model systems. This allowed the description of a nitrogen-independent, high pH-related stress that resulted in cell-cycle inhibition and indirectly in TG accumulation. A similar pH effect on cell growth and the cell cycle, but not lipid accumulation, was described by Malis-Arad and McGowan (1982b). In our experiments, the high pH stress (above pH 10) caused longer cell division cycles. When the cell division rate declines because of a particular stress imposed by the medium, there is a possibility that one stage of the algal cell cycle will be more sensitive to the stress than others. This will result in a preferential lengthening of that stage of the cell cycle [Olson et al., 1986]. One way, therefore, to identify the sensitive stage is to determine where the cells arrest when population growth ceases. The morphological data represented in Figures 4A-D indicate that the autosporangial cell stage, i.e. prior to autospore release but after nuclear division, is sensitive to high pH in Chlorella CHLOR1. This verified the previously-described high pH-stress which resulted in a functional synchrony at this stage due to a possible pH-dependent increased flexibility of the mother cell wall. This in turn prevented its rupture and thus inhibited autospore release [Malis-Mad and McGowan, 1982 a,b].

Badour and Gergis [1965] suggested the presence of an "autotoxin" in media from stationary phase cultures of the diatom Nitzschia sp. that caused a nitrogen-independent inhibition of cell division and an accumulation of intracellular lipid droplets. This effect was not reversed by nitrate additions, but cells did revert to dividing cultures when resuspended in fresh medium. When cells began dividing again, the lipid droplets declined. It is possible that the "autotoxin," which could not be isolated [Opute, 1974], might indeed, have been no more than an effect of high pH. The initial pH of the medium was adjusted to 7.0-7.4, but the medium used does not appear to have been buffered. In addition, in the presence of the "autotoxin" diatom cell division was arrested after nuclear division but before cell separation, i.e. the situation was analogous to the high pH-stress with Chlorella (Figs. 4A-D). This work, and ours, suggests that the mechanism of TG accumulation is not related directly to either high pH stress or nutrient deprivation, as has been previously reported [Suen et al., 1987; Taguchi, et al., 1987]. Instead, these stresses appear to have effects on the microalgal cell division cycle.

The accumulation of TG as a function of the pH of the growth medium cannot be explained simply by an interference with the progression of the cell cycle and a concomitant oversynthesis of triglyceride. This is because during this accumulation of triglyceride, the fatty acid profiles of the membrane lipids, as well as their quantity, changed also. An attempt to explain these changes requires that we consider the synthetic pathways and their activity within the cell cycle for all three classes of lipid i.e. storage triglyceride and membrane phospho- and glycolipids. TG and membrane lipids are synthesized sequentially during the cell cycle [Otsuka and Marimura, 1966; Beck and Levine, 1977; Klyachko-Gurvich et al., 1981]. Because of this sequential synthesis, Chlamydomonas

reinhardi, for example, was shown to be phospholipid and glycolipid rich at early stages of its cell cycle, probably because synthetic rates for these membrane lipids declined later in the cycle [Beck and Levine, 1977]. In Chlorella sp. K, a partial decomposition of glycolipids was shown to occur immediately prior to autospore release [Klyachko-Gurvich, et al., 1981]. This same decline in membrane lipids (glycolipids and polar lipids) was seen in Chlorella CHLOR1 stressed at high pH (Fig. 5). These cells also have been shown to be functionally synchronized at the cell cycle stage just prior to cell separation, as indicated by the increased proportion of autosporangial complexes in culture [see also Malis-Arad and McGowan, 1982b].

The two-pathway model of plant lipid biosynthesis was developed to explain the fatty acyl composition of plant glycerolipids [Roughan, 1987; Frentzen, 1986]. The lipid class fatty acid profiles for Chlorella CHLOR1 (data not shown) indicate that here lipid biosynthesis might be modeled in a similar fashion. In non-stressed cells (pH<10), the GLFA of the chloroplast membranes were a mixture of fatty acids derived from the prokaryotic pathway (the precursors 16:0/18:1w9) and the unsaturated 16-carbon fatty acids, as well as the subsequent eukaryotic (extra-chloroplastic) pathway products, the polyunsaturated 18-carbon fatty acids [Roughan, 1987]. However, positional identification of the acyl species on the complex lipids would be required to verify this conclusion. The PLFA of the plasma and other non-chloroplastic membranes were primarily products of the eukaryotic pathway with the precursors and polyunsaturated 18-carbon fatty acids balanced according to the functional requirements for plasma membrane fluidity. The unsaturated 16-carbon fatty acids found in the PLFA may be contributed by the phosphatidyl glycerol synthesized by the prokaryotic pathway and incorporated into the chloroplast membranes [Frentze, 1986].

Once the precursor fatty acids have been exported to the endoplasmic reticulum, esterified and the lipid modified to form diacylglycerols (DAG), there are at least two possible pathways for their subsequent modification. To form membrane lipid, further desaturation occurs through a phosphatidyl choline intermediate [Roughan, 1987]. To form storage lipid, a fatty acid is esterified to C-3 by a non-specific C-3-acyl-transferase [Frentzen, 1986]. It appears that TG was synthesized in Chlorella CHLOR1 with little further modification of the precursor fatty acids, regardless of the amount of TG accumulated in the culture. This result suggested that the Chlorella DAG pool was not closely connected to the phosphatidyl choline pool where desaturation normally occurs [Frentzen, 1986]. If the sole function of algal TG is carbon/energy storage during the cell cycle [Tosuka and Morimura, 1966], further desaturation is unnecessary, and in fact, detrimental because of loss of energy during beta-oxidation would be caused by the introduction of an unsaturated linkage [Schulz, 1985]. Other algae, especially the marine diatoms [Opute, 1974] have TGFA profiles which are highly polyunsaturated, indicating that TG

biosynthesis in their case is more like that in developing oil seeds with the DAG pool and PC-pool interconnected. This results in a more unsaturated DAG pool [Frentzen, 1986].

Where previous reports have quantified only total lipid fatty acid changes during TG accumulation, the increased proportions of precursor fatty acids have always been interpreted based on the increasing accumulation of the precursor fatty acid-rich TG [e.g. Suen et al., 1987; Fisher and Schwarzenbach, 1978; Sicko-Goad et al., 1988; Piorreck et al., 1984; Ben-Amotz et al., 1985; Millie, 1986]. The fatty acid profile changes during TG accumulation we have found suggest another interpretation and this is discussed below.

The storage lipid (TG) fatty acid profile of Chlorella appeared to be constant in composition (Table 1), regardless of the amount of TG accumulated (Fig. 5), i.e. little modification of the precursor fatty acids occurred following their esterification to the glycerol backbone. The membrane lipid (GL, PL) fatty acid profiles of Chlorella were not stable during TG accumulation induced by high pH. When the cells were incubated in medium pH>10, the GLFA and PLFA profiles contained significantly decreased unsaturated to precursor fatty acid ratios (Table 1). Thus, significantly less modification of the precursor fatty acids occurred in membrane lipids than during non-TG accumulating conditions (Table 1).

Some triglyceride has been shown to contaminate the glycolipid fraction when it is eluted with acetone from silicic acid columns [Suen et al., 1987]. This is a potential explanation for the shifts in GLFA profile during TG accumulation. However, if this were a major artifact in our work, we would predict that the GLFA fraction of cells incubated in CAPS (pH 10.3) would be greater than cells in CH+C (pH 9.6), because of the higher TG accumulation at the high pH (Fig. 1). We did not find this. There have been no reports wherein TG was found to contaminate the polar lipid during its elution with methanol from silicic acid [Suen et al., 1987]. Further purification of the lipids or each lipid class after silicic acid chromatography will be required to address conclusively the possibility that these shifts in fatty acid composition of the gross lipid fraction are artifactual.

If we dismiss the question of artifacts, our results suggest that the enrichment of precursor fatty acids during TG accumulation reported previously [e.g. Suen et al., 1987; Fisher and Schwarzenbach, 1978; Sick-Goad et al., 1988; Piorreck et al., 1984; Ben-Amotz et al., 1985; Millie, 1986] was not due solely to an increase in TGFA. It appears that algal lipid biochemistry was shifted in such a manner that less further desaturation of precursor fatty acids occurred in membrane lipid fractions. However, if TG accumulation functioned merely as storage for excess carbon fixed by the cell, these changes in membrane fatty acid profiles would not be predicted. Instead, we suggest a regulation point in TG synthesis at the level of the DAG pool and a possible

inhibition of the algal desaturation enzyme system (through the phosphatidyl choline intermediate). Shaw's [1966] distinction of storage and structural lipid defined solely by their fatty acid profiles may need to be modified therefore. Our preliminary data obtained with Amphora indicate that lipid biochemistry of this organism differs from that of Chlorella. •

These results emphasize the importance of a complete model for a shift in lipid metabolism from membrane lipid synthesis to storage lipid synthesis. A model which only argues for an increased synthesis of fatty acids is incomplete. A biochemical model for lipid accumulation must take into account that fatty acids can be esterified to either storage lipids (triglycerides) or membrane lipids (glycolipids and polar lipids), but only triglycerides accumulate during nutrient limitation. The importance of an adequate model for triglyceride accumulation is emphasized by our results obtained with synchronous cultures. These cells were not stressed nutritionally, yet they synthesized triglyceride to levels twice that of the dark-adapted cells. However, prior to DNA synthesis and cell division, this lipid disappeared from the cells and was probably utilized. If the cells could be poised biochemically at the stage they are in during synchrony at the 7th hour (Fig. 6b), then presumably they would continue to synthesize triglyceride. In triglyceride-accumulating batch cultures stressed by elevated pH, the division cycle was arrested during the autosporangial stage i.e. after DNA synthesis had taken place. These two seemingly contradictory observations could be accommodated if the autosporangial cells were incapable of undertaking a further round of DNA synthesis. The regulation of the onset of triglyceride utilization and the triggering of cell division are probably associated. Experiments with inhibitors of specific stages in the cell cycle may be useful in investigating the timing of these processes.

ACKNOWLEDGEMENTS

We thank Nicholas J. Cooksey for technical help (J.B.G.), Dr. Martin Hamilton for statistical and graphic advice, Dr. Larry Jackson for discussions of the work, Dr. Kennedy Gauger for assistance in the preparation of the figures, and the Solar Energy Research Institute for support through sub-contract XK-5-05073-1.

REFERENCES CITED

1. Badour, S.S. and Gergis, M.S. 1965. "Cell division and fat accumulation in Nitzschia sp. grown in continuously illuminated mass cultures." Arch fur Mikrobiol 51:94-102.

2. Beck, J.C. and Levine, R.P. 1977. "Synthesis of chloroplast membrane lipids and chlorophyll in synchronous cultures of Chlamydomonas reinhardi." Biochim Biophys Acta 489:360-369.

3. Ben-Amotz, A., Tornabene, T.G. and Thomas, W.H. 1985. "Chemical profile of selected species of microalgae with emphasis on lipids." J. Phycol 21:71-81.

4. Cohen, D. and Parnas, H. 1976. "An optimal policy for the metabolism of storage materials in unicellular algae." J Theor Biol 56:1-18.

5. Cooksey, K.E., Guckert, J.B., Williams, S.A. and Callis, P.R. 1987. "Fluorometric determination of the neutral lipid content of microalgal cells using Nile Red." J Microbiol Methods 6:333-345.

6. Fisher, N.S. and Schwarzenbach, R.P. 1978. "Fatty acid dynamics in Thalassiosira pseudonana (Bacillariophyseae): Implications for physiological ecology." J Phycol 14:143-150.

7. Frentzen, M. 1986. "Biosynthesis and desaturation of the different diacylglycerol moieties in higher plants." J Plant Physiol 124:193-209.

8. Guckert, J.B., Cooksey, K.E. and Jackson, L.L. 1987. "Biochemical elucidation of neutral lipid synthesis in microalgae." IN: FY87 Aquatic Species Program Annual Report. SERI/SP231-3206 (Johnson, D.A., Sprague, S. Eds), pp. 175-189.

9. Klyachko-Gurvich, G.L., Tsoglin, L.N. and Mozhaitseva, G.I. 1981. "Lipid metabolism during the course of ontogenesis of Chlorella in connection with activity of the photosynthetic apparatus." Sov Plant Physiol 28:304-311.

10. Malis-Arad, S. and McGowan, R.E. 1982a. "Alkalinity-induced aggregation in Chlorella vulgaris II. Changes in the cell wall during the cell cycle." Plant Cell Physiol 23:11-17.

11. Malis-Arad, S. and McGowan, R.E. 1982b. "A "point of no return" in the cell cycle of Chlorella." Plant Cell Physiol 23:397-401.

12. Millie, D.F. 1986. "Nutrient-limitation effects on the biochemical composition of Cyclotella meneghiniana (Bacillariophyta): an experimental and statistical analysis." Can J Bot 64:19-26.

13. Nichols, H.W. and Bold, H.C. 1965. "Trichosarcina polymorpha gen. et sp. nov." J Phycol 1:34-38.

14. Olson, R.J., Vaulot, D. and Chisholm, S.W. 1986. "Effects of environmental stresses on the cell cycle of two marine phytoplankton species." Plant Physiol 80:918-925.

15. Opute, F.I. 1974. "Studies of fat accumulation in Nitzschia palea Kutz." Ann Bot 38:889-902.

16. Opute, F.I. 1974. "Lipid and fatty-acid composition of diatoms." J Exp Botany 25:823-825.

17. Otsuka, H. 1963. "Contents of sterols in Chlorella cells at different developmental stages." Plant Cell Physiol 4:293-297.

18. Otsuka, H. and Morimura, Y. 1966. "Change of fatty acid composition of Chlorella ellipsoidea during its cell cycle." Plant Cell Physiol 7:663-670.

19. Paul, J.G. and Meyers, B. 1982. "Fluorometric determination of DNA in aquatic microorganisms by use of Hoechst 33258." Appl Env Microbiol 43:1393-1399.

20. Piorreck, M., Baasch, K-H. and Pohl, P. 1984. "Biomass production, total protein, chlorophylls, lipids and fatty acids of freshwater green and blue-green algae under different nitrogen regimes." Phytochemistry 23:207-216.

21. Roughan, P.G. 1987. On the control of fatty acid compositions of plant glycerolipids. IN: The Metabolism, Structure, and Function of Plant Lipids, Stumpf, P.K., Mudd, J.B., Nes, W.D. (Eds). Plenum Press, New York, pp. 247-254.

22. Schulz, H. 1985. Oxidation of fatty acids. IN: Biochemistry of Lipids and Membranes, Vance, D.E., Vance, J.E. (Eds). Benjamin/Cummings, Menlo Park, CA, pp. 116-142.

23. Shaw, R. 1966. "The polyunsaturated fatty acids of microorganisms." Adv Lipid Res 4:107-173.

24. Shifrin, N.S. and Chisholm, S.W. 1981. "Phytoplankton lipids: interspecific differences and effects of nitrate, silicate and light-dark cycles." J Phycol 17:374-384.

25. Sicko-Goad, L., Simmons, M.S., Lazinsky, D. and Hall, J. 1988. "Effect of light cycle on diatom fatty acid composition and quantitative morphology." J Phycol. 24:1-7.

26. Suen, Y., Hubbard, J.S., Holzer, G. and Tornabene, T.G. 1987. "Total lipid production of the green alga Nannochloropsis sp. QH under different nitrogen regimes." J Phycol 23:289-296.

27. Taguchi, S., Hirata, J.A. and Laws, E.A. 1987. "Silicate deficiency and lipid synthesis of marine diatoms." J Phycol 23:260-267.

Microalgal Fuel Production Processes: Analysis of Lipid Extraction and Conversion Methods

Nick Nagle
Peter Lemke

Solar Fuels Research Division, Solar Energy Research Institute
1617 Cole Blvd., Golden CO 80401

ABSTRACT

Microalgae are unique photosynthetic organisms that are known to accumulate storage lipids in large quantities and thrive in saline waters. Before these storage lipids can be used they must first be extracted from the microalgae and converted into usable fuel. Transesterification of lipids produces fatty acid methyl esters that can be used as a diesel fuel substitute.

Three solvents, 1-butanol, ethanol, and hexane/2-propanol were evaluated for extraction efficiency of microalgal lipids. Type of catalyst, concentration of catalyst, time of reaction, temperature of reaction, and quality of lipid were examined as variables for transesterification. The most efficient solvent of the three for extraction was 1-butanol (90 % efficiency), followed by hexane/2-propanol and ethanol. Optimal yield of fatty acid methyl esters was obtained using 0.6 N hydrochloric acid in methanol for 0.1 h at 70^{o} C.

MICROALGAL FUEL PRODUCTION PROCESSES: ANALYSIS OF EXTRACTION AND CONVERSION METHODS

INTRODUCTION

World-wide energy shortages and the oil embargo of the 1970's forced many nations to evaluate energy sources and supplies. Energy from biomass is an attractive solution because it is renewable. One of the goals of U.S. Department of Energy and the Solar Energy Research Institute is to develop a technology base for the large scale production of lipid-producing microalgae and conversion of microalgal lipids into substitutes for traditional fuels.

Neenan et al. (1986) analyzed the production of gasoline and diesel fuel substitutes using mass culture of microalgae. Large scale raceways of microalgae could yield 150-400 barrels of oil/acre/year. Two methods of conversion have been proposed (Neenan, et al., 1986): (1) transesterification for ester fuel production and (2) zeolite catalysis for gasoline production. While production of methyl esters from seed crops has been studied extensively, research on methyl esters from microalgal lipids is limited. This paper will report the results of our study which examined several solvent systems for lipid extraction from microalgae and identified the impact of major variables in transesterification of microalgal lipids.

MATERIALS AND METHODS

BIOMASS PRODUCTION

Biomass was produced for lipid extraction and conversion work at two locations - the Solar Energy Research Institute Field Test Laboratory Building (FTLB), and the Solar Energy Research Institute Outdoor Test Facility (OTF) in Roswell, New Mexico (Johnson et al. 1987). At the FTLB, the diatom Chaetoceros muelleri (SERI designation CHAET9, Johansen et al. 1987) was grown in five 1.4 m^2 ponds in a greenhouse. The ponds were filled to a depth of 20 cm with SERI Type II/10 water as a growth medium (Barclay et al., 1986). The ponds were heated to maintain a minimum temperature of 19° C. High pressure sodium lamps (Applied Hydroponics, San Rafael, CA) were used to continuously maintain a minimum light intensity of 400 $\mu E \cdot m^{-2} \cdot S^{-1}$. Growth medium was pH-controlled at an upper limit of 9.5, by carbon dioxide injection. Ambient air and water temperature and light intensity were monitored, and pH was controlled by an Apple computer using a Strawberry Tree data acquisition card (Sunnyvale, CA). Growth rates and nutrient status were monitored daily. The maximum growth rate obtained was 28 $g \cdot m^{-2} \cdot d^{-1}$ of ash free dry weight.

At the OTF, the alga Monoraphidium minutum (SERI designation MONOR2, Barclay et al., 1986) was grown in three 3.0 m^2 ponds outdoors. The ponds were filled to a depth of 15 cm using on-site saline ground water as a growth medium. The ponds were not heated and received only natural illumination. pH was controlled to an upper limit of 9.5.

HARVESTING

At the FTLB, biomass was harvested by pressure filtration. A filter press (Star Systems, Timmonsville, SC) with twenty plates and frames (30 cm in diameter) with 5 μm pore size paper filters was used to harvest the algae.

Growth medium and cells were pumped through the press at a rate of 800 $L \cdot h^{-1}$. Filtrate (growth medium) was returned to the ponds, through four cycles of growth and harvest. The biomass was collected on the paper filters. Biomass was concentrated from an initial concentration in the ponds of 0.5 % solids, to a final concentration of 8.0 % solids.

At the OTF, polymer flocculation (Weissman, unpublished) was the harvest method chosen. Biomass was concentrated from an initial density of 0.5 % solids to a final density of 4.0 % solids.

EXTRACTION

Lipid extractions were performed with a variety of solvents to determine the extraction efficiency compared with a control method. Three replicate trials of each solvent extraction were performed on C. muelleri. All extractions were batch runs, timed for 90 min. Temperature was varied, depending on the boiling point of the solvent. Solvent to biomass ratio in all trials was three:one (see below). All biomass percentages are expressed on a wet weight per volume basis.

The solvents used were 1-butanol, ethanol, and a mixture of hexane and 2-propanol. The hexane/2-propanol solvent system was 40 % hexane and 60 % 2-propanol, by volume. The control method was run in triplicate. This was a five step water/methanol/chloroform extraction (Roessler 1986).

Harvested biomass (8.0 % solids) was concentrated by centrifugation to 15.0 % solids, to reduce handling difficulty and volume of solvent needed. A 400 g sample of concentrated biomass was mixed with 1200 g of solvent. The mixture was heated to near boiling and maintained at that temperature for 90 min. The mixture was well-agitated during the extraction, then vacuum-filtered through a glass fiber filter to separate the lipid and solvent from the solid residue. Next, the solvent was removed by distillation. The lipid was further purified by a chloroform/methanol/water phase separation. A second distillation was run to remove the solvent from the purified lipid. The extracted lipid was then weighed. Purity was quantitatively determined (Delamas et al. 1984) using a thin layer chromatography scanner with flame ionization detector (Iatron Laboratories, Inc., Tokyo). The resulting yield of the pure lipid was compared with the control yield, to arrive at the relative efficiency for each extraction.

CONVERSION OF MICROALGAL LIPID

A Plackett-Burman screening design (Murray 1984) was used to screen major variables that affect transesterification. Variables examined were type of catalyst (hydrochloric acid-methanol and sodium hydroxide-methanol), concentration of catalyst (0.12 N and 0.6 N), time of reaction (0.1 and 3.0 h), temperature of reaction (20^{0} and 70^{0} C), and type of feedstock used, (lipid extracted from M. minutum and C. muelleri). A sample of 250 mg of the designated lipid was weighed into a teflon screw-cap tube, 5 mL of the catalyst-methanol solution was added and incubated at the appropriate time and temperature. The samples were agitated every 10 min. Fatty acid methyl esters (FAME) were extracted by addition of 5 mL of petroleum ether followed by vortexing and centrifugation. The top layer was drawn off, evaporated at 50^{0} C and weighed. The dependent variable in the regression model was called YIELD, which was the amount of FAMEs produced by the individual treatment. FAME identification was done using the Iatroscan. The efficiency of methylation of known algal lipids was determined using individual lipid

standards, at conditions chosen using the Plackett-Burman screening design.

RESULTS

EXTRACTION

For C. muelleri, the highest and most consistent extraction efficiency and lipid purity was obtained by using 1-butanol. Average extraction efficiency for the butanol trials was 90 % (w/w), with a relative standard deviation (RSD) of 3 %. The fraction of pure lipid in total extractables was 0.94.

Ethanol (95 % ethanol, 5 % propanol, v/v) gave an average lipid extraction efficiency of 73 % (RSD of 13 %), and a pure lipid fraction of 0.90. The hexane/2-propanol solvent system gave an extraction efficiency of 78 % (RSD of 26 %), and a pure lipid fraction of 0.90 (See Table 1). All efficiency and purity results are averages of three "large scale" (150 to 400 g of biomass feedstock) extraction trials. Each large scale trial was run with three small scale (1.0 to 1.5 g of biomass) controls to determine theoretical 100 % yields.

One large scale extraction was run on the alga M. minutum. M. minutum was grown outdoors at the Roswell, New Mexico Test Facility. The solvent used for this extraction was 1-butanol. Extraction efficiency was 81 %, with a pure lipid fraction of 0.96.

CONVERSION

Variables examined in the Plackett-Burman screening design were time, temperature, type of catalyst, concentration of catalyst, and type of lipid used. Results indicate (Table 2) that type of catalyst was the most important variable. Time, concentration of catalyst, lipid type, and temperature of reaction were not as important. The explained coefficient of determination (R^2) was 74 %. Type of catalyst alone could explain over 55 % of the variation in the model. The maximum yield of FAMEs was achieved at the following conditions: 0.6 N hydrochloric acid-methanol catalyst, for 0.1 h, at 70^{o} C, using the extracted lipid from C. muelleri. Conversion yields of known algal lipids (Table 3) indicate that fatty acids had the highest yield (93 %), while monogalactosyl diglyceride had the lowest yield, 46 %.

DISCUSSION

EXTRACTION

Solvents were selected for analysis based on several criteria. These were low carcinogenicty, ease and safety of handling, volatility, availability and cost, and previous research. Ethanol, 1-butanol, and hexane/2-propanol appeared to be the most promising solvents.

All solvents were fairly effective at extracting a pure lipid product, at reasonably high efficiencies, with 1-butanol obviously being the best of the three. Butanol extractions were also the most consistent from trial to trial, in efficiency and purity. Alhough all solvents were relatively easy to handle, the consistency of the butanol results indicates a lower sensitivity to changes (or errors) in extraction procedure. This may be a considerable benefit as the process is scaled up.

The source of biomass (C. muelleri vs M. minutum) does not appear to significantly affect extraction efficiency. While only one extraction trial with M. minutum was run, its efficiency was not significantly different from the C. muelleri extractions.

All conversion studies were run with lipid extracted with 1-butanol. While all three solvents provided comparably pure lipid, downstream effects (conversion efficiency) were not investigated as a function of extraction method. Future work may include studies of the downstream effects of extraction solvent choice.

CONVERSION

Transesterification of seed oils has been well documented (Engler 1983). Freedman et al. (1984) optimized the variables for ester formation from triacylglycerols. The feedstock should have less than 0.5 % free fatty acids, 1 % sodium hydroxide-methanol should be used in a 6:1 molar ratio of alcohol to oil, and the mixture should be refluxed for 1 h at 60^{o} C. Freedman found that yields from seed oils using acid catalyst were lower, the reaction took longer, and higher temperatures were required when hydroxide catalyst was used. Freedman (1984) and Nye (1983) recommended acid catalyst when starting materials are low grade or have a high concentration of free fatty acids; the fatty acids would deactivate an alkaline catalyst. The concentration of free fatty acids in the lipid from C. muelleri and M. minutum was 24.6 %; thus an acid catalyst would be more effective than a base catalyst. The high confidence coefficient for the hydrochloric acid-methanol catalyst over the sodium hydroxide catalyst confirms this. The negative coefficient for time suggests that longer incubation times are deleterious to FAME yields. Temperature was not significant. A possible explanation might be related to the high concentration of free fatty acids in the algal lipid. The lower conversion yields from the phosphatidyl choline, phosphatidyl glycerol, mono- and digalactosyl diglyceride esters can be explained by the substitution of fatty acid groups by carbohydrate and phosphate groups.

Acknowledgements

This research was supported through the Aquatic Species Program of the DOE Biofuels and Municipal Waste Technology Division under BF71 (656-87). We would like to thank Joseph Weissman, of Microbial Products, Inc., for cultivation and harvesting of M. minutum for this project.

REFERENCES

Barclay, W., Johansen, J., Chelf, P., Nagle, N., Roessler, P. and Lemke, P., 1986, Microalgae Culture Collection 1986-1987, Solar Energy Research Institute, Golden, CO. SERI/SP-232-3079.

Delamas, R.P., Parrish, C.C. and Achman, R.G., 1984, Determination of Lipid Class Concentration in Seawater by Thin Layer Chromatography with Flame Ionization Detection, Anal. Chem., Vol. 56, pp. 1272-1277.

Engler, C.R., Johnson, L.A. Jegasothy, H., Reddy, M.S. and Yarbrough, C.M. 1983. Vegetable Oil as a Diesel Fuel. Agricultural Reviews and Manuals, Agricultural Research Service. USDA/ARM-NC-28.

Freedman, B., Pryde, E.H. and Mounts, T.L., 1984, Variables Affecting the Yields of Fatty Esters From Highly Unsaturated Triglycerides, J. Am. Oil Chem. Soc., Vol. 61, pp. 1638-47.

Harrington, K.J., 1986, Chemical and Physical Properties of Vegetable Esters and Their Effect on Diesel Fuel Performance, Biomass, Vol. 9, pp. 1-17.

Johansen, J., Lemke, P., Nagle, N., Chelf, P., Roessler, P., Galloway, R., and Toon, S., 1987, Addendum To Microalgae Culture Collection 1986-1987, Solar Energy Reseach Institute, Golden, CO, SERI/SP-232-3079a.

Johnson, D.A., Sprague S., 1987, FY 1987 Aquatic Species Program Overview, Solar Energy Research Institute, Golden, CO, SERI/PR-231-2358.

Lepage, G. and Roy, C.C., 1984, Improved Recovery of Fatty Acids Through Direct Transesterification Without Extraction or Purification, J. Lipid Res., Vol. 25, pp. 1391-1396.

Murray, J.S. 1984. X-STAT. Wiley Professional Software.

Neenan, B., Feinburg, D., Hill, A., Mcintosh, R., and Terry, K., 1986, Fuels from Microalgae: Status, Potential, and Research Requirements, Solar Energy Research Institute, Golden, CO, SERI/SP-231-2550.

Nye, M.J., Williamson, T.W., Deshpande, S., Schrader, J.H. Snively, W.H., Yurkewich, T.P. and French, C.L., 1983, Conversion of Used Frying Oil to Diesel Fuel by Transesterification: Preliminary Tests, J. Am. Oil Chem. Soc., Vol. 60, p. 1598.

Roessler, P.G., 1986, Biochemical Aspects of Lipid Accumulation in Silica-Deficient Diatoms, Solar Energy Research Institute, Golden, CO, SERI/SP-231-3071, pp. 257-271.

Weissman, J. 1987. Microbial Products Polymer Harvesting Process, Microbial Products Inc., Fairfield, CA, Unpublished.

A:\AICHE

TABLE 1. Efficiency of lipid extraction from C. muelleri for several different solvents. All extractions were heated to near-boiling and run batchwise for 90 min. All results below are averages of three trials, with coefficients of variation in parentheses. Gross efficiency is actual lipid yield divided by theoretical yield from control extractions. Net efficiency accounts for the purity of extracted lipid. Purity is determined by thin layer chromatography (IATROSCAN).

SOLVENT	GROSS EFFICIENCY	PURITY	NET EFFICIENCY
1-butanol	94 % (3)	0.94 (3)	90 % (3)
ethanol	82 % (12)	0.90 (4)	73 % (13)
hexane/2-propanol	87 % (25)	0.90 (6)	78 % (26)

Note: One extraction trial was run with M. minutum feedstock and 1-butanol solvent. The results were gross efficiency of 84 %, purity fraction of 0.96, and net efficiency of 81 %.

TABLE 2. Regression coefficients for yield of fatty acid methyl esters using a Plackett-Burman screening design. Lipids from C. muelleri and M. minutum. were transesterified at different combinations of time, temperature, catalyst, and catalyst concentration. Type of catalyst was identified as the most important, having the largest coefficient of determination.

Coefficient	Term	Std. Error	Confidence Coef.
8.2	Lipid	11.1	49.4 %
0.3	Temp	0.4	49.9 %
-10.7	Time	7.7	77.9 %
39.9	Catalyst	11.1	98.5 %
5.2	Conc	4.5	69.5 %

TABLE 3. Yield of fatty acid methyl esters (FAME) from standards representing lipids found in algae. All yields are the mean of two samples of lipid standards. Reactions took place using 5 mL of 0.6 N hydrochloric acid in methanol at 70° C for 1.5 h. Yield is based on mass of FAME produced divided by mass of starting material.

LIPID	% YIELD
Palmitic acid	93.4%
Triolein	87.6%
Phosphatidyl glycerol	54.4%
Phosphatidyl choline	65.1%
Monogalactosyl diglyceride	46.6%
Digalactosyl diglyceride	55.8%

Document Control Page	1. SERI Report No. SERI/SP-231-3579	2. NTIS Accession No. DE89009472	3. Recipient's Accession No.

4. Title and Subtitle
Aquatic Species Program

5. Publication Date
September 1989

6.

7. Author(s)
W.S. Bollmeier, S. Sprague

8. Performing Organization Rept. No.

9. Performing Organization Name and Address
Solar Energy Research Institute
1617 Cole Boulevard
Golden, Colorado 80401-3393

10. Project/Task/Work Unit No.

11. Contract (C) or Grant (G) No.
(C)
(G)

12. Sponsoring Organization Name and Address

13. Type of Report & Period Covered
Annual Report

14.
through May 1989

15. Supplementary Notes

16. Abstract (Limit: 200 words)

Researchers have learned that many species of aquatic microalgae produce lipids, or oils, when stimulated by environmental stress. These oils can then be processed into diesel fuel or gasoline. Scientists in the Department of Energy (DOE) / Solar Energy Research Institute (SERI) Aquatics Species Program have collected and screened more than 3,000 strains of microalgae from desert and saline environments. The most promising of these strains are maintained in a culture collection at SERI, and research is now focusing on applying genetic techniques to enhance lipid production of microalgae. Researchers are also studying ways to optimize microalgae lipid production by growing the microalgae in intensive cultures of large outdoor ponds. Because microalgae require large amounts of carbon dioxide as a nutrient, these microalgae facilities could be coupled with a power plant or other source of carbon dioxide. Thus, this technology offers not only the potential of producing renewable liquid fuels, but a possible way to improve the environment at the same time.

17. Document Analysis

a. Descriptors Microalgae ; lipid production ; genetic techniques ; renewable liquid fuels

b. Identifiers/Open-Ended Terms

c. UC Categories 244

18. Availability Statement
National Technical Information Service
U.S. Department of Commerce
5285 Port Royal Road
Springfield, Virginia 22161

19. No. of Pages
173

20. Price
A08

Form No. 0069 (3-25-82) ★U.S. GOVERNMENT PRINTING OFFICE: 1989 -773-107/ 00026